The dissertation Committee for Jane Jaeyon Lee certifies that this is the approved version of the following dissertation:

Assessment of Body Composition: Total, Central, and Regional Adiposity via Stereovision Body Imaging

Committee:

Jeanne Freeland-Graves, Supervisor

Bugao Xu

Christopher Jolly

Richard Finnell

Hirofumi Tanaka

Assessment of Body Composition: Total, Central, and Regional Adiposity via Stereovision Body Imaging

by

Jane Jaeyon Lee, B. A.; B. S.; M. S. Stat.

Dissertation

Presented to the Faculty of the Graduate School of

The University of Texas at Austin

in Partial Fulfillment

of the Requirements

for the Degree of

Doctor of Philosophy

The University of Texas at Austin

August 2014

Acknowledgements

First of all, I extend my deepest gratitude towards my dear supervisor, Dr. Jeanne Freeland-Graves, who guided me to be a successful scholar. I will always remember the discipline that you taught me and cherish the time that we spent together.

I would like to express my sincere appreciation toward my committee members and professors at the University of Texas at Austin who always supported me: Drs. Bugao Xu, Christopher Jolly, Richard Finnell, Hirofumi Tanaka, Deanna Staskel, Lydia Steinman, Monica Meadows, Tasah Beretvas, Matt Hersh, and Erika Hale.

I am willing to convey my gratitude to the precious people in my life, Andrew Knieberg, Kyoung-Jin Lee, Lauran Mangini, Ji-Eun Lee, Kyung-Jun Lee, Randy Metzger, Donald Garrett, Miriam Pashby, Kathy McWilliams, Yeyi Zhu, Reese Pepper, Tamara Tabbakh, Namrata Sanjeevi, Tamara Mousa, Jimi Kim, Jaehyun Joo, and Seongjoon Kang.

Also, special thanks to Jim Battey, who has been my mentor and friend since I started graduate school. I greatly appreciate your patience with helping me and for believing in me that I am capable of completing my long journey.

Last but not least, I am grateful to my family, Dr. Young Dae Lee, Young Oak Jang, and Jae Woo Lee, and God who are the constants in my world. I learned how to be persistent and to keep pursuing the purpose of my life because of your endless love.

Assessment of Body Composition:

Total, Central, and Regional Adiposity

via Stereovision Body Imaging

Jane Jaeyon Lee, Ph.D.

The University of Texas at Austin, 2014

Supervisor: Jeanne Freeland-Graves

This research utilized stereovision body imaging (SBI) as a method for determining total, central and regional body composition. In Aim 1, prediction equations for abdominal adiposity were developed via anthropometrics, SBI, and magnetic resonance imaging. R^2 for total abdominal, subcutaneous, and visceral adiposity were 89.9%, 90.4% and 71.7%, respectively. The prediction of visceral fat was improved when SBI was included as a method. In Aim 2, body size and shape of men and women, as well as risks associated with accumulation of visceral adiposity, were determined by body measurements via SBI. Men had higher total body, torso and abdomen-hip volumes and waist circumference, while women exhibited greater thigh volume, hip circumference, and lower body-volume ratios ($p<0.05$), while the BMI values for men and women did not differ ($p>0.05$). Thigh to torso [odds ratios (OR) 0.44] and abdomen-hip (OR 0.41) volume ratios were associated with decreased risks of accumulating visceral adiposity.

SBI was effective for determination of body size and shape and the prediction of visceral adiposity accumulation in adults. In Aim 3, the efficacy of body measurements assessed by SBI was explored for the determination of android and gynoid body fat via SBI and dual-energy x-ray absorptiometry. The R^2 of the mathematical equations established by body measurements assessed via SBI for fat mass and percent body fat were 93.2% and 76.4% for android, and 91.4% and 66.5% for gynoid, respectively. These prediction values indicate that SBI is good for estimation of android and gynoid body fat mass; but less effective for percent body fat. An improved understanding of human body composition was achieved by this research.

Table of Contents

List of Tables

List of Figures

CHAPTER 1. INTRODUCTION

Obesity is a significant epidemic health problem associated with diseases such as hypertension, dyslipidemia, coronary heart disease, and type 2 diabetes (1-4). Other unfavorable effects of obesity include negative body image, negative self-esteem, and poor health-related quality of life (5-7). The prevalence of obesity in the United States is an epidemic, as 33.3% of adults are overweight [body mass index (BMI) 25-29.9 kg/m^2], 34.9% are obese class I and II (BMI 30.0-39.9 kg/m^2), and 6.6% are obese class III (BMI $\geq$ 40 kg/m^2) (8-10).

To date, BMI is the most commonly used method to determine body size and shape that reflects overall obesity status. The classifications of BMI are generally divided into six categories: underweight (BMI <18.50 kg/m^2), healthy weight (BMI 18.5-24.99 kg/m^2), overweight (BMI 25-29.99 kg/m^2), obese class I (BMI 30-34.99 kg/m^2), obese class II (BMI 35-39.99 kg/m^2), and obese class III (BMI $\geq$ 40 kg/m^2) (11, 12). Values of $\geq$ 30.0 kg/m^2 are documented to be associated with increased risks of developing hypertension, dyslipidemia, cardiovascular disease, type 2 diabetes, and metabolic syndrome (13-17). Thus, BMI is ideal for epidemiological and preliminary screening in clinical and field settings. However, the sensitivity involved with screening populations by this method is relatively crude because the index is oversimplified. It is limited in differentiation of muscle and fat mass, as well as android and gynoid shape between individuals (18-20).

Current methods to determine total, central, and regional body compositions have numerous shortcomings, such as high expense, non-portability, or lack of accuracy/availability. Consequently, newer instruments and techniques are needed to create more practical methods for assessing and monitoring different types of obesity.

Total body fat mass and percentage are utilized mainly to determine overall obesity status. Central obesity measures include surrogate measurements of abdominal adiposity, such as: waist circumference, sagittal diameter, waist-to-hip ratio, waist-to-height ratio, and skinfold thickness, as well as direct measurements of abdominal adiposity (total abdominal, subcutaneous, visceral fat, and android fat). Other body measurements used to assess regional obesity include: arm fat, gynoid fat, thigh circumference, thigh fat, sagittal abdominal diameter to thigh circumference ratio, and leg length, volumes, fat, and leg to trunk fat ratio.

This research will discuss the obstacles in using existing instruments and methods to measure overall, central, and regional obesity and provide a better solution for detection of body composition. The primary objective of this study was to enhance assessment of total, central, and regional body composition by comparing a three-dimensional (3D) stereovision body imaging (SBI) system, versus the "gold standards" of air displacement plethysmography (ADP), dual-energy x-ray absorptiometry (DXA), and magnetic resonance imaging (MRI).

Approaches for Specific Aims

Aim 1. To develop mathematical models for the prediction of total abdominal, subcutaneous, and visceral adiposity using measurements derived via SBI.

Hypothesis: Body measurements obtained by a SBI will serve as accurate determinants for prediction of total abdominal, subcutaneous, and visceral adiposity.

Rationale: Mathematical models derived from measurements obtained by SBI can be predictors of abdominal adiposity with the application of newly developed technology. SBI can be utilized for predicting the presence and type of abdominal fat in clinical and field settings. This information will aid physicians and health providers to make better informed decisions regarding the risks of abdominal adiposity.

Aim 2. To determine the body size and shape via a SBI system assessed total/regional body volume and volume ratios in men and women.

Hypothesis: Total/regional body volumes and volume ratios measured by SBI are accurate measurements for determination of body size and shape in men and women.

Rationale: SBI is a reliable instrument that utilizes a precise and valid method for assessing total and regional body volumes. Body volume ratios, including the upper- and lower-body volume, can reflect the body size and shape of men and women. This stereovision instrument will serve as a useful tool for clinical and field studies as a rapid, non-invasive, objective method of obesity assessment.

Aim 3. To examine the efficacy of SBI for assessment of regional body fat distribution, including android and gynoid fat mass and percentages.

Hypothesis: Regional body fat can be estimated effectively by the use of SBI. This system will provide a more accurate analysis of regional body fat, volume, and circumferences more easily and at a lower cost than other instruments currently available.

Rationale: Determination of the total body volume or percent fat of an individual is oversimplified and lacks information on regional fat distribution. The distribution of fat in different regions of the body can influence health risks in relation to chronic diseases. Current methods for measuring body fat regions are expensive and not convenient when compared to the relative cost effectiveness and ease-of-use of a SBI system. It is estimated that the SBI system will market for ~$10,000, as opposed to the much higher costs of CT, DXA and MRI. It is believed that SBI will be an accurate measurement of both android and gynoid fat mass and percent body fat.

Assessment of Overall Obesity

A wide variety of methods are used to estimate overall obesity, including: traditional anthropometrics, bioelectrical impedance analysis (21), hydrodensitometry (22), abdominal ultrasonography (23), ADP or BOD POD® (24), DXA (25), computed tomography (CT) (26), and MRI (27).

Traditional anthropometric measurements achieved by manual methods are the most commonly utilized because they are practical, cost-efficient and the least difficult to

obtain. Weight and height are measured primarily to calculate BMI, which provides an estimation of overall weight status. Skinfold thickness (28, 29) is an older procedure that utilized interrelationships among subcutaneous fat, internal fat, and whole body density to determine overall obesity. Other anthropometric indices (30-33) predict percent body fat from circumferences and skeletal diameters, but the predictive accuracy of equations is not improved greatly by adding measures of skinfold thickness. Waist circumference is the most significantly related to health risks (34, 35), as it reflects central obesity. In addition, sagittal diameter, a measure of anteroposterior thickness of the abdomen at the umbilicus (36), may be an indirect measure of visceral fat (37, 38). However, manual methods are known to be problematic in inter rater reliability (39).

The technique of bioelectrical impedance analysis utilizes the contrast of electric impedance of tissues (40, 41). The aqueous tissues are suitable conductors due to their dissolved electrolytes; whereas, fat and bone have relatively poor conductance properties. Consequently, this device provides body fat percentage by estimating fat free mass (or total body water) from measurements of impedance and reactance (40, 41). However, the percent fat value may vary according to the hydration status of individuals, thus limiting its usefulness in severe obesity (42).

Hydrodensitometry was once considered the gold standard for assessment of body fat. It is based on body density, estimated by measuring total body volume from water displaced when the body is fully submerged. If the body is assumed to be composed of two components, including fat and fat-free mass with known densities, then the percent

body fat can be calculated from body density by equations such as Siri, Brozek, Lohman, Ortiz, and Schtte (43-47). The principle of hydrodensitometry is simple and it is the oldest established method to estimate body density, as it has been in existence since 1945 (48). However, this method is not suitable for the elderly and children due to severe subject burden, such as the stress of being submerged repeatedly in a small enclosure of water, the inability to climb into a tub, and having to bend forward and exhale while in a small space under the water (49, 50).

Abdominal ultrasonography is one of the methods that is capable of assessing abdominal adiposity by incorporating transducer (probe), transmission (gel) and high-frequency sound waves to capture the image of the abdominal anatomical structures (i.e. organs and blood vessels) (51). Visceral adiposity assessed by ultrasonography was closely linked with metabolic risk factors, such as homeostasis model assessment (HOMA) index ($r=0.41$, $p<0.001$). These associations were stronger than subcutaneous adiposity assessed by ultrasonography ($r=0.17$, $p<0.05$) (52). The reproducibility of measuring abdominal adiposity is relatively high with ultrasonography, as the coefficient of variation was 0.8%, as reported by Ribeiro-Filho et al. (2004) (23). Moreover, the utilization of abdominal ultrasonography is beneficial compared to CT or DXA due to the fact that it is not associated with ionizing radiation. Yet, the diagnostic concordance for visceral adiposity was only 74% when compared to CT. This indicates that ultrasonography cannot be considered as an accurate means to assess visceral adiposity (23).

ADP (or BOD POD®) is a newer method that displays good agreement for percent body fat compared with DXA (within 1%) (53). It is more accommodating in that it is less difficult for the subject than hydrodensitometry (53, 54). This system is based on theoretical constructs of Dempster and Aitkens (55), and the methods of Ginde et al. (24). Under isothermal conditions, body density is estimated in a specially designed capsule via variations in pressure and body volume. The breathing circuit system measures thoracic gas volume while the subject breathes normally. Five prediction equations (Siri, Brozek, Lohman, Ortiz, Schtte) are available in the BOD POD® software in order to measure percent body fat for different populations, including the general population (44), African American males (47), African American females (46), lean and obese individuals (56), and children under 17 years old (45). These prediction equations are based on measurements of body volume and body mass to estimate fat and fat-free mass. In comparison to hydrodensitometry, this method underestimates body fat percentage in men, yet it overestimates body fat percentages in women, perhaps due to their excess body hair (57). Body density measured via ADP was significantly correlated with hydrodensitometry ($r=0.94$, $p<0.001$) (54). But, measurements generated using this technique can be influenced by alterations in body temperature. Also, it requires the subject to remain still (for ~ 100 seconds) which may be difficult for children. This technique can induce claustrophobia due to the small size of the chamber (24).

Instruments that utilize advanced techniques and are capable of assessing detailed information include DXA (58), CT (59), and MRI (60). DXA differs from

hydrodensitometry and ADP in that it is a three-compartment model of body composition estimation, which is based on assumptions concerning the absorption of x-rays by bone, non-bone lean tissue or protein, and fat (61). The separation of fat-free mass into protein and bone mass increases accuracy because it accounts for inter-individual variations in these components. This device uses a technique based on different attenuations of X-rays through bone, lean tissue, and fat that decline with increasing photon energy (58, 62). The amount of tissues is estimated by the transmittance rates of X-rays at varying energies. This system is known to be accurate for measurement of bone mass, but it can underestimate percent body fat by 2-4%, and fat mass by 1.9 kg, as compared to hydrodensitometry (63). It also has been reported that DXA overestimates fat mass and body fat (64). Presumably, the bias that exists in DXA is due to variations in body size, fat mass, sex, and disease state. In addition, this method is limited because instruments have a weight and size limit. For example, some instruments have a weight limit of 300 lbs (GE/Lunar Prodigy densitometer, software version 10.5); other instruments are limited to 250 lbs (50, 53). Moreover, values for DXA differ according to the manufacturer, scanner, and software-specific algorithms, yielding higher (53, 65-67) and lower measurements (49, 68, 69) than comparable methods. Nonetheless, DXA has been reported to be sensitive for assessing moderate weight loss (64).

Both CT and MRI estimate body composition by imaging internal body structures. CT measures the differences in the attenuation of computer programmed X-rays through the tissues. It creates cross-sectional 3D slices to capture detailed images of

the body, such as brain, internal organs, and fat tissues. (59). MRI utilizes radio waves in the magnet fields, and measures the abundance of hydrogen nuclei in different tissues. This technique results in the production of high quality, 3D anatomic images without the risks of ionizing radiation (70). Both DXA and CT involve the use of radiation during the assessment. In addition, ADP, DXA, CT, and MRI are limited in their practical use due to their lack of portability, large size, and high expense associated with these devices, which limits practicality for large population studies.

Determination of Central Obesity

In the assessment of obesity, measurement of central obesity may be just as important as determination of overall adiposity (71-74). Central obesity is defined as excess fat around the abdominal area. Assessment of central obesity is complicated by the fact that there are three basic types of fat within this area, including subcutaneous adiposity (abdominal fat depots underneath skin), visceral adiposity (abdominal fat depots around organs), and ectopic fat (fat depots in locations not associated with accumulation of adipose tissue) (75). Excess subcutaneous fat is associated with insulin resistance (9,10) and cardiovascular disease risk factors (76). An abundance of fat accumulation within the visceral area has been linked to diabetes (77), hypertension (78) and metabolic syndrome (71). Finally, ectopic fat (i.e. liver fat) is associated with obesity-related vascular and coronary artery disease (79, 80). Abdominal visceral

adiposity is widely classified as part of ectopic fat because it is not supposed to accumulate in this area (81).

In the abdominal fat depots, a preponderance of evidence supports that abdominal visceral fat has greater implications for diabetes-related risk factors, as compared to abdominal subcutaneous adiposity (71, 74, 82-84). However, assessment of abdominal adiposity, especially visceral adiposity, is difficult because it requires instruments that utilize advanced techniques, such as MRI or CT; whereas, subcutaneous adiposity can be measured by traditional anthropometric methods (i.e. skinfold thickness).

It is recognized that over-accumulation of visceral fat tends to act as a dysfunctional adiposity that induces excess storage of ectopic fat (muscle, epicardial, and liver fats) (82). Consequently, abnormal free fatty acid metabolism may trigger the dysfunctional release of adipokines (82). Accumulation of the ectopic fats influences the metabolic profile and, eventually, increases the risks of developing metabolic syndrome (82). In contrast, subcutaneous fat is characterized by some as a "healthy adiposity," which does not appear to influence the development of metabolic syndrome (82). Thus, assessment of visceral adiposity may be more important for ascertainment of health risks, as compared to prediction of subcutaneous adiposity.

Traditional anthropometric measurements achieved by manual methods are utilized to a great extent because they are practical, cost-efficient and the least difficult to obtain. Those that reflect central obesity include waist circumference (85, 86), sagittal abdominal diameter (87, 88), waist-to-hip ratio (85, 89), waist-to-height ratio (90), and

skinfold thicknesses (86). Waist circumference is the most commonly used surrogate measurement of central obesity because it is simple to obtain. In addition, it demonstrates a high correlation with visceral adiposity volume (r=0.87), as compared to waist-to-hip ratio (r=67) (87). Greater waist circumferences than 102 cm in men and 88 cm in women are associated with a substantial increase of metabolic dysfunctions (91). For example, a larger waist circumference is related to increased metabolic disease risks (91), diabetes (92), cardiovascular diseases (93), and mortality (94). Sagittal diameter is a measure of anteroposterior thickness of the abdomen at the umbilicus in the supine position (95). Previously this measure has been shown to be an effective predictor of visceral adiposity in adults (96), but not in adolescents (97). Sagittal abdominal diameter is utilized as a surrogate of abdominal adiposity, as it is demonstrated to be a consistent predictor of cardiovascular disease. The hazard ratio for men and women was 1.42 and 1.44, respectively (98). Moreover, sagittal abdominal diameter was strongly related with cardiovascular risk factors (95, 99) and metabolic syndrome (100), even compared to waist circumference. Yet, Valsamakis et al. (2004) demonstrated that waist circumference showed stronger associations with visceral adiposity, as compared to sagittal diameter (101).

Waist-to-hip ratio is another of the most commonly used measurements for estimation of central obesity. The cut-off points for waist-to-hip ratio for predicting greater metabolic implications indicated by the World Health Organization (WHO) are 0.90 cm for men and 0.85 cm for women (91). Along with waist circumference, waist-to-

hip circumference showed strong associations with cardiovascular risk factors (93), type 2 diabetes (102), hypertension, and overall mortality (103). Waist-to-height ratio was introduced in the 1990s for detecting abdominal obesity and related health risks (104). Previously, waist-to-height ratio has been previously reported as a better predictor for cardiovascular diseases (105) and diabetes (106), as compared to waist-to-hip ratio or BMI. Waist-to-height ratio was more effective for predicting cardiometabolic risk than either waist circumference or BMI (90). Furthermore, waist-to-height ratio is utilized as an index of central obesity, which is more effective in defining metabolic syndrome than waist circumference (107).

Manual methods have potential for errors in inter rater reliability. For example, measurements can differ depending on the amount of training undertaken by the measurer for both waist and hip circumferences (108), and skinfold thickness (109). Furthermore, protocols for anthropometric measurements may not be consistent across different investigations and have not resulted in reliable outcomes (39, 110-113). In a literature review, Wang et al. (2003) found 14 different descriptions in three different manuals used as reference guides for the measurements of waist circumference (39).

Mason and Katzmarzyk (2009) explored the impact of the four major measurement sites of waist circumference on prevalence of metabolic syndrome (110). These include the superior border of the iliac crest, midpoint between the iliac crest and the lowest rib, and the umbilicus, and smallest circumference of the waist (110). Associations with morbidity/mortality (112) and abdominal adiposity (subcutaneous and

visceral fat) differed (113), depending on the sites or the protocols used to assess the body measurements. Thus, traditional anthropometric parameters appear to be an imprecise means for the accurate measurement of central obesity (39, 111).

Finally, the problem of awkwardness resulting from the close proximity between the researcher and subject remains when obtaining anthropometric data by manual methods. Devices such as abdominal BIA or ultrasonography (23, 114) are alternatives to assess central obesity in a cost-efficient and uncomplicated manner. Nonetheless, BIA is sensitive to hydration status and body geometry (in which water distribution differs), which may be limiting its usefulness in severe obesity (54). Previously, abdominal ultrasonography showed only 74% of the diagnostic concordance compared to CT (23). Thus, BIA or ultrasonography may not be as an accurate assessment tool for visceral adiposity, as opposed to MRI or CT, which directly assess the fat mass in the abdominal area and differentiate subcutaneous and visceral adiposity.

Evaluation of Regional Obesity

The overall fat distribution of humans can be classified crudely into android (apple shape or upper-body obesity) or gynoid (pear shape or lower-body obesity) shapes (115, 116). An android body shape is more closely linked with increased metabolic dysfunction, as opposed to a gynoid body type. Accumulation of body adiposity in the upper or lower regions has a more significant association with adverse metabolic functions (117). Specifically, greater fat accumulation in the lower body region is

believed to be protective. In contrast, fat depots in the upper region are more closely linked to obesity-related conditions, such as elevated insulin and glucose levels (118-121), metabolic dysfunctions (122-124), and greater risks of cardiovascular disease (123, 125, 126) and diminished longevity and mortality (123, 127). Knowledge of specific shapes and sizes of bodies and segments, with varying distribution of regional fat distribution, may provide beneficial information for clinical applications.

Measures of lower body fat have been explored previously by other researchers including hip and thigh circumference, thigh fat, leg fat, and gynoid fat (118-121). Greater waist circumference and smaller hip circumference were observed in type 2 diabetic patients, as compared to healthy participants, regardless of age, lifestyle factors, and intensity of obese status (as classified by BMI) (128). Both hip and thigh circumferences were inversely related to type 2 diabetes risks (32). Especially, thigh circumference was associated with positive levels of glucose in women (33). Furthermore, thigh adiposity was negatively linked to metabolic syndrome in elderly obese adults (9), a higher presence of glucose in men, and increased levels of glucose and lipids in men and women (33). Moreover, leg adiposity was related to low levels of glucose (34).

Aasen et al. (2008) noted that greater leg fat, as compared to trunk fat assessed by DXA, was associated with reduced insulin resistance in obese (120) and obese postmenopausal women ($p<0.05$) (83). Similar associations were identified with cardiometabolic variables (blood pressure, insulin resistance, high density lipoprotein,

triglycerides, high-sensitivity C-reactive protein) in healthy postmenopausal women (124). Similarly, positive relationships exist between larger waist and smaller hip circumferences and elevated cardiovascular disease risk factors (129). In addition, greater leg fat mass (kg) compared to whole body fat mass (kg) or trunk fat mass (kg), that was assessed by DXA, were associated with decreased metabolic risk factors (blood pressure, cholesterol, low and high density lipoprotein cholesterol, triacylglycerol, fasting blood glucose and serum insulin, C-reactive protein) in Caucasians, African Americans, and Hispanic men and women ($p<0.05$) (130). Gynoid fat, as determined by DXA, demonstrated decreased odds of metabolic risk factors, including blood pressure [odds rstios (OR) 0.5, $p<0.01$], fasting plasma glucose (OR 0.5, $p<0.01$) and triacylglycerol (OR 0.6, $p<0.01$) (131). Thus, assessment of specific regional body composition may be just as essential as determination of overall obesity.

The limitations of using regional body measurements obtained via traditional anthropometrics, MRI, CT, or DXA are similar to those associated with the assessment of central obesity. These measures are inaccurate, invasive, non-portable, expensive, or inefficient. Thus, alternative instruments are needed for the assessment of regional body composition.

System of Stereovision Body Imaging

Alternative methods that provide more practical and cost efficient means for obtaining accurate body measurements are essential for researchers and practitioners

because of the limitations of current measures to assess total, central, and regional obesity. To address issues of reliability and accuracy, 3D body scanners have been utilized for obtaining body images and measurements (46, 30). Previous studies confirm that 3D body scanners are efficient and reliable instruments that can replace some traditional manual methods to accurately measure body circumferences (47-49). Moreover, the 3D surface imaging of the human body has received considerable attention due to its broad range of applications, such as in the clothing industry (132, 133), movies and computer games (117), biometrics (134), dermatology and cosmetics (135), and breast and plastic surgery (136, 137). In recent years, this technique has been employed for obesity assessment due to the fact that the technique is easy to use, safe, and cost-effective (138).

Previous photonic body scanners have been used to measure body composition and compare body size and shape of different populations. The SBI incorporated in this study was validated for accuracy in measuring body volume and percent body fat, as the difference between ADP and SBI for assessing body volume was only −0.165 ± 0.692 (p=0.30) and 0.789 ± 4.178 for percent body fat (p=0.41) (138). The Hamamatsu Bodyline Laser Scanner was validated initially in adults and children to measure body volume. It showed less than a 3% error for assessment of body volume, as compared to that measured by underwater weighing and ADP. These results confirmed the accuracy of the system (139). Subsequently, a 3D photonic scanner $[TC]^2$ was utilized to assess body circumferences, including head, mid-upper arm, chest, waist, hips, mid-thigh, knee and

calf in diverse populations (American, British, Thai) (140-143). Values of body circumference ratios also were explored, according to different sex and age categories, in order to determine the disparities of body size and shape (142). The body measurements obtained via a Chang Gung Total Body Scanner determined relationships with BMI, somatotype index, and anthropometric data (144). Based on these data, a health index (145, 146) was developed with an anthropometric chronic disease risk factor score (147). This health index will allow clinicians to identify health risks.

The SBI system that was utilized in this research was designed and assembled by Dr. Bugao Xu at the University of Texas. It is a novel device that is capable of providing specific body measurements, including volumes for total body, torso (neck to umbilicus), abdomen-hip (umbilicus to hip), and thigh (crotch to top of knee); circumferences of shoulder (widest girth of upper torso including arms), chest (widest girth of chest), abdomen (smallest girth of torso), hip (widest girth of lower torso), crotch (lowest point of torso), upper thigh (highest point of thigh), lower thigh (lowest point of thigh), knee (bottom of knee), and calf (widest girth of lower leg); length of front and back (neck to waist), front and back upper torso (shoulder to waist), lower torso (umbilicus to crotch), crotch (abdomen to crotch), front and back shoulder slope (diagonal shoulder to waist), and thigh (crotch to top of knee); and breadth at the shoulder (138, 148). This device has been validated against ADP to accurately measure body volume and body fat percentage, as the differences were -0.165 ± 0.692 (p=0.30) for fat mass and 0.789 ± 4.178 for percent body fat (p=0.41) (138). Moreover, the visual representation of a human body

provided by the SBI improves the assessment of body size and shape in men and women because it can be rotated 360º in all directions (**Figure 1.1**).

The amount of time required to perform the measurement via SBI is brief, as the subject remains motionless for only 200 milliseconds per scan. More than 1 million data points are acquired, with a resolution under 1 mm. Less than 1 minute of processing time is required for surface modeling, during which a 3D image with numerous body circumferences at desired landmarks is generated (138, 148). An additional advantage of using a 3D stereovision device is that it is relatively inexpensive and much more portable than cumbersome equipment, such as DXA and ADP. This device has been validated for assessment of body volume and fat in 10 men and 10 women, as compared to ADP (138).

An innovation of SBI is that it measures central obesity utilizing two new parameters: central obesity width and central obesity depth (149). The definition of central obesity width is a measurement of the largest width on the coronal plane, at the level of the umbilicus. Central obesity depth is the length between the mid-point of the central obesity width and umbilicus. The two measurements lie perpendicularly on the same plane. It is believed that these surrogate measurements of central obesity will be effectively utilized for the assessment of central adiposity.

In sum, the current research was undertaken to explore the efficacy of a 3D SBI system as an instrument for determining total, central, and regional obesity in order to provide a more accurate and efficient means for obesity assessment and monitoring. It is believed that this newly developed state-of-the-art SBI will be effective for the

assessment of total, central and regional adiposity. The ability to accurately estimate body adiposity will provide health practitioners an enhanced ability to assess and monitor types of obesity.

Figure 1.1. Diverse body sizes and shapes of men and women determined by a three-dimensional stereovision body imaging system

(a) Men, starting from the left side, BMIs are 20, 24, 29, 36, 40 kg/m^2, respectively.

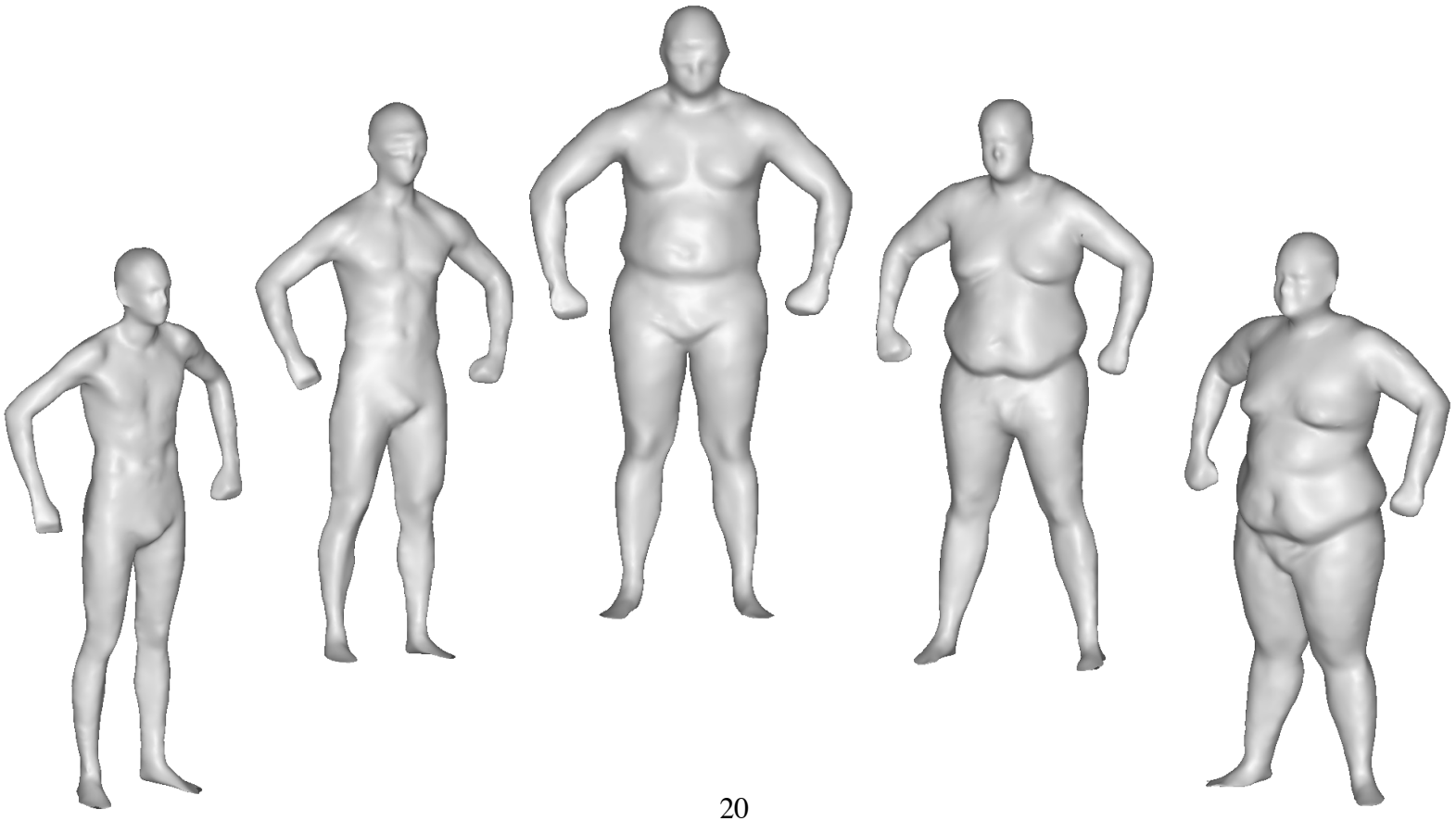

(b) Women, starting from the left side, BMIs are 19, 25, 30, 35, 39 kg/m^2, respectively.

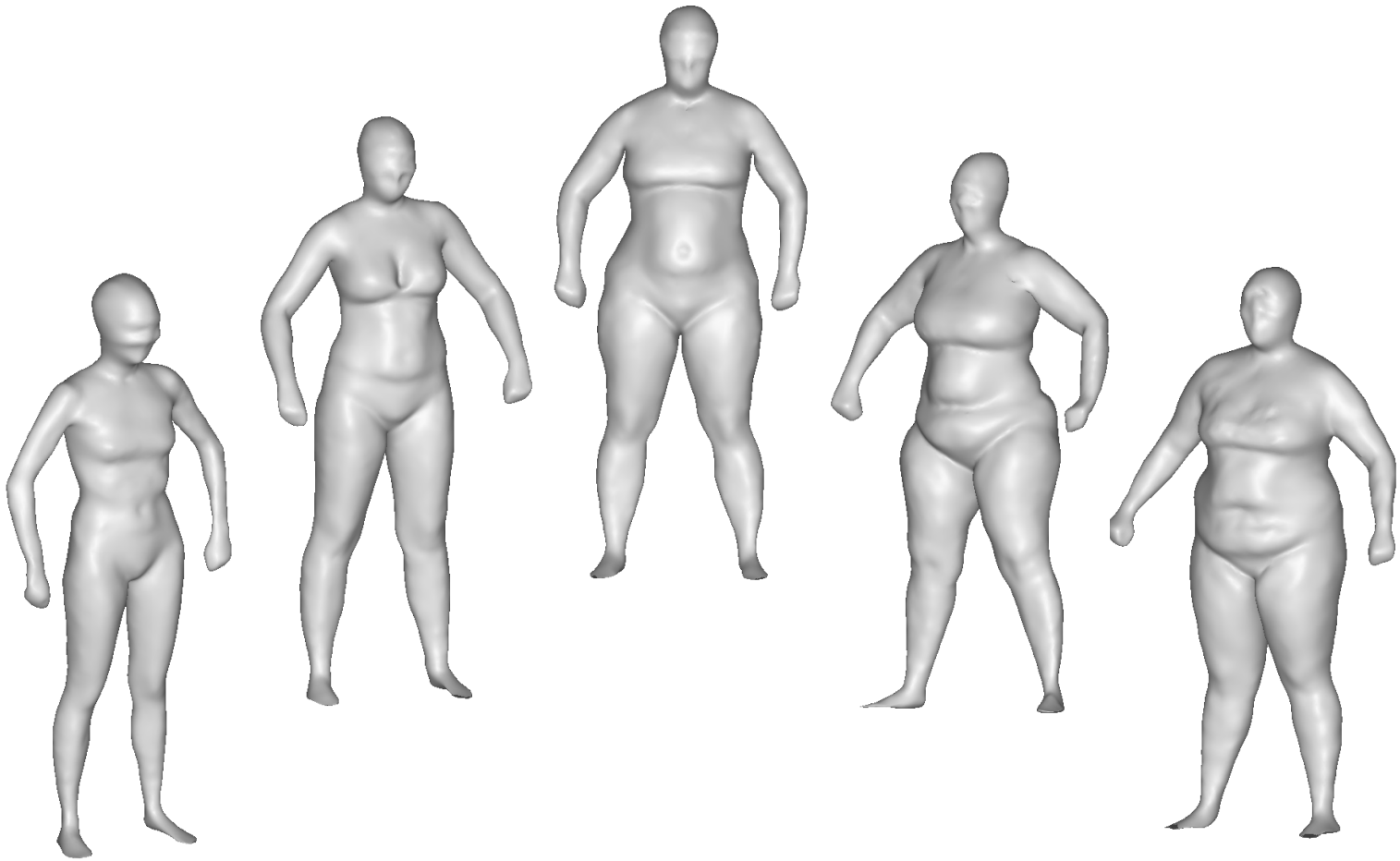

CHAPTER 2. PREDICTIVE EQUATIONS FOR CENTRAL OBESITY VIA ANTHROPOMETRICS, STEREOVISION IMAGING, AND MAGNETIC RESONANCE IMAGING IN ADULTS[1]

Abstract

Abdominal visceral adiposity is related to risks for insulin resistance and metabolic perturbations. Magnetic resonance imaging (MRI) and computed tomography are advanced instruments that quantify abdominal adiposity; yet field use is constrained by their bulkiness and costliness. The purpose of this study is to develop prediction equations for total abdominal, subcutaneous, and visceral adiposity via anthropometrics, stereovision body imaging (SBI), and MRI. Participants (67 men and 55 women) were measured for anthropometrics, and abdominal adiposity volumes evaluated by MRI umbilicus scans. Body circumferences and central obesity were obtained via SBI. Prediction models were developed via multiple linear regression analysis, utilizing body measurements and demographics as independent predictors, and abdominal adiposity as a dependent variable. Cross-validation was performed by the data-splitting method. The final total abdominal adiposity prediction equation was – 470.28 + 7.10 waist circumference – 91.01 sex + 5.74 sagittal diameter (R^2=89.9%); subcutaneous adiposity was – 172.37 + 8.57 waist circumference – 62.65 sex – 450.16 stereovision waist-to-hip ratio (R^2=90.4%); and visceral adiposity was – 96.76 + 11.48central obesity depth – 5.09 central obesity width + 204.74 stereovision waist-to-hip ratio – 18.59 sex (R^2=71.7%). R^2

[1] Portion of this chapter has been published in Obesity (Silver Spring) (149) "Lee JJ, Freeland-Graves JH, Pepper MR, Yao M, Xu B. Predictive equations for central obesity via anthropometrics, stereovision imaging and MRI in adults. 2014;22:852-62."

significantly improved for predicting visceral fat when SBI variables were included, but not for total abdominal or subcutaneous adiposity. SBI is effective for predicting visceral adiposity and the prediction equations derived from SBI measurements can assess obesity.

Introduction

Obesity is a significant health problem associated with diseases, such as diabetes (150), coronary heart disease (4), and nonalcoholic fatty liver (151, 152). In the United States, approximately 34.2% of the population is overweight [body mass index (BMI) ≥ 25.0 to 29.9 kg/m^2], and 33.8% and 5.7% exhibit obesity (BMI ≥ 30.0 to 39.9 kg/m^2) or extreme obesity (BMI ≥ 40 kg/m^2), respectively (152).

The most common method to classify the degree of weight status is BMI, due to its simplicity. Since values ≥ 30.0 kg/m^2 are linked to greater mortality and morbidity in populations, this method is ideal for epidemiological and preliminary screening in clinical and field settings. However, BMI does not distinguish between those with high muscle mass versus high fat, or the distribution of fat in different regions of the body. The distribution of fat is important, as excess subcutaneous fat (underneath the skin) is related to insulin resistance (153) and cardiovascular disease risks (76). In contrast, an abundance of visceral fat (between/around the organs) is associated with diabetes (77), hypertension (78), and metabolic risk factors (71).

Traditional anthropometric measurements ascertained by manual methods are the most commonly utilized for obesity assessment because they are practical, cost-efficient,

and the least difficult to obtain. Measurements that reflect central obesity may include waist circumference (86), waist-to-hip ratio (89), skinfold thicknesses (86), and sagittal diameter (88).

Investigations of anthropometric measurements and risk for obesity-related diseases have shown that waist circumference and waist-to-hip ratio are positively related to coronary heart disease in women (89); and that greater waist circumference and thickness of abdominal skin folds are associated with increased risk for metabolic syndrome (154). Also, sagittal diameter appears to be more related to cardiovascular risk factors than waist circumference or waist-to-hip ratio (95).

Manual body measurements are readily accessible, but their accuracy may be subject to low inter-rater reliability, inadequacy of training, and variances in the type of methods utilized (108). For example, Wang et al. (2003) reported 14 different descriptions in three different manuals used as reference guides for measurements of waist circumference (39). In addition, awkwardness is created by the close proximity between researcher and subject. Thus, traditional anthropometric parameters are an imprecise means for accurate measurement of abdominal adiposity. It is clear that devices that incorporate advanced techniques, such as magnetic resonance imaging (MRI) or computed tomography (CT) may provide more precise assessment (71). Yet, the large size and high expense associated with these instruments limit their use in field settings. Furthermore, the utilization of dual-energy x-ray absorptiometry (DXA) and CT may be precluded by the risk of radiation exposure.

A further step in the assessment of obesity can be the application of mathematical prediction equation models. Traditionally, these models have been developed by combining manual anthropometric measurements (weight, height, BMI, waist-to-hip ratio, sagittal diameter, body circumferences, skinfold thicknesses) and demographic characteristics (age, sex, ethnicity) (155, 156). However, the final prediction model is only as precise as the accuracy of the measurements inputted.

This research will test the efficacy of using a method of photogrammetry to be incorporated into prediction models for assessing central obesity. To date, 3D body scanners have been utilized for obtaining body images and measurements (138). These scanners are reliable instruments that can replace manual methods to accurately measure body circumferences (142, 157). This technique has been proven useful for tailoring clothing for textile manufacturing purposes, as well as for the assessment of obesity (138). The present study will utilize a SBI system to acquire fast, noncontact 3D whole body images and measurements, in order to develop algorithms for prediction of total, subcutaneous, and visceral abdominal adiposity. Parameters measured by SBI also will include unique measurements of central obesity, such as central obesity depth and central obesity width. Three variations of measurements will be tested: traditional anthropometrics, SBI, and a combination of the two. Accuracy between the prediction models will be compared to determine the best methods for prediction of central obesity.

Method and Procedures

Design of Study

The convenience sample consisted of 122 adults who were instructed to fast for 4 hours and avoided heavy exercise, alcohol or caffeine for 10 hours prior to the visit. Subjects made two visits to the: 1) university laboratory and 2) MRI research center.

At visit 1, demographic and health history questionnaires were completed and subjects were assessed for traditional anthropometrics measurements, including weight, height, body circumferences, and sagittal diameter. Body scans were performed via SBI to assess body size, shape, circumferences, composition, and central obesity. At visit 2, MRI scans were obtained for assessment of central adiposity measurements. To minimize errors, all measurements were completed at the laboratory within 3 hours and MRI assessment was made within 5 days.

Subjects

Hispanic and Non-Hispanic White men (n=67) and women (n=55) were recruited for the study via posted notices and word-of-mouth. Participants were aged 18 to 65 years old, with BMI ranging from 18.5 to 39.9 kg/m^2. Subjects were excluded from the study for any serious illness that could interfere with their ability to participate. Additionally, individuals who had exposure to metallic fragments or implants were eliminated due to the risks involved with utilizing MRI. Women who were or could be pregnant, or were lactating also were excluded due to university regulations. The study was approved by the University of Texas at Austin Institutional Review Board.

Anthropometrics

Standard protocols for the anthropometric measurements established by the National Institutes of Health guidelines (NIH guidelines) were performed by trained nutrition experts. Subjects were measured for height in centimeters to the nearest 0.1 centimeter without shoes and socks by a stadiometer (Health o meter, South Shelton, CT), and weight in kilograms by an electronic scale (Tanita, Arlington, IL) to the nearest 0.01 kilogram. Body circumferences, including arm, waist, hip, and thigh circumferences, were assessed via a MyoTape body tape measure (AccuFitness, Greenwood Village, CO). Sagittal diameter was measured horizontally from the umbilicus to the back via an abdominal caliper (Lafayette Instrument, Lafayette, IN). BMI was calculated by weight (kg) divided by height (m^2). Waist-to-hip ratio was computed by waist circumferences (cm) divided by hip circumferences (cm) and measurement for waist-to-height ratio was obtained by waist circumferences (cm) divided by height (cm).

System of Stereovision Body Imaging

Participants wore light-colored undergarments to facilitate accurate measurement of body size and shape with a swimming cap to conceal hair, and a blindfold to protect the eyes from the lights of the projectors. Subjects were instructed to place both arms at their sides with elbows bent, making a fist with both hands, with arms placed about 10 cm away from the body. Legs were spread approximately shoulder-width apart. Each subject remained motionless and was asked to hold their breath for 1 second during the 200-millisecond body scan. A total of 10 body scans were obtained to acquire the mean value.

The SBI system was fabricated with four pairs of monochromatic CMOS cameras

(Videre Design, Menlo Park, CA), with a resolution of 1280 × 960, and four ultrashort throw NEC 575VT LCD projectors (NEC Corporation, Tokyo, Japan) (138). Projectors were required to generate artificial texture on the scanned surface since human skin is not rich in texture. Four pairs of cameras simultaneously captured the body image when the body was illuminated by the projectors. The SBI is a novel device that calculates specific body measurements, including volumes, length, breadth, and central obesity parameters, via a rapid and non-invasive method. It can be assembled in a relatively small space and provides visual representation of body size and shape that can be rotated 360º in all directions. Advantages of this system over CT or MRI are: a) portability, which allows it to be used in field setting; b) cost, which is much lower than other equipment available; and c) lack of radiation.

SBI measurements included: shoulder, chest, abdomen, hip, crotch, upper thigh, lower thigh, knee, and calf circumferences, as well as central obesity depth and central obesity width. Central obesity width was defined as the largest width on the coronal plane, at the level of the umbilicus. Central obesity depth is the length between the mid-point of the central obesity width and umbilicus. These two measurements lie perpendicularly on the same plane (**Figure 2.1**).

Measurements for ratios computed were SBI waist-to-hip (waist circumference divided by hip circumference), waist-to-thigh (waist circumference divided by thigh circumference), and waist-to-height (waist circumference divided by height).

Magnetic Resonance Imaging

Figure 2.1. Central obesity depth (COD) and central obesity width (COW) at the umbilicus level, with minimal subcutaneous at the nearest site

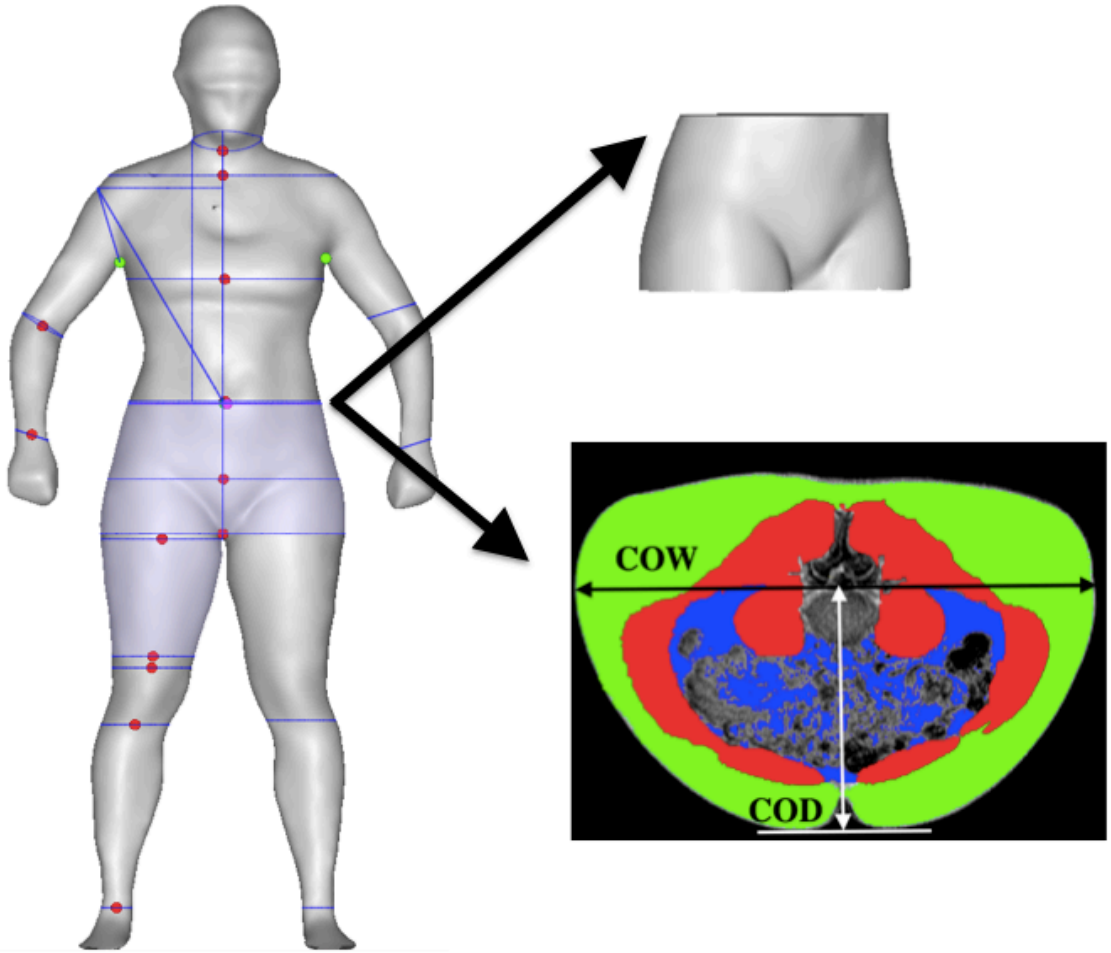

Participants were scanned for MRI via a 3.0 T general Electric scanner (GE Healthcare, Milwaukee, WI). When each subject was positioned on the center of the magnet, a 4-second 3-plane localizer scan was conducted, allowing visualization of anatomical landmarks. A slice of T1 axial images were obtained, centered at the navel, with TR 140, TE 2.1, flip angle 80, slice thickness 8.0 mm, gap 5.0 mm, FOV 40 x 40, matrix size 512 x 192, and bandwidth 62.5 kHz. MRI slices were analyzed by MRI software, SliceOmatic 4.3 (Tomovision, Montreal, CAN). Subcutaneous and visceral adiposity volumes were obtained from the umbilical slice, based on a volume of 3D pixels meeting the adipose shading threshold within the region of interest. The total abdominal volume was computed by summing the calculation for subcutaneous and visceral adiposity volumes.

Analysis of Statistics

All statistical analyses and data management were performed using Predictive Analytics Software Statistics 18.0 (IBM SPSS, Chicago, IL). Subjective characteristics were computed as a measure of descriptive statistics and described in terms of a mean, standard error of the mean (SEM), and minimum and maximum values of demographic variables and body measurements. P-values (p) less than 0.05 were adopted for the significance level.

All of the traditional anthropometrics measurements were assessed twice, and coefficients of variation of each value were obtained to examine the intra-observer reproducibility of the measurements. Coefficient of variation was also implemented to evaluate the reproducibility of SBI over 10 body scans. Total abdominal, subcutaneous

and visceral adiposity volumes were quantified from MRI umbilicus scans by two trained observers to acquire a coefficient of variation to confirm the reliability of the central obesity values. Reproducibility of the traditional anthropometrics, SBI and MRI measurements were assessed from a subset of 50 participants. The value of coefficient of variation was calculated as the standard deviation of the observations divided by the mean of the observations and these values were multiplied by 100 to be expressed as a percentage.

Subjects were assigned randomly into two groups: primary (70%, n=85) and validation (30%, n=37). The primary group was used to create prediction equations for estimation of central adiposity initially. Then the prediction equations were fit into the data derived from the validation group to assess the validity of the equations.

Pearson's correlation coefficients (r) were used to examine relationships between MRI measurements of total abdominal, subcutaneous and visceral fat volumes with 1) demographic parameters, 2) anthropometric measurements assessed by traditional manual methods, and 3) body measurements measured by SBI. A total of nine measurements (sex, waist circumference, waist-to-hip ratio, sagittal diameter, SBI waist circumference, SBI hip circumferences, SBI waist-to-hip ratio, central obesity depth, central obesity width) that exhibited high correlations with abdominal adiposity were selected to be included for the prediction of abdominal adiposity.

Parameters from three methods were applied to develop prediction equations for total abdominal, subcutaneous, and visceral adiposity. These included: 1) traditional anthropometric body measurements (waist circumference, waist-to-hip ratio, sagittal

diameter) and demographics (sex) as independent variables; 2) SBI parameters (SBI waist circumference, SBI hip circumferences, SBI waist-to-hip ratio, central obesity depth, and central obesity width) and demographics (sex) as independent variables; and 3) a combination of traditional anthropometrics, SBI measurements, and demographic parameters as independent variables. Sex was dummy coded as women=0 or men=1, and ethnicity, as Caucasian=0 or non-White Hispanic=1.

Prediction models were developed by conducting stepwise multiple linear regression analysis. Three different methods for independent predictors were applied with dependent variables of abdominal adiposity. Equations that contained the strongest predictor variables were selected as the optimal means for predicting total abdominal, subcutaneous and visceral fat. Independent variables that exhibited a variance inflation factor of 10 or higher in the results were removed to eliminate the impact of collinearity among the variables in a regression model. The remaining independent variables were included in the resultant stepwise multiple linear regression analysis.

The final prediction models were applied to the validation group as a means of cross-validation. R^2 described the percentages explained for the dependent variable for prediction equations; these are composed of a combination of independent variables to describe how well the model fits the data. The value of R^2 (%), mean error (observed value – predicted value) and 95% confidence intervals were examined to assess the validity of the prediction equations in the validation group.

Results

Statistics of Description

Characteristics of the participants in the primary and validation groups did not differ significantly (**Table 2.1**). In addition to descriptors presented in **Table 2.1**, the mean ± SEM for the primary and validation groups were 0.88 ± 0.01 and 0.87 ± 0.01 for waist-to-hip ratio, 0.85 ± 0.01 and 0.84 ± 0.02 for stereovision waist to hip ratio, 0.56 ± 0.01 and 0.56 ± 0.01 for waist-to-height ratio, 0.54 ± 0.01 and 0.55 ± 0.01 for stereovision waist-to-height ratio, and 1.44 ± 0.02 and 1.39 ± 0.41 for stereovision waist and thigh ratio. Among the 122 participants, 54.9% (n=67/122) were men and 45.1% (n=55/122) women; 65.6% (n=80/122), Caucasian and 34.4% (n=42/122), non-White Hispanic. Also, 33.6% (n=41/122) had healthy weights, 32.8% (n=40/122) were overweight, or 33.6% (n=41/122) exhibited class I and II obesity.

Reproducibility of Anthropometric, MRI, and SBI Measurements

All of the coefficients of variation values for traditional anthropometric measurements including weight, height, sagittal diameter, and circumferences of arm, waist, hip, and thigh were less than 1%, which ensured that the anthropometric variables were highly replicable. The reliability of the repeated measurements evaluated by coefficients of variation for SBI also exhibited strong agreements for abdominal adiposity volumes over 10 repeated body scans. Values of coefficients of variation for circumferences of waist, hip, thigh, central obesity depth and width were 0.6, 0.4, 0.6, 2.4, and 0.9%, respectively.

Table 2.1. Characteristics of subjects

Measurement Method	Group				
	Primary (n=85)		Validation (n=37)		
	Mean ± SEM[a]	Range	Mean ± SEM[a]	Range	*p* value[b]
Traditional Anthropometric					
Height (cm)	170.38 ± 0.96	148.59 – 189.23	170.04 ± 1.69	147.32 – 189.48	0.85
Weight (kg)	80.86 ± 1.96	49.80 – 129.64	83.71 ± 2.89	47.36 – 128.05	0.42
BMI (kg/m^2)	27.81 ± 0.60	18.85 – 40.33	28.90 ± 0.85	18.20 – 40.07	0.31
Waist circumference (cm)	91.92 ± 1.52	67.11 – 127.47	92.96 ± 2.27	65.40 – 115.00	0.71
Hip circumference (cm)	106.78 ± 1.28	80.50 – 132.08	108.62 ± 1.78	86.00 – 134.00	0.42
Sagittal diameter (cm)	23.64 ± 0.56	15.80 – 37.00	23.62 ± 0.73	15.40 – 33.00	0.99
Stereovision Body Imaging					
Stereovision waist (cm)	99.41 ± 1.78	75.00 – 133.08	101.05 ± 2.37	76.43 – 124.48	0.60

Table 2.1 (continued)

Stereovision hip (cm)	107.79 ± 1.21	91.71 – 136.93	110.97 ± 1.83	86.89 – 134.33	0.15
Stereovision thigh (cm)	64.60 ± 1.06	47.41 – 109.10	67.87 ± 1.97	55.18 – 122.95	0.11
Central obesity depth (cm)	15.39 ± 0.41	8.91 – 22.79	16.05 ± 3.77	8.83 – 22.08	0.38
Central obesity width (cm)	34.91 ± 0.58	21.25 – 46.41	35.97 ± 0.81	25.52 – 47.94	0.31
Magnetic Resonance Imaging					
Abdominal adiposity (cm^2)	284.35 ± 16.49	64.23 – 652.63	267.56 ± 22.73	20.64 – 510.43	0.57
Subcutaneous adiposity (cm^2)	218.72 ± 14.05	13.70 – 514.84	201.98 ± 18.23	18.09 – 412.03	0.50
Visceral adiposity (cm^2)	65.63 ± 4.57	7.28 – 187.17	65.58 ± 7.00	2.55 – 188.91	0.99

[a] Standard error of mean

[b] Significant level by independent samples t-test

Two trained observers displayed strong agreement in quantifying abdominal adiposity via MRI umbilicus scans. Values of coefficients of variation regarding MRI were 0.7, 0.8, and 0.9% for total abdominal, subcutaneous and visceral adiposity, respectively.

Correlations between Central Adiposities and Potential Variables

Pearson correlation coefficients (r) between abdominal adiposity volumes and demographics, traditional anthropometrics, and SBI measurements are shown in **Table 2.2**. The correlations between total abdominal adiposity and all independent variables were statistically significant, except for sex (p=0.10), ethnicity (p=0.10), and height (p=0.73). Total abdominal adiposity was highly related to BMI, waist circumference, hip circumference, waist-to-height ratio, and sagittal diameter. Relationships between total abdominal adiposity and SBI waist circumference, central obesity depth, and SBI waist-to-height ratio are depicted in **Figure 2.2a**.

All variables measured were significantly related to subcutaneous adiposity except ethnicity (p=0.08), height (p=0.55), and stereovision waist-to-thigh ratio (p=0.34), with age approaching significance (p=0.06) (**Table 2.2**). Linear relationships between subcutaneous adiposity and SBI waist circumference, central obesity depth, and waist-to-height ratio are illustrated in **Figure 2.2b**. Subcutaneous adiposity and BMI, waist-to-height ratio, and SBI hip circumference also were significantly related.

Table 2.2. Pearson correlation coefficients between total, subcutaneous, and visceral abdominal adiposity volumes, by using demographics, traditional anthropometrics and stereovision body imaging parameters

Parameters	Abdominal Adiposity Volume[a]		
	Total	Subcutaneous	Visceral
Demographic			
Age	0.29**	0.17	0.50**
Sex	– 0.15	– 0.23**	0.16
Ethnicity	0.15	0.16	0.05
Traditional Anthropometric			
Height (cm)	– 0.03	– 0.05	0.05
Weight (kg)	0.75**	0.73**	0.47**
Body mass index (kg/m^2)	0.85**	0.84**	0.51*
Waist circumference (cm)	0.85**	0.81**	0.60**
Hip circumference (cm)	0.83**	0.83**	0.45**
Waist-to-hip ratio	0.59**	0.50**	0.60**
Waist-to-height ratio	0.88**	0.84**	0.60**
Sagittal diameter (cm)	0.84**	0.78**	0.63**
Stereovision Body Imaging			

Table 2.2 (continued)

Stereovision waist (cm)	0.79**	0.72**	0.67**
Stereovision hip (cm)	0.81**	0.84**	0.36**
Stereovision thigh (cm)	0.54**	0.61**	0.09
Stereovision waist-to-hip ratio	0.36**	0.22*	0.62**
Stereovision waist-to-thigh ratio	0.23*	0.09	0.55**
Stereovision waist-to-height ratio	0.81**	0.74**	0.65**
Central obesity depth (cm)	0.83**	0.75**	0.71**
Central obesity width (cm)	0.82**	0.81**	0.47**

[a] Determined by magnetic resonance imaging

** Correlation is significant at 0.01 level (2-tailed)

* Correlation is significant at 0.05 level (2-tailed)

For visceral adiposity, all of the correlation coefficients with variables measured were also significant, with the exception of sex (p=0.08), ethnicity (p=0.55), height (p= 0.59), and SBI thigh circumference (p=0.33) (**Table 2.2**)**.** The highest correlations of visceral adiposity were found with central obesity depth (r=0.71), SBI waist circumference (r=0.67), and SBI waist-to-height ratio (r=0.65). Of these, central obesity depth provided the best correlation to visceral adiposity. Scatter plots of abdominal adiposity volumes according to these measurements are shown in **Figure 2.2c**.

Mathematical Model for Predicting Total Abdominal Adiposity

The best prediction equation for total abdominal adiposity was obtained by traditional anthropometric methods: total abdominal adiposity volume (cm^2) = – 470.28 + 7.10 waist circumference (cm) – 91.01 sex (women=0, men=1) + 5.74 sagittal diameter (cm) (**Table 2.3**). Equations obtained by traditional anthropometric methods resulted in the same ultimate model as the combination method due to the fact that the SBI parameters were not ideal predictors for predicting total abdominal adiposity. Thus, the final model for total abdominal adiposity did not include SBI body measurements. The optimal equation for total abdominal adiposity exhibited the highest R^2 (89.9%) and lowest standard error of the estimate (SEE) (49.18) among ten mathematical models (**Table 2.3**) developed by three different methods; traditional anthropometrics, SBI, and a combination. The R^2 for this model was not significantly different from the R^2 for the equation created by the stereovision imaging method (R^2 = 84.2%).

Figure 2.2. Abdominal adiposity volume determined by magnetic resonance imaging, according to body measurements

(a) total abdominal, (b) subcutaneous, and (c) visceral adiposity volume according to stereovision body imaging waist circumference, central obesity depth, and waist-to-height ratio

(a)

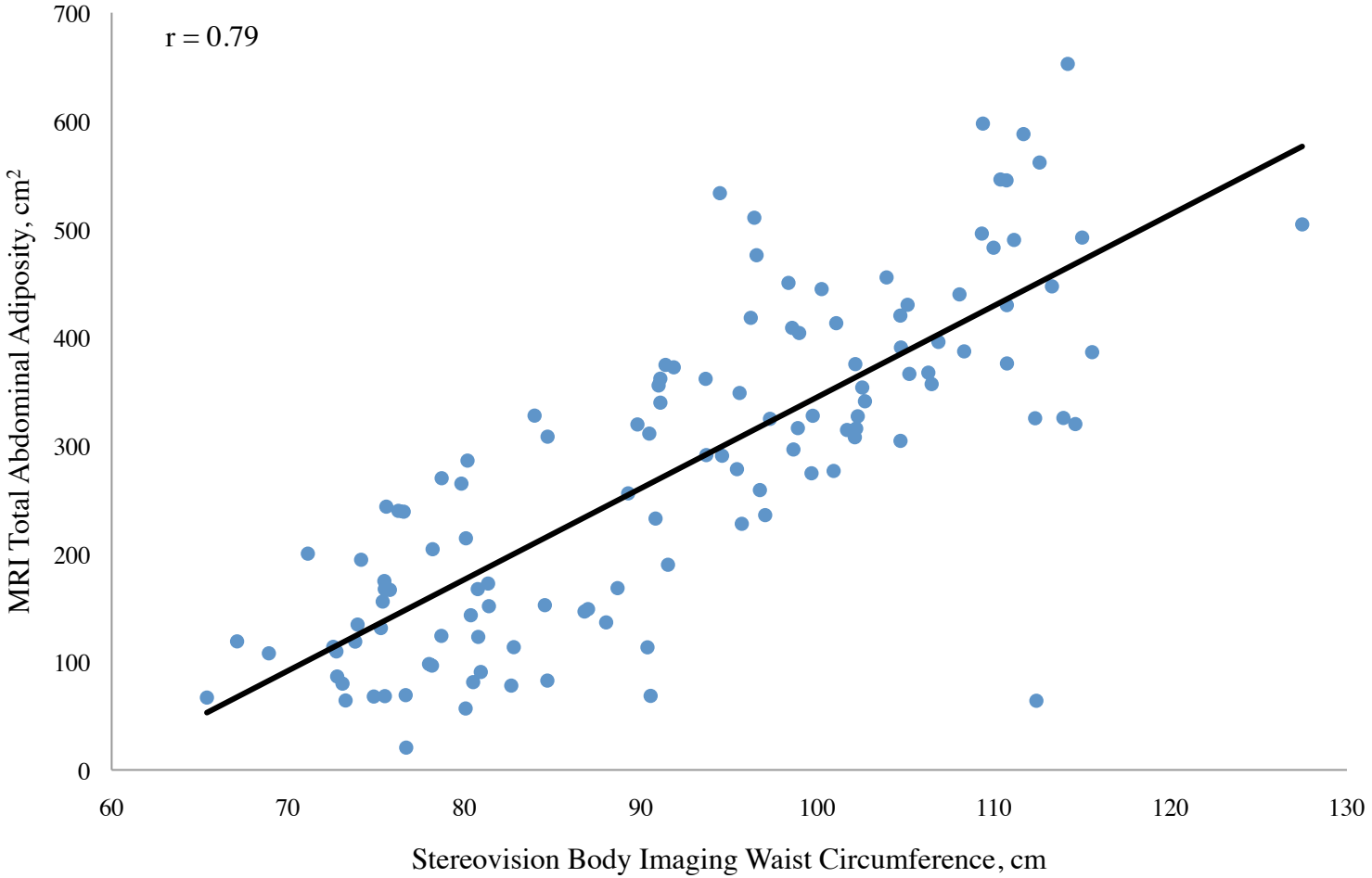
r = 0.79
MRI Total Abdominal Adiposity, cm2
700
600
500
400
300
200
100
0
60
70
80
90
100
110
120
130
Stereovision Body Imaging Waist Circumference, cm

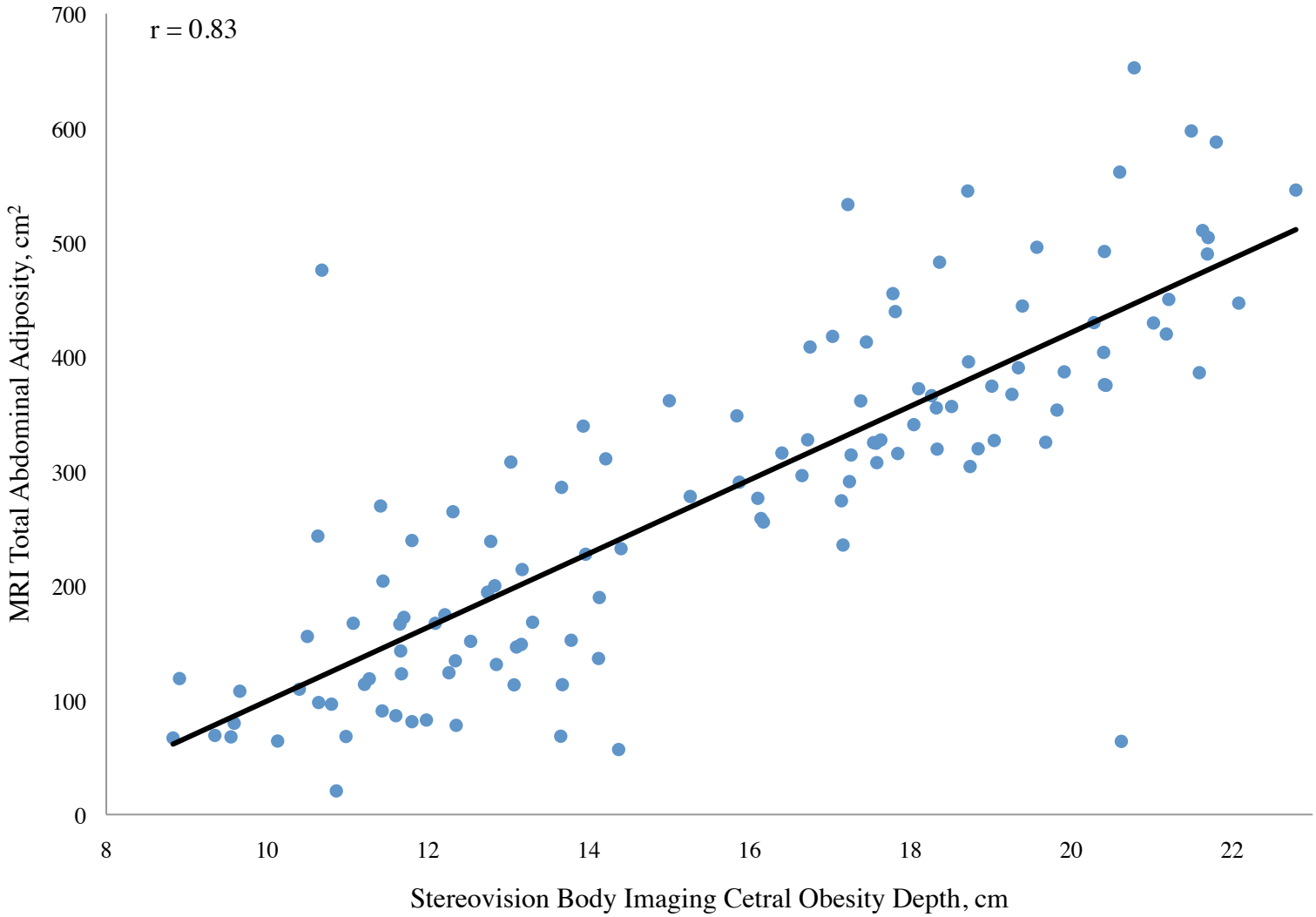
r = 0.83
MRI Total Abdominal Adiposity, cm²
700
600
500
400
300
200
100
0
8
10
12
14
16
18
20
22
Stereovision Body Imaging Cetral Obesity Depth, cm

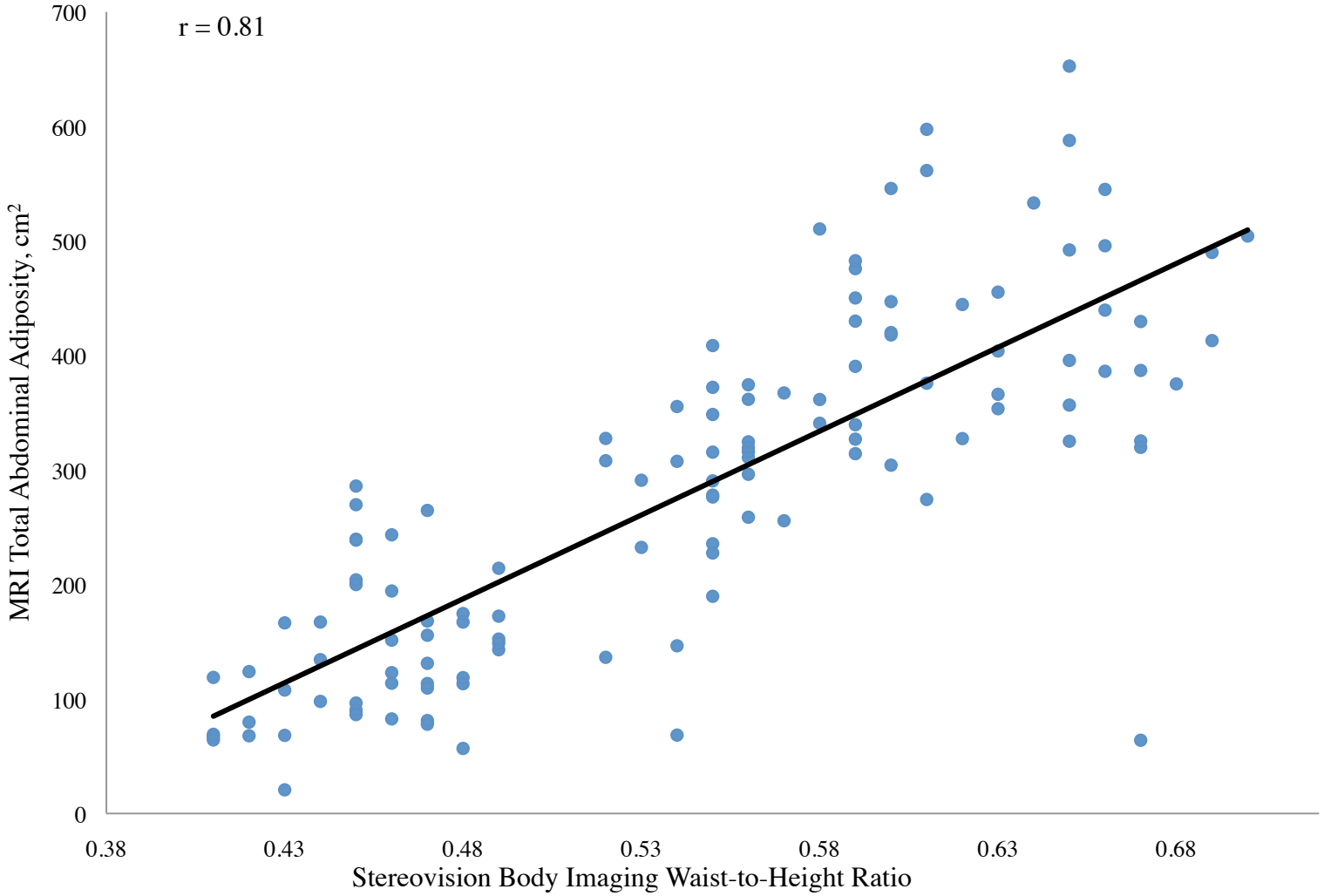
r = 0.81
MRI Total Abdominal Adiposity, cm²
700
600
500
400
300
200
100
0
0.38
0.43
0.48
0.53
0.58
0.63
0.68
Stereovision Body Imaging Waist-to-Height Ratio

b.

(b)

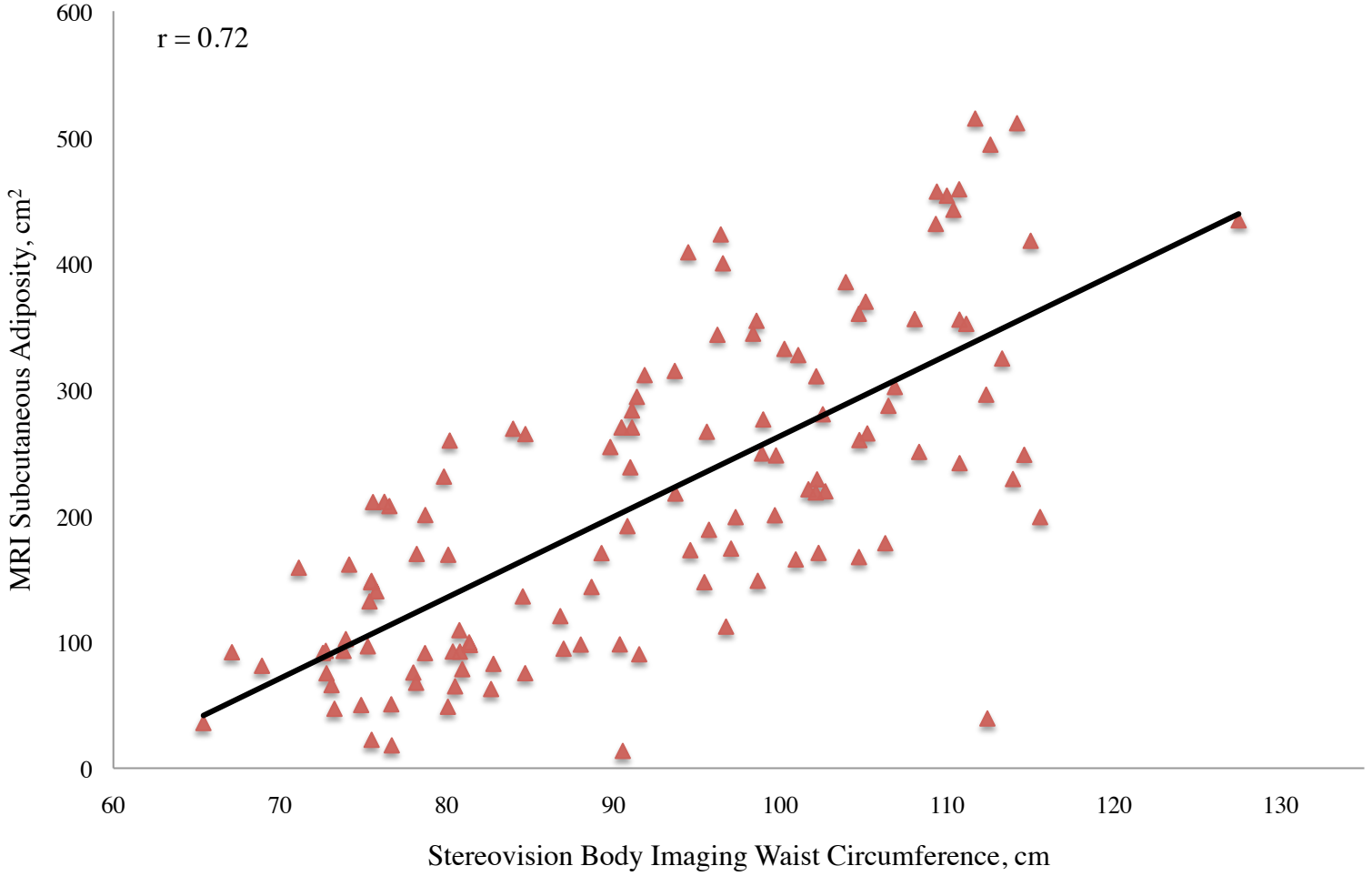
r = 0.72
MRI Subcutaneous Adiposity, cm2
600
500
400
300
200
100
0
60
70
80
90
100
110
120
130
Stereovision Body Imaging Waist Circumference, cm

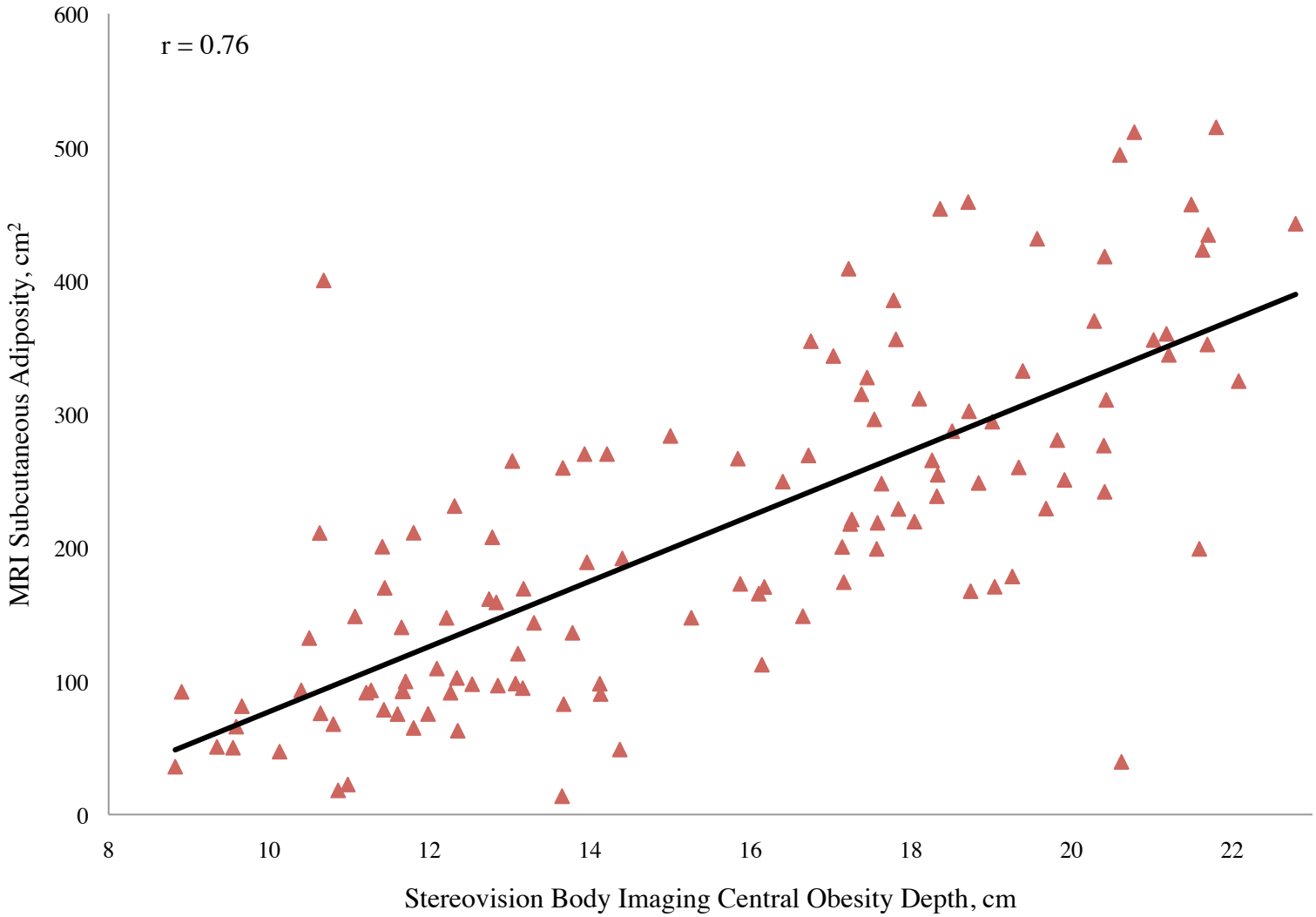
r = 0.76
MRI Subcutaneous Adiposity, cm2
600
500
400
300
200
100
0
8
10
12
14
16
18
20
22
Stereovision Body Imaging Central Obesity Depth, cm

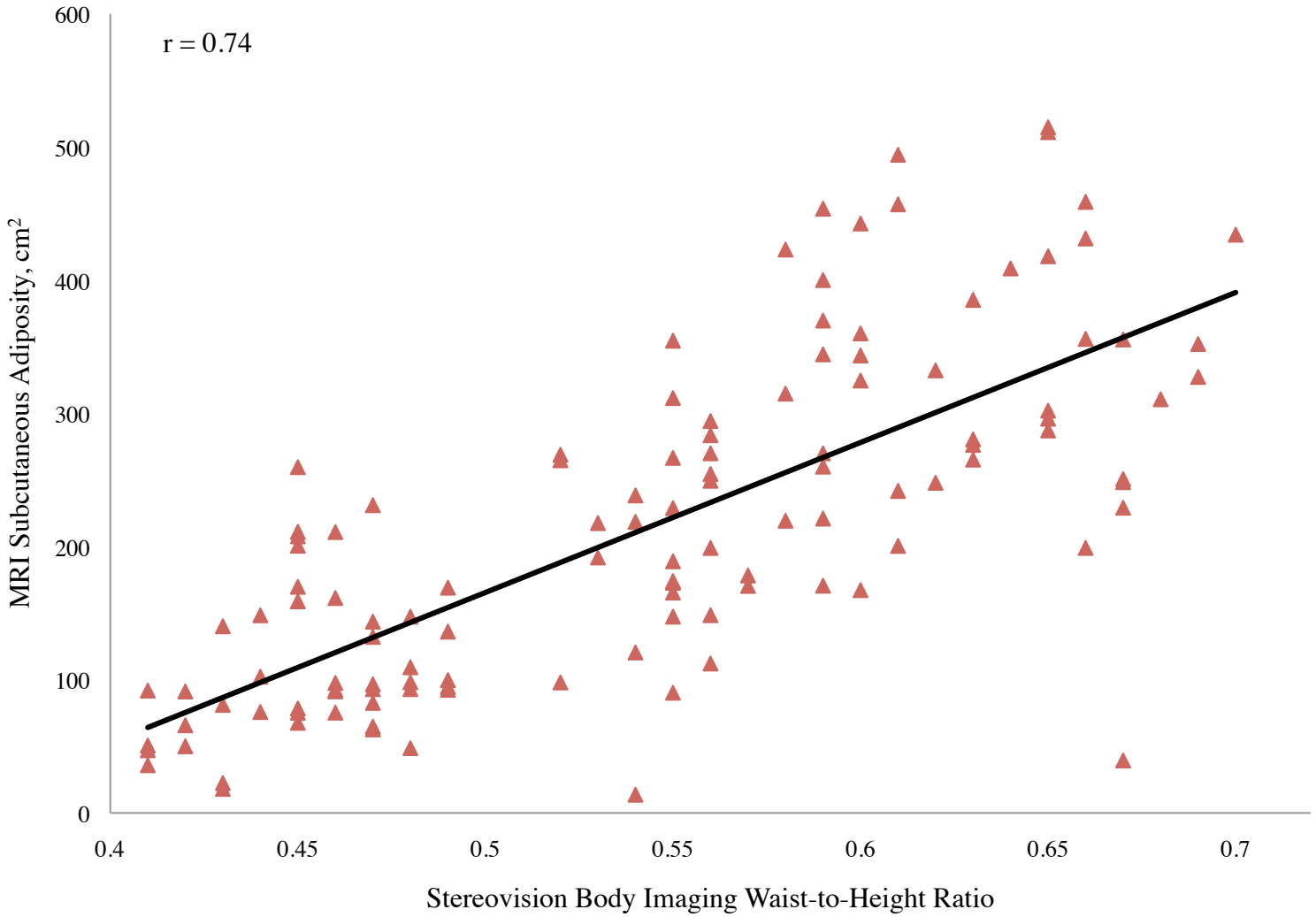
r = 0.74
600
500
400
300
200
100
0
MRI Subcutaneous Adiposity, cm2
0.4
0.45
0.5
0.55
0.6
0.65
0.7
Stereovision Body Imaging Waist-to-Height Ratio

(c)

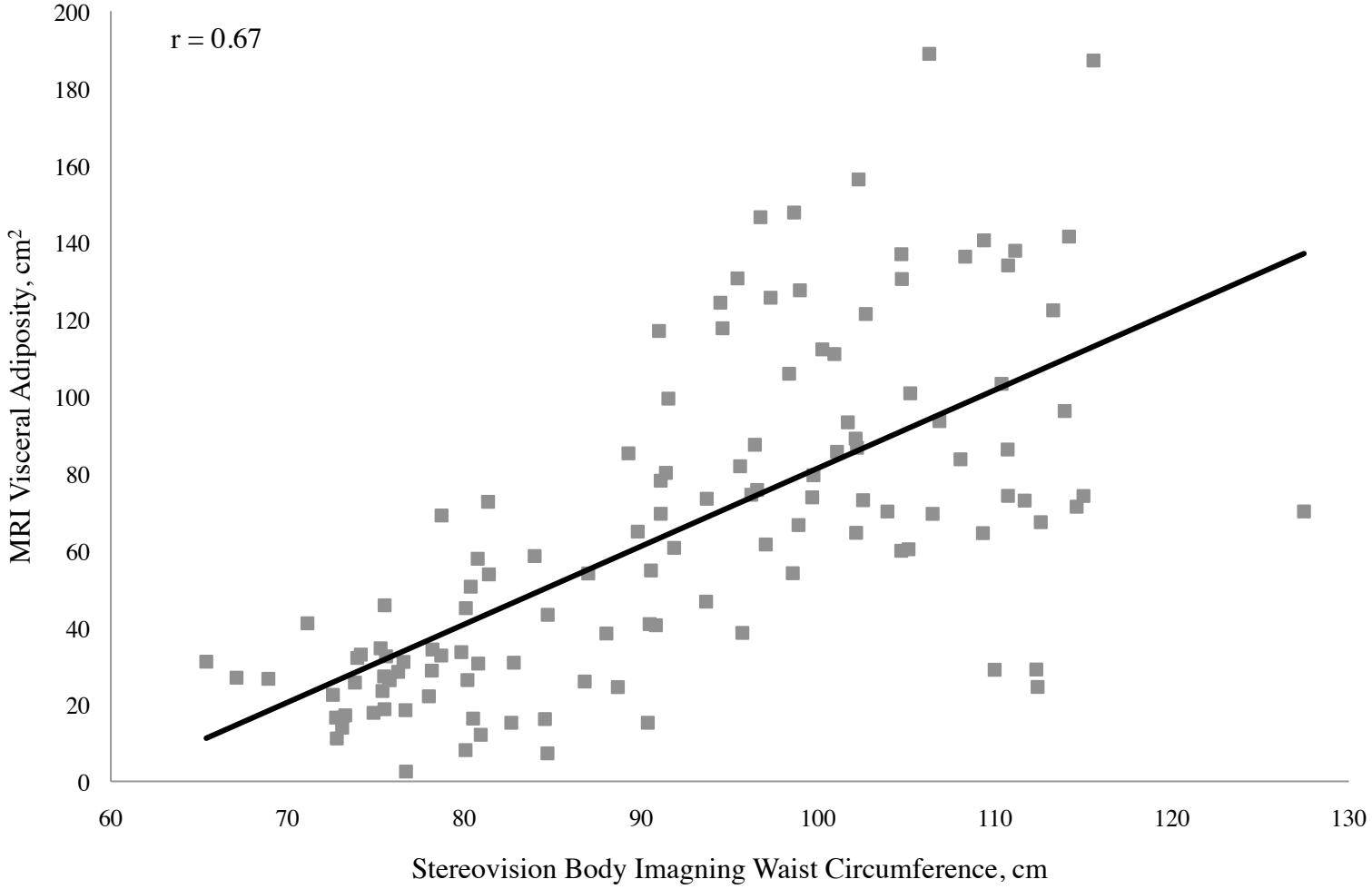
r = 0.67
MRI Visceral Adiposity, cm2
200
180
160
140
120
100
80
60
40
20
0
60
70
80
90
100
110
120
130
Stereovision Body Imagning Waist Circumference, cm

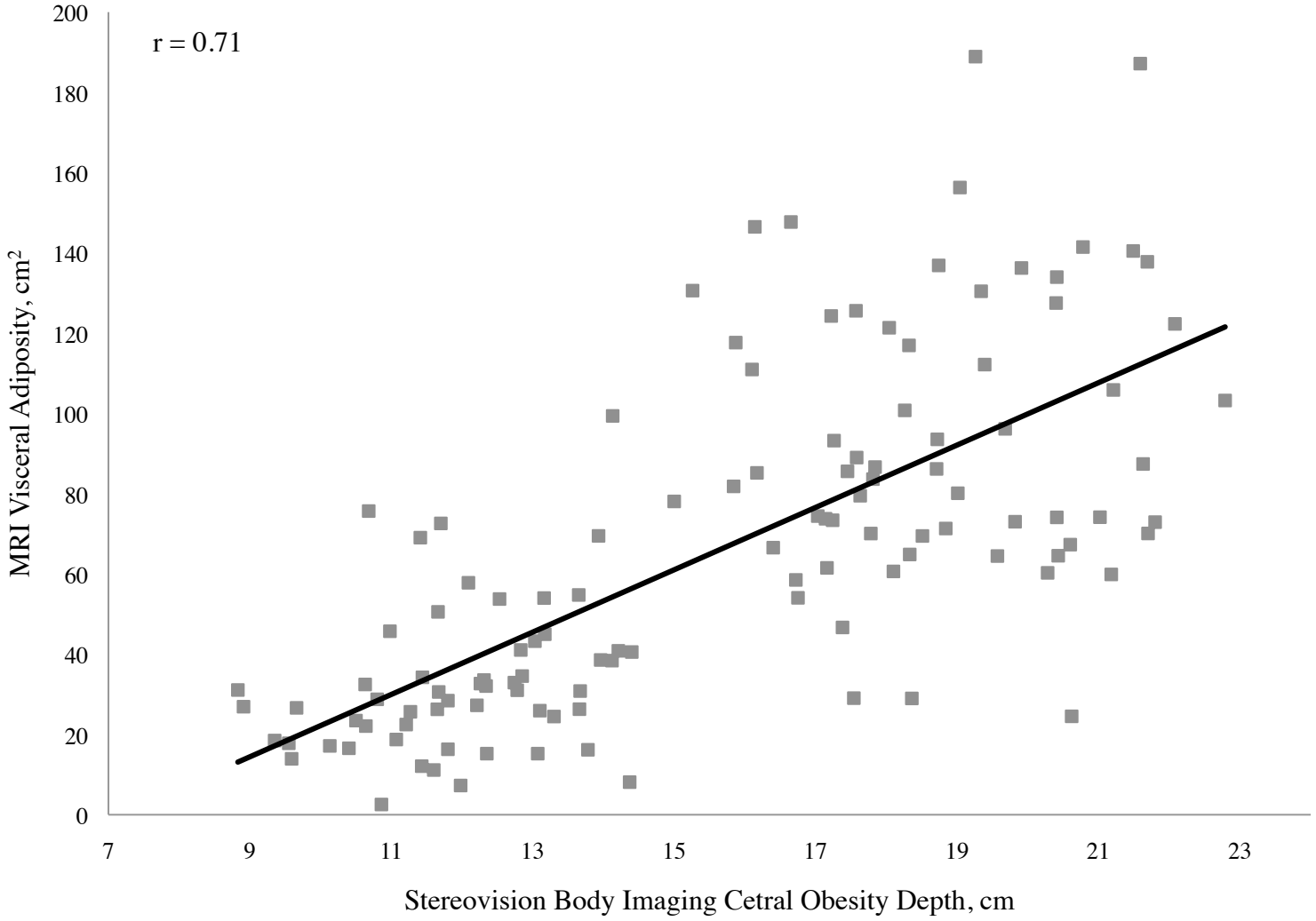
r = 0.71
MRI Visceral Adiposity, cm2
200
180
160
140
120
100
80
60
40
20
0
7
9
11
13
15
17
19
21
23
Stereovision Body Imaging Cetral Obesity Depth, cm

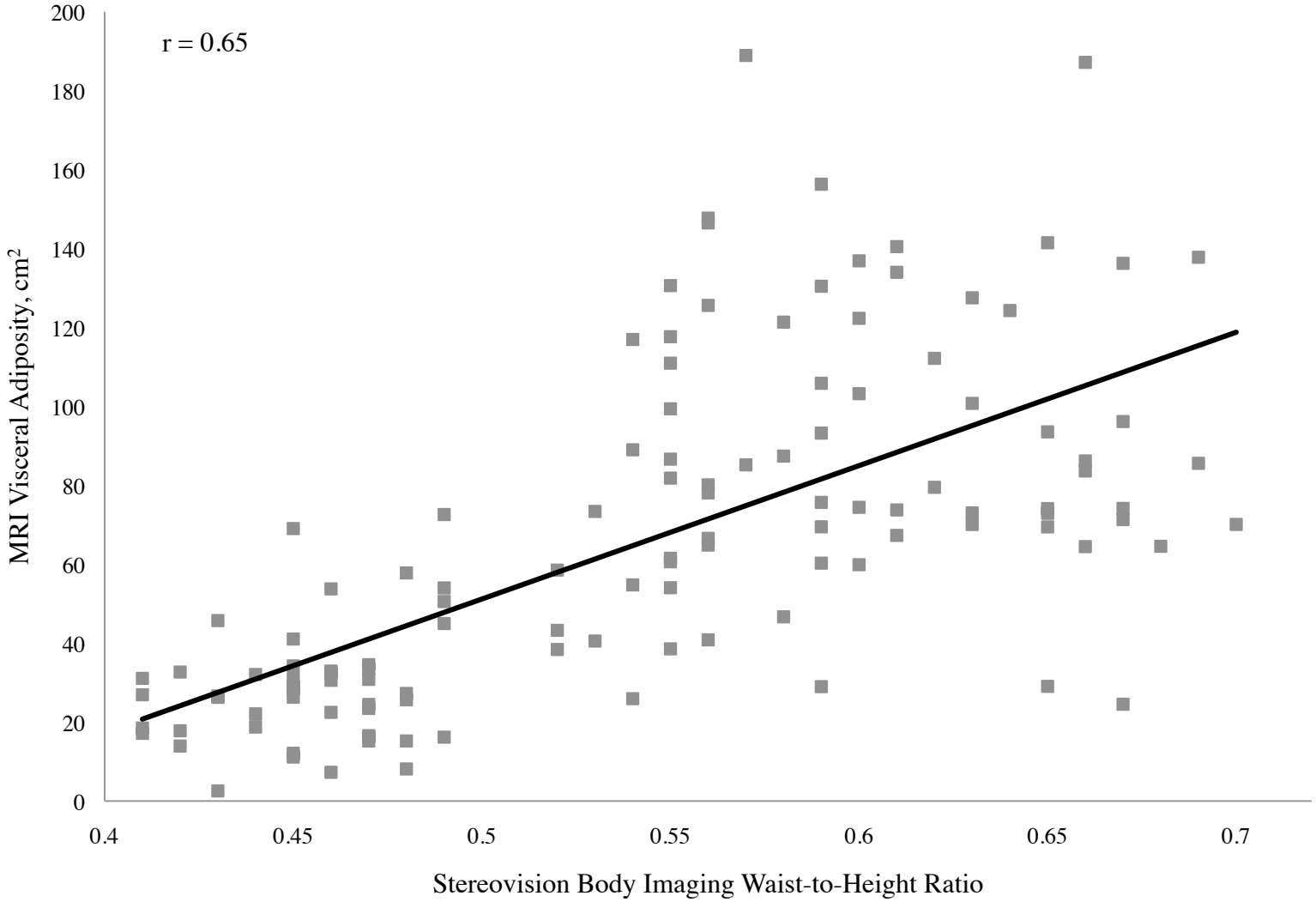
r = 0.65
MRI Visceral Adiposity, cm²
200
180
160
140
120
100
80
60
40
20
0
0.4
0.45
0.5
0.55
0.6
0.65
0.7
Stereovision Body Imaging Waist-to-Height Ratio

Mathematical Model for Predicting Subcutaneous Adiposity

The final equation for subcutaneous adiposity was selected from models developed by the combination method: subcutaneous adiposity volume (cm^2) = – 172.37 + 8.57 waist circumference (cm) – 62.65 sex (women=0, men=1) – 450.16 stereovision waist-to-hip ratio (**Table 2.4**). From a total of ten models (**Table 2.4**), this model contained the highest R^2 of 90.4%, with the lowest SEE of 40.85. The model developed by the stereovision imaging method had a lower R^2 of 79.3%, with the highest SEE of 59.65: subcutaneous adiposity volume (cm^2) = – 827.48 + 7.43 stereovision hip circumference (cm) + 7.02 central obesity width (cm). Thus, the optimal model for subcutaneous adiposity was a combination of demographic (sex), anthropometric (waist circumference), and SBI WHR (SBI waist-to-hip ratio) measurements.

Mathematical Model for Predicting Visceral Adiposity

The final multiple regression model for the prediction of visceral adiposity was best described by the utilization of stereovision and combination methods, which resulted in an identical model: visceral adiposity volume (cm^2) = – 96.76 + 11.48 central obesity depth (cm) – 5.09 central obesity width (cm) + 204.74 stereovision waist-to-hip ratio – 18.59 sex (women = 0, men = 1) (**Table 2.5**). The most important influences for prediction of visceral adiposity were central obesity depth, central obesity width, stereovision waist-to-hip ratio, and sex. The addition of traditional anthropometric measurements did not improve the variance, thus the model was identical. Note that with

the exception of sex, all variables included in the model were derived from the SBI system. Among 11 possible models (**Table 2.5**), the R^2 for the final model (R^2=71.7%) was significantly higher than the model derived from traditional anthropometric measurements (R^2=54.2%), and the SEE was only 22.97: visceral adiposity volume (cm^2) = – 214.28 + 306.03 waist-to-hip ratio + 5.78 sagittal diameter – 1.34 waist circumference (cm) (SEE=29.04).

The prediction equations were then applied to the validation group data and 95% confidence intervals were computed in order to check the cross-validity of the developed mathematical equations (**Tables 2.3, 2.4, 2.5**). All of the 95% confidence intervals included zero, which implies that the predicted abdominal adiposity (total, subcutaneous, and visceral abdominal adiposity) did not differ from the measured values of the abdominal adiposity at the level of 0.05. In addition, the mean error (ME) in **Tables 2.3, 2.4,** and **2.5** exhibit the differences between the observed values of abdominal adiposity measured by MRI and predicted values obtained by the mathematical equations.

The final prediction equation models for total abdominal, subcutaneous, and visceral adiposity are summarized in **Table 2.6**. All of the predictive models provided large effect sizes (larger than 0.35) due to the high R^2 values. Consequently, the observed power of abdominal adiposity equations among the given sample size ranged from 0.94 to 1. The optimal equation for predicting total abdominal adiposity was derived via traditional anthropometrics; whereas, subcutaneous and visceral adiposity were obtained by combination and stereovision imaging measurement methods, respectively.

Table 2.3. Regression coefficients for prediction of total abdominal adiposity by using traditional anthropometric, stereovision body imaging and combination measurement methods

Measurement Method	Eq[a]	Independent Variables							R^2 (%)	ME (CI)[b]
		Intercept	Waist[a]	Sex	SD[a]	COD[a]	sHip[a]	sWaist[a]		
Traditional[c, d]	1	– 509.05	– 8.38	–	–	–	–	–	80.1	– 21.09 (–79.56, 37.37)
	2	– 492.20	8.78	– 94.04	–	–	–	–	89.2	– 33.40 (– 91.64, 24.84)
	3[e]	– 470.28	7.10	– 91.01	5.74	–	–	–	89.9	– 32.04 (– 90.70, 26.61)
Stereovision Body Imaging[f]	4	– 237.02	–	–	–	33.88	–	–	72.2	– 39.32 (– 99.96, 21.31)
	5	– 708.42	–	–	–	19.99	6.36	–	81.8	– 50.28 (– 112.88, 12.32)
	6	– 612.78	–	– 36.73	–	22.63	5.29	–	82.9	– 53.33 (– 116.07, 9.41)
	7[e]	– 645.08	–	– 61.37	–	12.97	3.79	3.89	84.2	– 49.36 (– 111.03, 12.30)

Table 2.3 (continued)

Combination[g]	8	– 509.05	– 8.38	–	–	–	–	–	80.1	– 21.09 (– 79.56, 37.37)
	9	– 492.20	8.78	– 94.04	–	–	–	–	89.2	– 33.40 (– 91.64, 24.84)
	10[e]	– 470.28	7.10	– 91.01	5.74	–	–	–	89.9	– 32.04 (– 90.70, 26.61)

[a] Eq, equation; Waist, waist circumference; SD, sagittal diameter; COD, central obesity depth; sHip, stereovision body imaging hip circumference; sWaist, stereovision body imaging waist circumference

[b] Mean error = observed – predicted (confidence interval)

[c] Manual

[d] Independent variables include sex, waist circumference, waist-to-hip ratio, sagittal diameter

Table 2.4. Regression coefficients for prediction of subcutaneous adiposity by using traditional anthropometric, stereovision body imaging and combination measurement methods

Measurement Method	Eq[a]	Independent Variables							R^2 (%)	ME (CI)[b]
		Intercept	Waist[a]	Sex	WHR[a]	sHip[a]	COW[a]	sWHR[a]		
Traditional[c, d]	1	– 425.91	6.81	–	–	–	–	–	72.8	– 20.22 (– 67.38, 26.93)
	2	– 408.19	7.23	– 98.81	–	–	–	–	86.8	– 33.20 (– 80.70, 14.30)
	3[e]	– 204.92	8.82	– 86.07	– 409.19	–	–	–	88.6	– 35.86 (– 83.92, 12.21)
Stereovision Body Imaging[f]	4	– 877.72	–	–	–	10.17	–	–	76.5	– 49.07 (– 100.10, 1.97)
	5[e]	– 827.48	–	–	–	7.43	7.02	–	79.3	– 47.76 (– 99.18, 3.66)
Combination[g]	6	– 877.72	–	–	–	10.17	–	–	76.5	– 49.07 (– 100.10, 1.97)
	7	– 769.53	3.37	–	–	6.21	–	–	82.7	– 38.15 (– 87.87, 11.58)

Table 2.4 (continued)

8	– 566.98	5.59	– 76.30	–	2.80	–	–	88.1	– 38.36 (– 86.96, 10.24)
9	– 96.94	9.21	– 64.91	–	– 0.83	–	– 504.72	90.5	– 33.88 (– 81.38, 13.61)
10[e]	– 172.37	8.57	– 62.65	–	–	–	– 450.16	90.4	– 35.17 (– 83.00, 12.66)

[a] Eq, equation; Waist, waist circumference; WHR, waist-to-hip ratio; sHip, stereovision body imaging hip circumference; COW, central obesity width; sWHR, stereovision body imaging waist-to-hip ratio

[b] Mean error = observed – predicted (confidence interval)

[c] Manual

[d] Independent variables include sex, waist circumference, waist-to-hip ratio, sagittal diameter

[e] Recommended model by stepwise multiple regression analysis

[f] Independent variables include sex, stereovision body imaging waist circumference, stereovision body imaging hip circumferences, stereovision body imaging waist-to-hip ratio, central obesity depth, central obesity width

[g] Independent variables include sex, waist circumference, waist-to-hip ratio, sagittal diameter, stereovision body imaging waist circumference, stereovision body imaging hip circumferences, stereovision body imaging waist-to-hip ratio, central obesity depth, central obesity width

Table 2.5. Regression coefficients for prediction of visceral adiposity by using traditional anthropometric, stereovision body imaging and combination measurement methods

Measurement Method	Eq[a]	Independent Variables								R^2 (%)	ME (CI)[b]
		Intercept	WHR[a]	SD[a]	Waist[a]	COD[a]	COW[a]	sWHR[a]	Sex		
Traditional[c,d]	1	– 245.98	352.89	–	–	–	–	–	–	44.4	2.93 (– 13.04, 18.89)
	2	– 192.17	211.14	3.02	–	–	–	–	–	51.1	1.77 (– 14.35, 17.90)
	3[e]	– 214.28	306.03	5.78	– 1.34	–	–	–	–	54.2	3.29 (– 12.98, 19.56)
Stereovision Body Imaging[f]	4	– 57.33	–	–	–	7.99	–	–	–	52.3	– 5.36 (– 22.14, 11.43)
	5	41.65	–	–	–	15.62	– 6.20	–	–	66.0	– 3.91 (– 21.63, 13.80)
	6	– 55.72	–	–	–	12.23	– 4.84	119.89	–	68.9	– 1.84 (–19.89, 16.22)
	7[e]	– 96.76	–	–	–	11.48	– 5.09	204.74	– 18.59	71.7	– 2.00 (– 20.36, 16.37)

Table 2.5 (continued)

Combination[g]	8	– 57.33	–	–	–	7.99	–	–	–	52.3	– 5.36 (– 22.14, 11.43)
	9	41.65	–	–	–	15.62	– 6.20	–	–	66.0	– 3.91 (– 21.63, 13.80)
	10	– 55.72	–	–	–	12.23	– 4.84	119.89	–	68.9	– 1.84 (–19.89, 16.22)
	11[e]	– 96.76	–	–	–	11.48	– 5.09	204.74	– 18.59	71.7	– 2.00 (– 20.36, 16.37)

[a] Eq, equation; WHR, waist-to-hip ratio; SD, sagittal diameter; Waist, waist circumference; COD, central obesity depth; COW, central obesity width; sWHR, stereovision body imaging waist-to-hip ratio

[b] Mean error = observed – predicted (confidence interval)

[c] Manual

[d] Independent variables include sex, waist circumference, waist-to-hip ratio, sagittal diameter

[e] Recommended model by stepwise multiple regression analysis

[f] Independent variables include sex, stereovision body imaging waist circumference, stereovision body imaging hip circumferences, stereovision body imaging waist-to-hip ratio, central obesity depth, central obesity width

[g] Independent variables include sex, waist circumference, waist-to-hip ratio, sagittal diameter, stereovision body imaging waist circumference, stereovision body imaging hip circumferences, stereovision body imaging waist-to-hip ratio, central obesity depth, central obesity width

Table 2.6. Final prediction equations for total abdominal, subcutaneous and visceral adiposity volumes by using demographic, traditional anthropometric, stereovision body imaging and magnetic resonance imaging measurements

Adiposity Volume[a]	Measurement Method	Predictive Models	R^2 (%)
Total abdominal	Traditional[b, c, d]	– 470.28 + 7.10 Waist[e] – 91.01 Sex + 5.74 SD[e]	89.9
	Stereovision[f]	– 645.08 + 12.97 COD[e] + 3.79 sHip[e] – 61.37 Sex + 3.89 sWaist[e]	84.2
	Combination[g]	– 470.28 + 7.10 Waist[e] – 91.01 Sex + 5.74 SD[e]	89.9
Subcutaneous	Traditional[b, c]	– 204.92 + 8.82 Waist[e] – 86.07 Sex – 409.19 WHR[e]	88.6
	Stereovision[f]	– 827.48 + 7.43 sHip[e] + 7.02 COW[e]	79.3
	Combination[d, g]	– 172.37 + 8.57 Waist[e] – 62.65 Sex – 450.16 sWHR[e]	90.4
Visceral	Traditional[b, c]	– 214.28 + 306.03 WHR[e] + 5.78 SD[e] – 1.34 Waist	54.2
	Stereovision[d, f]	– 96.76 + 11.48 COD[e] – 5.09 COW[e] + 204.74 sWHR[e] – 18.59 Sex	71.7
	Combination[g]	– 96.76 + 11.48 COD[e] – 5.09 COW[e] + 204.74 sWHR[e] – 18.59 Sex	71.7

[a] Dependent variable measured by magnetic resonance imaging

[b] Manual

[c] Independent variables include sex, waist circumference, waist-to-hip ratio, sagittal diameter

[d] Optimal model for predicting central obesity by stepwise multiple regression analysis

[e] Waist, waist circumference; SD, sagittal diameter; COD, central obesity depth; sHip, stereovision body imaging hip circumference; sWaist, stereovision body imaging waist circumference; WHR, waist-to-hip ratio; COW, central obesity width; sWHR, stereovision body imaging waist-to-hip ratio

[f] Independent variables include sex, stereovision body imaging waist circumference, stereovision body imaging hip circumferences, stereovision body imaging waist-to-hip ratio, central obesity depth, central obesity width

[g] Independent variables include sex, waist circumference, waist-to-hip ratio, sagittal diameter, stereovision body imaging waist circumference, stereovision body imaging hip circumferences, stereovision body imaging waist-to-hip ratio, central obesity depth, central obesity width

Discussion

The current research is the first to develop mathematical equations for predicting abdominal adiposity by utilizing combined parameters derived from demographics, traditional anthropometric measurements, and measurements obtained by SBI. The results suggest that the body measurements derived from SBI improve the prediction of visceral adiposity volume. The R^2 in this study for prediction of visceral adiposity (71.7%) is lower than that found for both total abdomen (89.9%) and subcutaneous (90.4%) adiposity. Clearly, visceral adiposity is more difficult to measure without advanced instruments, such as MRI or CT that are stationary and expensive. In this study, predictive equations for total abdominal, subcutaneous, and visceral adiposity were created using measurements obtained from traditional anthropometrics, SBI parameters, and combinations. The most optimal result for the prediction of total abdominal adiposity was produced by traditional manual anthropometrics; for subcutaneous adiposity, a combination method was better. For visceral adiposity, the method of stereovision body imaging yielded the best results. These results were presumably due to the incorporation of new parameters of central obesity measured via the SBI system. Central obesity depth showed the highest correlation with visceral adiposity, as compared to other body measurements (demographics, traditional anthropometrics, and SBI variables). Moreover, measurements by SBI alone were not improved by adding traditional manual parameters since the SBI measurements were more strongly associated with visceral adiposity. In addition, central obesity depth, central obesity width, SBI waist-to-hip ratio and sex

appeared to contribute significantly to predict visceral adiposity.

Studies have shown that visceral adiposity is related to pathologies that include metabolic syndrome (71, 82), insulin resistance (84), and cardiovascular disease (158). While subcutaneous adiposity is a better indicator of metabolic syndrome in a specific population (159), visceral adiposity may have greater implications in terms of clinical health than subcutaneous adiposity (71, 74, 84).

A study by Goel (2008) developed prediction equations for total abdominal, subcutaneous, and visceral adiposity that included traditional anthropometric measurements as independent variables and abdominal adiposities, as measured by MRI, as a dependent variable (156). These prediction models explained 65%, 67.1% and 52.1% of the variances for total abdominal, subcutaneous, visceral adiposity volume, respectively. These values were somewhat lower than those obtained in the present research (89.9%, 90.4%, and 71.7%) for total abdominal, subcutaneous, and visceral adiposity volume.

Brundavani et al. (2006) also utilized MRI for the assessment of central obesity and developed prediction equations for visceral adiposity for men and women (160). The final prediction equations for men included weight, waist circumference and BMI as independent variables, and weight and waist circumference for women. The R^2 for visceral adiposity was higher for men (74%) than for women (63%) in the prediction equation. These values are similar to the results of the present study, in that the R^2 for men and women combined was 71.7%, and sex was included as a fourth independent

variable in the prediction equation for visceral adiposity. Moreover, sex was included in the prediction equations by Goel et al. (2008) (156). Collectively, these results imply that sex is a significant factor in order to predict visceral adiposity, as differences exist in fat distribution and accumulation between men and women. Previous studies reported that women have more subcutaneous adiposity compared to men (26); whereas, men have more visceral adiposity as opposed to women (161).

Janssen et al. (2002) developed prediction equations via multiple regression analysis (16). BMI and waist circumference were included as independent variables and MRI measured subcutaneous and visceral adiposity as dependent variables. Their model described 57% of visceral adiposity for men and 76% for women when BMI was added to the model as a first variable, and waist circumferences as a second variable. Waist circumference explained 49% of subcutaneous adiposity and 55% of visceral adiposity for men, and 52% of subcutaneous adiposity and 76% of visceral adiposity for women. The BMI explained 72% of subcutaneous adiposity and 46% of visceral adiposity for men and 53% of subcutaneous adiposity and 60% of visceral adiposity for women. These results suggest that BMI had a greater influence than waist circumference in describing the variance for subcutaneous adiposity; whereas, waist circumference was superior to BMI in the prediction of visceral adiposity volume.

Waist circumference was observed to be the most optimal variable for predicting subcutaneous adiposity in the equation model. In contrast to the study conducted by Janssen et al. (2002), BMI was not included as a predictor variable in either the

subcutaneous or visceral adiposity models (16). In addition, body measurements, such as central obesity depth and central obesity width, rather than waist circumference, were more precise components for predicting visceral adiposity. These results imply that variables derived from stereovision imaging were stronger predictors than waist circumference or BMI for predicting visceral adiposity.

The above mentioned studies utilized MRI for assessment of central obesity; other studies examined the use of CT to quantify abdominal adiposity (155, 162). Stanforth et al. (2004) compared prediction equations for visceral adiposity by using two different methods for men and women (155). A CT technique incorporated subcutaneous adiposity, sagittal diameter, age, and ethnicity as independent variables. The traditional anthropometric method utilized BMI, waist-to-hip ratio, waist circumference, age and ethnicity as independent variables. The R^2 for the CT method was 84% for men and 75% for women, with a R^2 of 78% for men and 73% for women for anthropometrics. These R^2 values are higher than the prediction value of the current study (71.7%), which includes both men and women. Since Wajchenberg et al. (2000) denoted that MRI showed lower reproducibility for measuring total and visceral adiposity, as opposed to CT (72), this suggests that CT may be slightly more precise. But the usage of CT is limited by radiation exposure and lack of portability.

Other prediction equations for visceral adiposity measured by CT were created in a Japanese adult population (n=112) (162). This model incorporated sex, age, waist-to-hip ratio, and internal fat mass (determined by DXA) as independent variables reported a

R^2 of 74.5%. In addition, a prediction equation for visceral adiposity with the components of sex, age, waist-to-hip ratio, and internal fat mass (measured by BIA) resulted in a similar R^2 of 77.3%. These two models utilizing DXA and BIA measures as independent variables produced slightly higher variances than did the measurements by the stereovision imaging system (71.7%).

CT and MRI derived measurements of subcutaneous and visceral adiposity were compared in previous studies (163, 164). Total and subcutaneous adiposity were overestimated when using CT compared to MRI, but not for visceral adiposity (163). Whereas, Seidell et al. have shown that subcutaneous adipose volume measured by CT and MRI did not differ statistically, but volume did significantly differ for visceral adiposity (164). Collectively, these studies suggest that the prediction equation for abdominal adiposity developed by CT-measured and MRI-measured may exhibit a disparity due to the error variances in the measurements of abdominal adiposity volumes.

A variety of 3-D body scanners have been validated for accuracy in measurement of waist and hip circumferences against manual tape measurements. Pepper et al. (2010) reported that correlations between waist and hip circumferences measured by 3-D laser body scanner and by tape were 0.998 and 0.989, respectively (165). Previously, Wells et al. (2007) found similar results via a 3-D photonic scanner (Textile and Clothing Technology Corporation, $[TC]^2$), with correlation efficients of 0.96 for waist circumference and 0.97 for hip circumference (142). Similarly, Zwane et al. (2010) observed hip circumference obtained from a 3D photonic scanner ($[TC]^2$) and tape

measurement were not statistically in the range of European size of 34 to 44 (157). In spite of the accuracy of the body measurements derived from body scanners, these body measurements have not been utilized to predict the quantity of abdominal adiposity.

Postmenopausal women have a higher amount of visceral adiposity, when compared to premenopausal women, which indicates that menopausal status or age could be a potential variable for predicting abdominal adiposity (166). However, age was excluded initially in the data analysis when other independent variables exhibited higher correlations with central obesity. The ineffectual correlation between age and abdominal adiposity compared to other variables could be explained by a lack of the power to detect the significance, since the age distribution among participants was evenly distributed and only 5.7% of the participants consisted of women over 50 years old. In addition, information on menopausal status was not available for this data set. Future research incorporating a higher percentage of elderly women could determine if the age of a woman or menopausal status has an impact on prediction of abdominal adiposity.

Thigh circumference has been suggested to be a significant variable for prediction of central obesity because this measure is inversely related to blood glucose, a parameter of risk for type 2 diabetes (167). Wells et al. (2008) demonstrated that waist adjusted for thigh girth ratio measured by photonic scanner linearly increased across BMI categories (143). However, in the prediction equation in the present study, both SBI thigh circumference and waist-to-thigh ratio were excluded due to non-significance.

Waist-to-height ratio (WHtR) also provides a mean for detecting abdominal

obesity and related health risks. Ashwell et al. (2011) reported that WHtR was a better predictor than waist circumference or BMI, in terms of monitoring cardiometabolic risk (90). Parikh et al. (2007) confirmed that WHtR serves as an index of central obesity and it was more effective in defining metabolic syndrome than waist circumference (168).

In this study, traditional and stereovision waist-to-height ratio exhibited high correlations with total abdominal, subcutaneous, and visceral adiposity. However, the former were excluded in the prediction model because other independent variables had stronger correlations with abdominal adiposity volumes. In addition, multicollinearity existed between independent variables that influenced the waist-to-height ratio, resulting in an exclusion from the prediction model. For example, in the creation of the visceral adiposity prediction model, waist-to-height ratio had a high correlation with central obesity depth ($r=0.89$, $p<0.001$). Yet, a substantial amount of visceral adiposity is explained by central obesity depth; thus, the waist-to-height ratio, which explains a similar portion of visceral adiposity, was excluded in the model. Then other variables were examined by the process of stepwise multiple regression analysis in order to ascertain whether they should be included in the model. For the total abdominal and subcutaneous models, waist-to-height ratio was excluded again, despite having the highest correlation with the adiposity volumes, because of the removal test in the stepwise multiple regression analysis. In this test, the least useful independent variable is removed from the equation when each variable is included in the equation.

The current research observed that body ratios (including waist-to-height ratio and

waist-to-thigh ratio) were not significant factors in the prediction of visceral adiposity, except for waist-to-hip ratio. The waist-to-hip ratio obtained via SBI was the third strongest predictor in the equation for subcutaneous and visceral adiposity. However, central obesity depth and central obesity width as measured by SBI were superior predictors for visceral adiposity, as compared to SBI waist-to-hip ratio.

In summary, the prediction equations for abdominal adiposity volumes were compared using traditional anthropometrics, SBI or a combination of both. For total and subcutaneous adiposity, traditional methods were just as effective as for SBI. However, for visceral adiposity, the most critical measure for assessing health risk, SBI provided a more optimal prediction model. Since the SBI system is inexpensive and non-invasive, it has potential for assessment of visceral adiposity in a field setting where CT or DXA are not available.

CHAPTER 3: EFFICACY OF THIGH VOLUME RATIOS ASSESSED VIA STEREOVISION BODY IMAGING AS A PREDICTOR OF VISCERAL ADIPOSITY MEASURED BY MAGNETIC RESONANCE IMAGING

Abstract

Central obesity, especially excessive accumulation of visceral adiposity, is a public health concern because it is associated with cardiovascular disease and type 2 diabetes. Assessment of this type of obesity via regional body volumes or proportions may be more crucial than overall adiposity, in terms of the clinical consequences. The purpose of this research was to explore the efficacy of regional volumes of thigh ratios assessed by stereovision body imaging (SBI) as a predictor of visceral adiposity, as measured by magnetic resonance imaging. Body measurements obtained via SBI also were utilized to explore the disparities of body size and shape in men and women and the risks associated with accumulation of visceral adiposity. A total of 121 adults were measured for total and regional body volumes, as well as volume ratios. Irrespective of body bass index (BMI) classification, men exhibited greater total body (80.95 L vs. 72.41 L), torso (39.26 L vs. 34.13 L), and abdomen-hip (29.01 L vs. 25.85 L) volumes, and waist circumference (95.21 cm vs. 88.46 cm) than women. Women had higher thigh volumes (4.93 L vs. 3.99 L), hip circumference (112.56 cm vs. 106.68 cm), and lower body-volume ratios [thigh to total body (0.07 vs. 0.05), thigh to torso (0.15 vs. 0.11), and thigh to abdomen-hip (0.20 vs. 0.15); $p<0.05$]. Thigh volume in relation to torso [odds

ratios (OR) 0.44] and abdomen-hip (OR 0.41) volumes were negatively associated with increased risks of a greater visceral adiposity deposition, even after controlling for age, sex, and BMI ($p<0.05$). The three-dimensional (3D) SBI provided an excellent method for determining body size and shape in men and women, and confirmed that women are more prone to exhibit a gynoid body shape as shown by greater lower-body volume ratios. In contrast, men are more likely to exhibit an android body type. The unique parameters of the volume of thigh, in relation to torso and abdomen-hip volumes, by SBI was highly effective in predicting visceral adiposity.

Introduction

Obesity is a significant public health concern associated with hypertension, dyslipidemia, coronary heart disease, and type 2 diabetes (1-4). In the United States, approximately one-third of the population is overweight (33.3%) and one-third is obese (34.9%) (8). At present, body mass index (BMI) is the most commonly used technique to assess obesity in populations due to its simplicity. Yet, this method is crude, in that body weight and height only estimate overall obesity, without consideration of the distribution of body fat (169).

Generally, fat depots are classified as visceral and subcutaneous adiposity (74). Within the abdominal area, visceral adiposity is the more metabolically active depot due to its associations with escalated risks of cardiovascular disease, diabetes, and metabolic syndrome; whereas, subcutaneous adiposity is linked with lower health risks (71, 74, 82,

84, 170). Since visceral adiposity is more of a primary concern than is subcutaneous, this research explored the relationships between visceral adiposity determined by magnetic resonance imaging (MRI) and body volume measurements estimated by three-dimensional (3D) stereovision body imaging (SBI).

Lower body factors (thigh circumference, thigh fat, leg fat, leg to trunk fat ratio, sagittal abdominal diameter to thigh circumference ratio) have been shown previously to have favorable effects on normal insulin and glucose levels (118-121), metabolic dysfunction (122-124), and risks of cardiovascular disease (123, 125, 126). Higher values of lower body factors have been suggested to exhibit protective effects on health risks associated with obesity-related diseases (121, 123, 124). It is predicted that lower body components, such as thigh volume in relation to total body, trunk, or abdomen-hip would be linked negatively with the accumulation of visceral adiposity.

To date, instruments that measure regional adiposity, such as dual-energy x-ray absorptiometry (DXA), computed tomography (CT), and MRI, are restricted in field settings due to their bulkiness, cost, and/or radiation exposure. An innovation of this research is the use of a 3D SBI system to collect body measurements in a rapid and inexpensive manner. This device provides a visual presentation of human body shape and size, including volumes of total body, torso (neck to umbilicus), abdomen-hip (umbilicus to crotch) and thigh (crotch to top of knee) (**Figure 3.1**). Previously, body volume measured via this system showed strong agreement with air displacement plethysmography (ADP) (R^2>0.99, p<0.01). No significant differences were found

between these methods (mean difference -0.17, $p>0.05$), indicating the preciseness of this technique (138). Also, measurements were highly reproducible, with intraclass correlation coefficient and coefficient of variation values lower than 0.99 and 1.9, respectively (138). In the present research, unique body volume measurements derived via SBI were utilized to assess the association with visceral adiposity.

Stereotypically, men accumulate more fat in the abdominal region, which is characterized by an android or apple shape; whereas, women have greater fat depots in the gluteal-femoral area, and exhibit a gynoid or pear-shaped body type (115, 171). Thus, men and women were assessed by SBI to document precise disparities in their body size and shape. Because central fat depots increase with age, especially for women with postmenopausal status (166, 172-174), demographics were taken into account for the examination of possible relationships between body volume measurements and obesity measures.

Method and Procedures

Design of Study

A total of 121 Caucasian and non-White Hispanic men (n=67) and women (n=54) made two visits to the The University of Texas at Austin SBI laboratory and the MRI Imaging Research Center. Subjects were instructed to fast for 4 hours prior to the visit and avoid excessive perspiration, heavy exercise, and caffeine or alcohol for 10 hours.

Demographic and health history questionnaires were administered at visit 1. Participants were measured for body size and shape by anthropometrics, including height, weight by a scale and a stadiometer; body circumferences (arm, waist, hip, thigh) by SBI; and total percent body fat by ADP within 3 hours. Ten body imaging scans of 200 milliseconds each were performed via SBI to assess body composition, such as body circumferences, total, and regional body volumes. At visit 2, MRI scans of the abdominal area were obtained for central obesity assessment within 5 days of the anthropometric measurements.

Subjects

Healthy Caucasian and non-White Hispanic men and women, aged 18 to 65 years with a BMI range of 18.5 to 40 kg/m^2 were recruited via notices posted online and on bulletin boards, and through word-of-mouth. Prescreening over the phone was performed before the first study visit. Criteria for exclusions were metallic/electronic implants or heavy metal ink tattoos, having known diseases, or being pregnant or breastfeeding. The risks and benefits of the study were explained and informed consents were obtained. The University of Texas at Austin Institutional Review Board approved this study.

Anthropometrics

Participants were measured for weight and height, wearing light clothing and barefoot, by an electronic scale (Tanita, Arlington, IL) to the nearest 0.1 kg and a

Figure 3.1. Total and regional body volumes according to BMI classification assessed by a stereovision body imaging system. Left to right: front of total body volume, back of total body volume, front of torso and thigh volums, front of abdomen-hip and thigh volumes, and back of abdomen-hip and thigh volumes.

(a) Men, BMI 20.2 kg/m^2, healthy weight

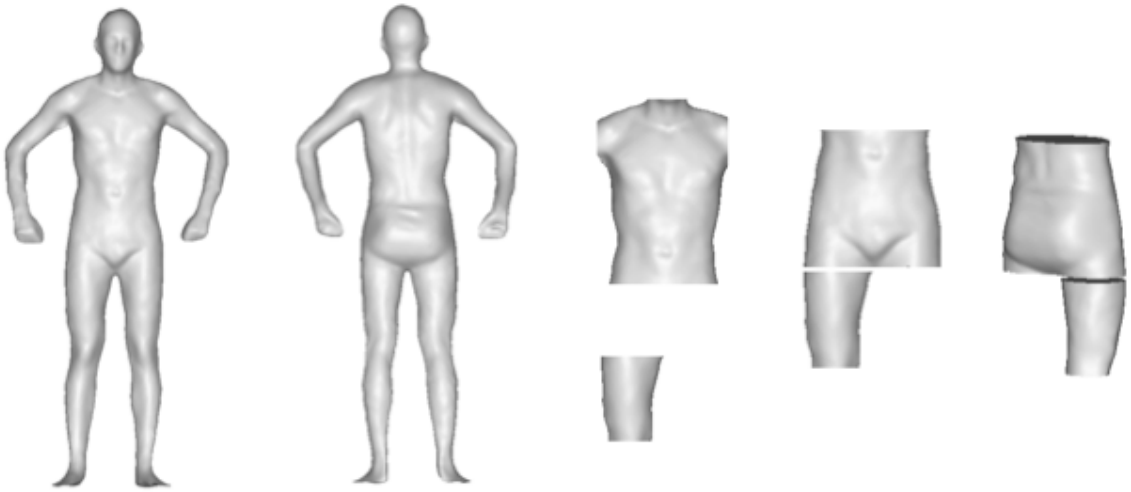

(b) Men, BMI 25.6 kg/m^2, Overweight

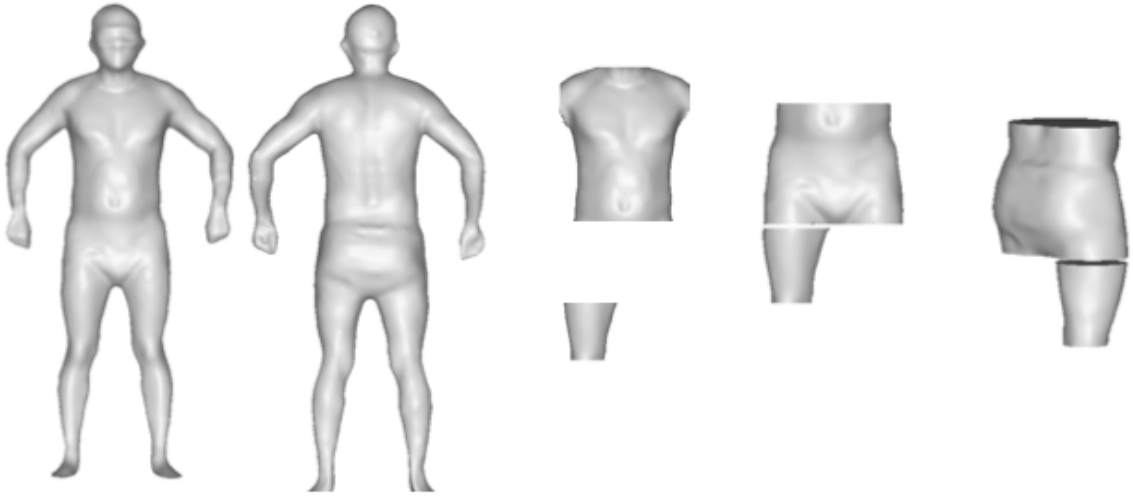

(c) Men, BMI 30.8 kg/m^2, obese class I

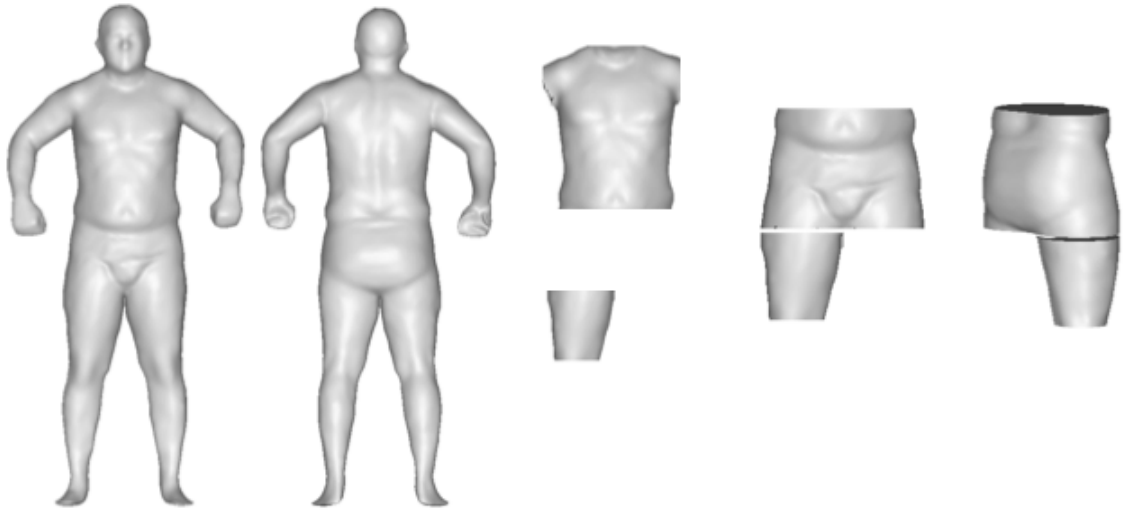

(d) Men, BMI 40.3 kg/m^2, obese class II

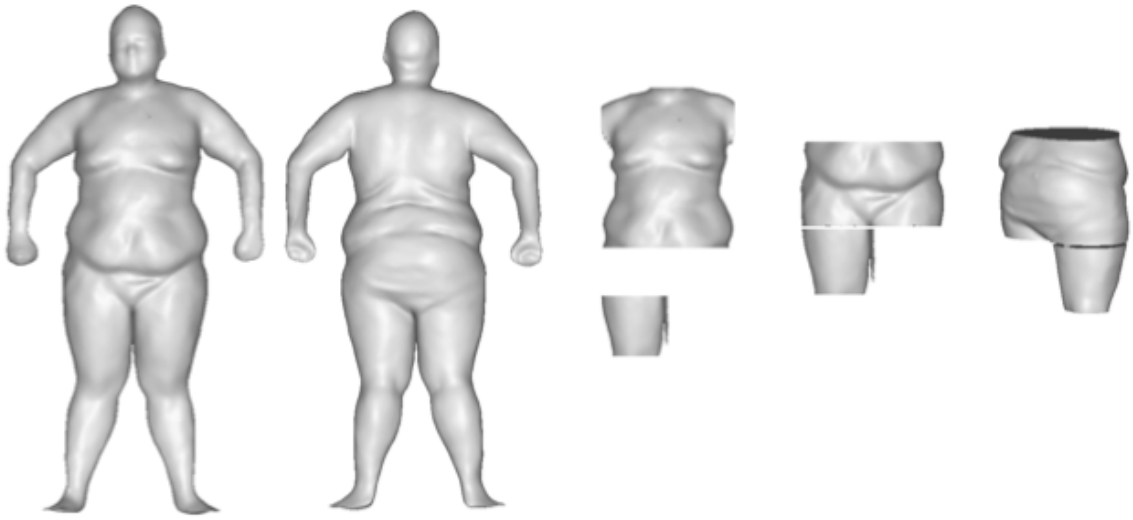

(e) Women, BMI 18.9 kg/m^2, healthy weight

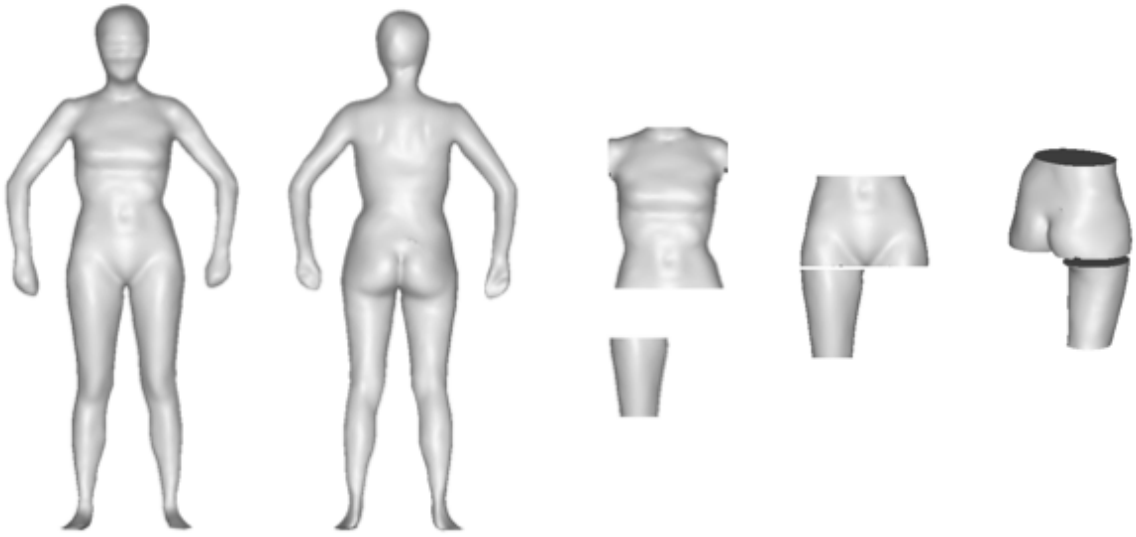

(f) Women, BMI 25.2 kg/m^2, overweight

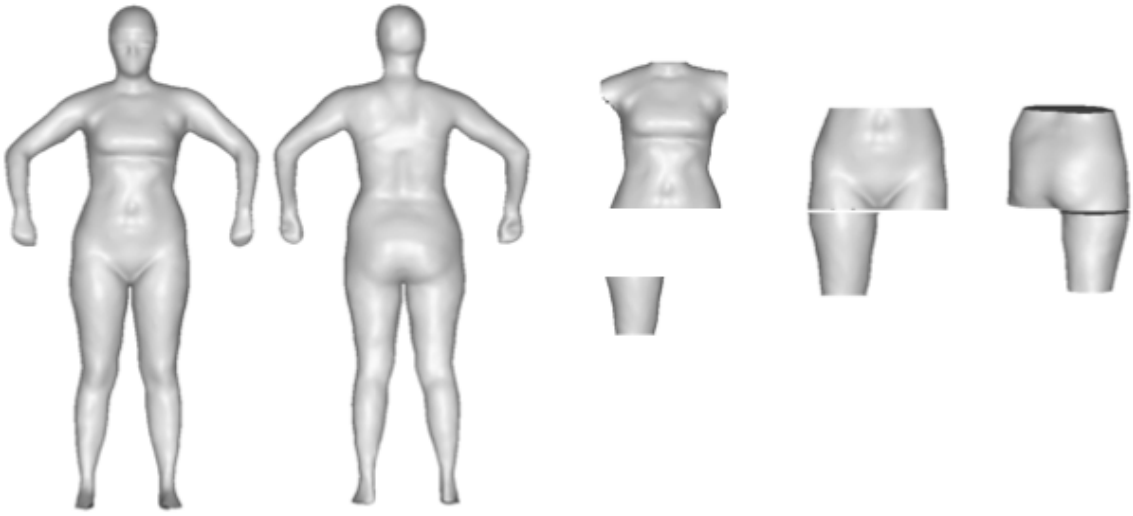

(e) Women, BMI 30.0 kg/m^2, obese class I

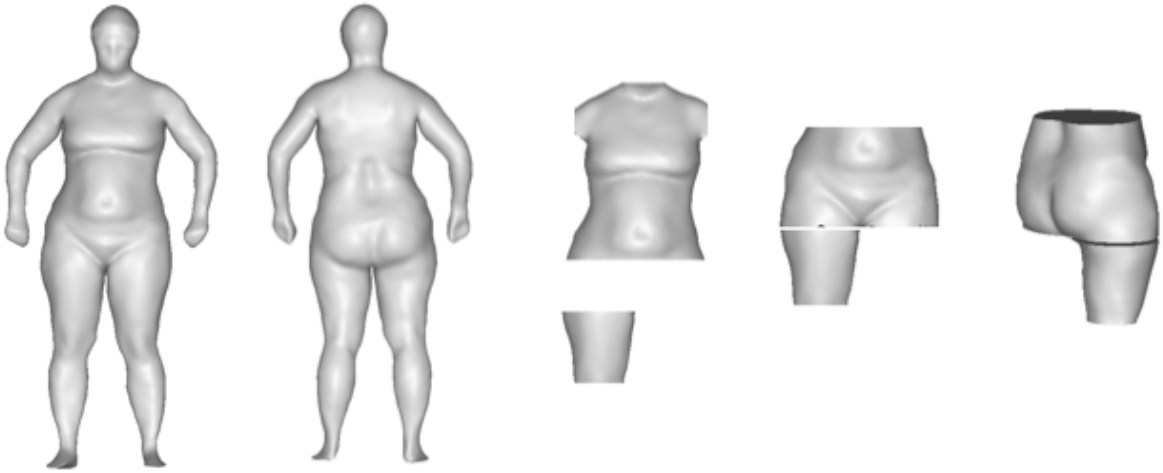

(f) Women, BMI 40.1 kg/m^2, obese class II

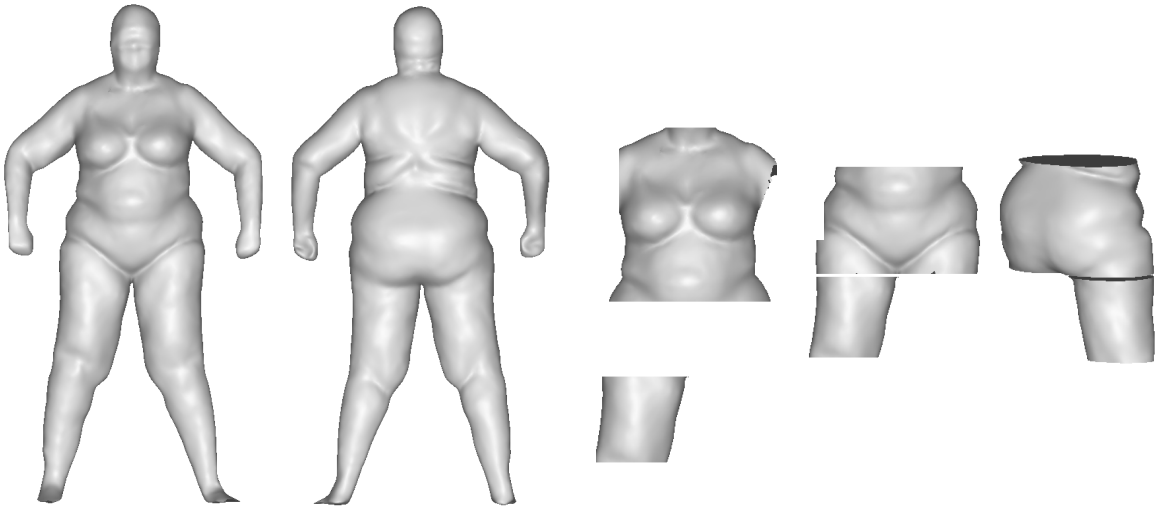

stadiometer (Health o meter, South Shelton, CT) to the nearest 0.1 cm, respectively. BMI was calculated as weight in kg divided by height in m^2 and classified as healthy weight (18.5-24.9 kg/m^2), overweight (25-29.9 kg/m^2), obese class I (30-34.9 kg/m^2), or obese class II (35-40 kg/m^2). A MyoTape body tape (AccuFitness, Greenwood Village, CO) measured body circumferences (arm, waist, hip, and thigh). Anthropometric assessments followed standard protocols for anthropometric measurements (175).

System of Stereovision Body Imaging

A 3D SBI measured body size and shape of the participants (138, 149). Subjects were instructed to wear minimal tight underwear and a swimming cap during the assessment. A blindfold was provided to protect the subjects' eyes from the bright light emanating from the projectors. During acquisition, participants posed with their legs slightly spread and arms extended from the torso while holding their breath for one second. A total of ten body scans of 200 milliseconds each was completed for the subjects. Detailed information regarding the instrument was previously reported by Xu et al. (2009) (138) and Lee et al. (2014) (149).

Body volume measurements assessed via SBI included total body, torso (neck to crotch), abdomen-hip (smallest point of waist to crotch) and thigh (crotch to mid-thigh). **Figure 3.1** shows the body image and regional body volumes assessed by SBI according to BMI classification. Subsequently, body volume ratios that reflect upper (torso/total body, abdomen-hip/total body, abdomen-hip/torso) and lower body volume ratios

(thigh/total body, thigh/torso, thigh/abdomen-hip) were computed. Body circumferences including shoulder, chest, abdomen, waist, hip, crotch, upper thigh, lower thigh, knee, and calf were assessed as well. A stereovision body imaging waist-to-hip ratio measurement was computed by waist circumferences (cm) divided by hip circumferences (cm).

Magnetic Resonance Imaging

The evaluation of abdominal adiposity volumes was performed using FDA-approved pulse sequences via a MRI 3.0 T General Electric scanner (GE Healthcare, Milwaukee, WI) by a certified MR technician. A 3-plane localizer scan was performed while centering the iliac crest after the subject was positioned on the magnet. A coronal slice was obtained as TR 140, TE 2.1, flip angle 80°, slice thickness 8.0 mm with gap 5.0 mm, FOV 40 x 40, matrix 512 x 93, and bandwidth 62.5 kHz, while centering at the navel. The coronal slice was analyzed for assessment of subcutaneous and visceral adiposity volume via SliceOmatic 4.3 (Tomovision, Montreal, CAN). Total abdominal adiposity was computed by adding the volumes of subcutaneous and visceral adiposity. Operation of the MRI scanner and maintenance of all the safety elements were performed only by imaging research center approved personnel.

Air Displacement Plethysmography

Percent fat mass and fat-free mass were calculated from body mass, density, and

volume, as determined by a BOD POD® body composition tracking system (Life Measurement System, Concord, CA). Participants were instructed to wear minimum clothing and cover their hair with a swimming cap to reduce error variance. Weights were measured by electronic scale and subjects were seated inside the sealed chamber. Under the isothermal conditions, body density was estimated via variations in pressure and body volume. The breathing circuit system measured thoracic gas volume while subjects breathed normally. Five prediction equations (Siri, Schtte, Ortiz, Brozek, Lohman) were available in the BOD POD® software in order to accurately measure body fat percentage for different populations, including the general population (44), African American males (47), African American females (46), lean and obese individuals (56) and children aged under 17 years old (45). These prediction equations were based on measurements of body volume and body mass to estimate fat and fat-free mass.

Analysis of Statistics

Statistical analyses were performed independently in men and women due to the sex differences in total and regional fat distribution. The normality of the distributions of the variables was examined by the Kolmogorov-Smimov test (176). Overall characteristics of the participants were described as mean and standard error of the mean. A one-way analysis of variance (ANOVA) was used to detect mean differences between different sex and BMI groups for demographic parameters and body measurements assessed via traditional anthropometrics, SBI, MRI, and ADP. When the results of

ANOVA were significant, pairwise comparisons detected where the differences might fall by post hoc analysis of Bonferroni correction. A univariate general linear model analysis also was conducted to explore disparities of total/regional body volumes and body volume ratio parameters among different sex and BMI groups. Line graphs were created to visually examine the associations between body volume parameters and BMI classification (healthy weight, overweight, obese class I and II).

Age-adjusted partial Pearson's correlation coefficients were used to describe the relationships between total/regional body volumes (torso, abdomen-hip, thigh) and upper/lower volume ratios with a) overall obesity measures (BMI, percent body fat); and b) central obesity parameters (subcutaneous and visceral adiposity). Scatter plots depicting the R^2 line of best fit were created to investigate linear associations between body fat percentage measured by ADP and total/regional body volumes determined via SBI, as well as visceral abdominal adiposity volume assessed by MRI and body volume ratios acquired by SBI, according to BMI classification.

The odds ratios (OR) were computed via multinomial logistic regression analysis to predict of the risks of being in the low tertile of visceral fat volume versus middle or high, with one standard deviation increases in total/regional body volume parameters. Analyses were preceded with unadjusted (model 1); adjusted for age and sex (model 2); and adjusted for age, sex, and BMI group (model 3) models in order to accurately explore risks involved while taking age, sex, and BMI into account. Total and regional body volume parameters were converted into Z-scores to compare the study results. The Z-

score was computed by subtracting the group mean value from the individual's observed value, and then dividing these subtracted values by the group sample standard deviation.

The level of significance adopted were $p<0.05$. All statistical analyses were performed by using Predictive Analytics Software Statistics 18.0 (IBM SPSS, Chicago, IL).

Results

Description of Statistics and line Graphs of Body Volumes According to BMI Groups

The general characteristics and body measurements of the subjects are shown in **Table 3.1**. The mean age, weight, height, and BMI of the overall subjects were 34.4 years, 81.6 kg, 170.3 cm, and 28.0 kg/m^2, respectively. Among the 121 participants, 35.5% had a healthy weight (n=24, men; n=19, women), 30.6% were overweight (n=23, men; n=14, women), 22.3% exhibited class I obesity (n=14, men; n=13, women), and 11.6% showed class II obesity (n=6, men; n=8, women). The BMI values for men and women in each BMI category did not differ as the group values were 22.3 kg/m^2 and 22.4 kg/m^2 in healthy, 27.7 kg/m^2 and 27.9 kg/m^2 in overweight, 32.7 kg/m^2 and 32.8 kg/m^2 in obese class I, and 37.2 kg/m^2 and 36.8 kg/m^2 in obese class II for men and women, respectively ($p>0.05$). In addition, 65% were Caucasian and 35% were non-White Hispanic. All parameters listed in **Table 3.1** were significantly different between men and women, except for age, BMI, and abdomen-hip to total body volume ratio, total

abdominal adiposity. Abdomen-hip volume (p=0.06), torso to total body volume ratio (p=0.07), and visceral adiposity (p=0.08) closely approached significance (**Table 3.1**).

In comparison to men, women possessed greater total abdominal and subcutaneous fat and less visceral fat, as determined by MRI. Yet only the difference in subcutaneous adiposity was statistically significant, with the higher visceral fat in men approaching significance (p=0.08). Moreover, a significantly higher percentage of total body fat, as assessed by ADP was observed in women, as opposed to men (p<0.05) (**Table 3.1**).

Regardless of the BMI classification, men exhibited greater total body, torso volumes, and waist circumference than women, while greater abdomen-hip volume (p=0.06) approached significance. Women had higher thigh volumes, hip circumference, and body volume ratio than men, including thigh to total body, thigh to torso, and thigh to abdomen-hip (**Table 3.1**).

Differences between total and regional body volumes and volume ratios in men and women are illustrated in **Figure 3.2**, according to BMI classification. Total and regional body volumes increased, with the exception of thigh volume, in correspondence with increasing BMI classification regardless of sex (**Figure 3.2a**). Thigh volume was statistically greater for the obese class II group, in comparison to healthy, overweight and obese class I groups, but not between overweight and obese class II groups (**Figure 3.2a**).

Table 3.1. Subject characteristics and body measurements by sex

Parameters	Sex				
	Men (n=67)		Women (n=54)		
	Mean ± SEM[a]	Range	Mean ± SEM[a]	Range	*p* value[b]
Demographics					
Age (years)	34.37 ± 1.42	18.6 – 59.8	34.39 ± 1.31	18.5 – 60.6	1.00
Ethnicity (%Caucasian/Hispanic)	65.7/34.3	–	64.8/35.2	–	–
Traditional Anthropometrics					
Height (cm)	175.78 ± 0.87	161.29 – 189.48	163.59 ± 0.95	147.32 – 178.82	0.00
Weight (kg)	86.26 ± 2.17	59.51 – 129.64	75.89 ± 2.25	47.36 – 126.69	0.00
BMI (kg/m^2)	27.68 ± 0.63	19.10 – 40.30	28.45 ± 0.76	18.61– 40.07	0.43
Stereovision Body Imaging					
Stereovision waist (cm)	95.21 ± 1.63	73.26 – 127.47	88.46 ± 1.89	65.40 – 115.00	0.01

Table 3.1 (continued)

Stereovision hip (cm)	106.68 ± 1.17	92.17– 132.36	112.56 ± 1.80	87.19 – 151.07	0.01
Waist-to-hip ratio	0.89 ± 0.01	0.74 – 1.09	0.79 ± 0.01	0.68 – 0.96	0.00
Volume (L):					
Total body	80.95 ± 2.19	54.66 – 122.89	72.41 ± 2.34	43.91 – 123.91	0.01
Torso	39.26 ± 1.37	23.59 – 67.70	34.13 ± 1.42	17.90 – 54.50	0.01
Abdomen-hip	29.01 ± 1.19	15.91 – 59.39	25.85 ± 1.16	12.14 – 45.31	0.06
Thigh	3.99 ± 0.15	2.24 – 9.01	4.93 ± 1.17	3.14 – 10.52	0.00
Volume Ratio:					
Torso to total body	0.48 ± 0.00	0.39 – 0.58	0.46 ± 0.01	0.35 – 0.59	0.07
Abdomen-hip to total body	0.35 ± 0.01	0.27 – 0.48	0.35 ± 0.01	0.27 – 0.45	0.90
Abdomen-hip to torso	0.73 ± 0.01	0.61 – 0.89	0.75 ± 0.01	0.65 – 0.88	0.04

Table 3.1 (continued)

Thigh to total body	0.05 ± 0.00	0.03 – 0.07	0.07 ± 0.00	0.05 – 0.10	0.00
Thigh to torso	0.11 ± 0.00	0.05 – 0.17	0.15 ± 0.01	0.08 – 0.27	0.00
Thigh to abdomen-hip	0.15 ± 0.01	0.06 – 0.24	0.20 ± 0.01	0.11 – 0.33	0.00
Magnetic Resonance Imaging					
Total abdominal adiposity (cm^2)	259.15 ± 18.54	20.64 – 652.63	300.56 ± 18.94	56.81 – 544.98	0.12
Subcutaneous adiposity (cm^2)	187.50 ± 15.41	13.70 – 514.84	242.62 ± 15.46	35.82 – 458.81	0.01
Visceral adiposity (cm^2)	71.65 ± 5.85	2.55 – 188.91	57.94 ± 4.48	8.12 – 137.78	0.08
Air Displacement Plethysmography					
Total body fat (%)	26.00 ± 1.20	9.00 – 49.70	37.18 ± 1.35	16.10 – 53.70	0.00

[a] Standard error of mean

[b] Significant level determined by one-way analysis of variance (ANOVA)

Lower-body volume ratios (thigh to total body, thigh to torso, thigh to abdomen-hip) decreased according to BMI groups, specifically from healthy weight to obese class I participants (**Figure 3.2b**). No significant differences were observed between obese class I and II participants for lower body volume ratios (thigh to total body, thigh to torso, and thigh to abdomen-hip) (**Figure 3.2b**).

Scatter plots of volumes according to overall and central obesity measures

Figure 3.3 presents scatter plots of total/regional body volumes (torso, abdomen-hip, and thigh) assessed by SBI and percent body fat measured by ADP in men and women, according to BMI classifications. Total body, torso, and abdomen-hip volumes were positively correlated with percent body fat and these relationships correspond with increasing BMI classification. Thigh volume also showed positive relationships with percent body fat (**Figure 3.3g,h**); however, the correlation coefficients were lower but still significant then that observed for values of other regional body volumes (**Figure 3.3a-f**). The scatter plots of visceral adiposity assessed by MRI and lower-body volume ratios (thigh to torso and thigh to abdomen-hip) measured by SBI, according to BMI classifications are illustrated in **Figure 3.4**. These lower-body volume ratios also showed negative associations with visceral adiposity and these relationships were more reliable in women. While in men, the scatter plots exhibited greater variations and did not show strong correspondence with BMI groups (**Figure 3.4**).

Figure 3.2. Total and regional body volumes and body volume ratios of men and women assessed by stereovision body imaging, according to BMI classification

(a) Total and regional body volumes

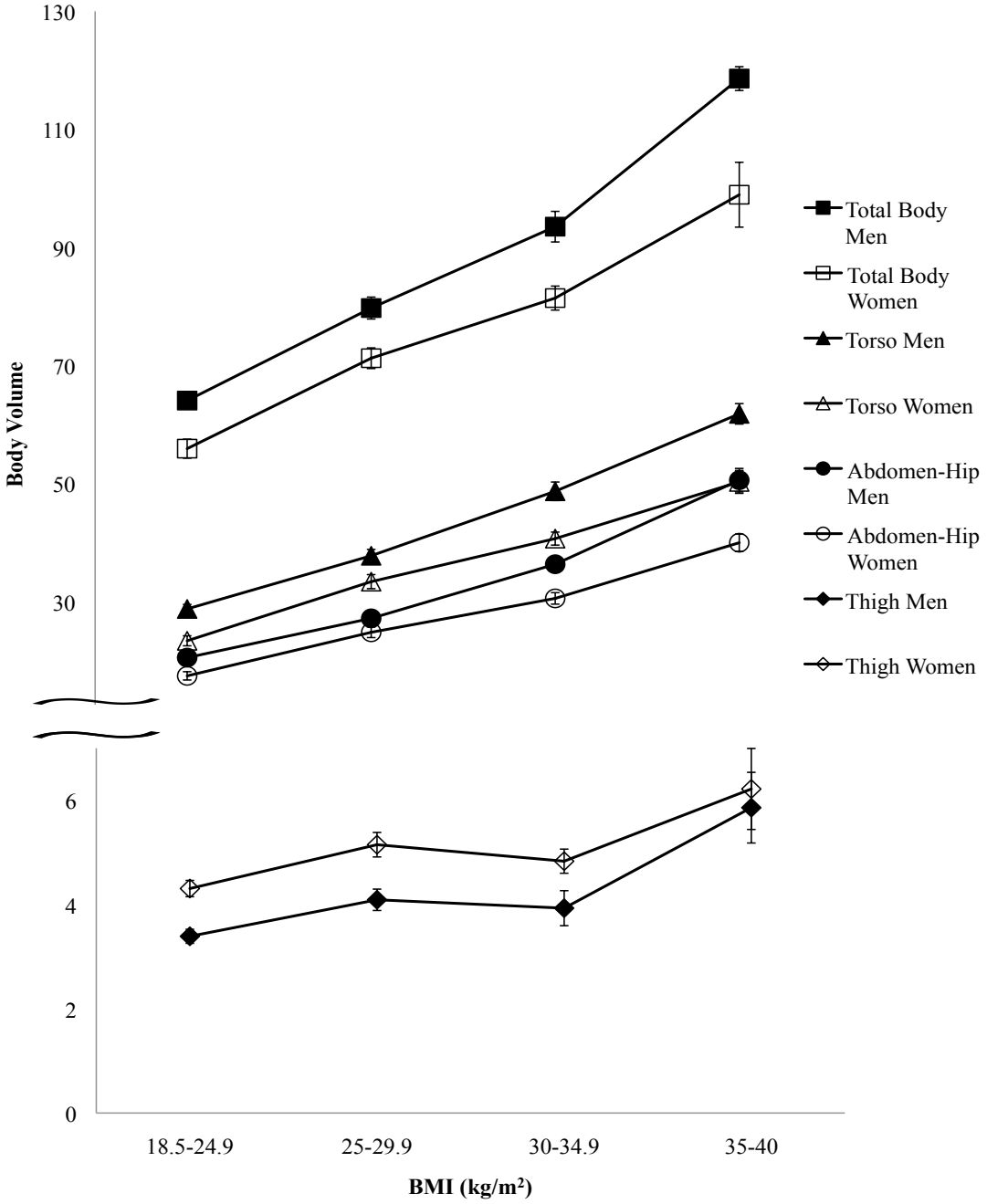

(b) Regional body volume ratios

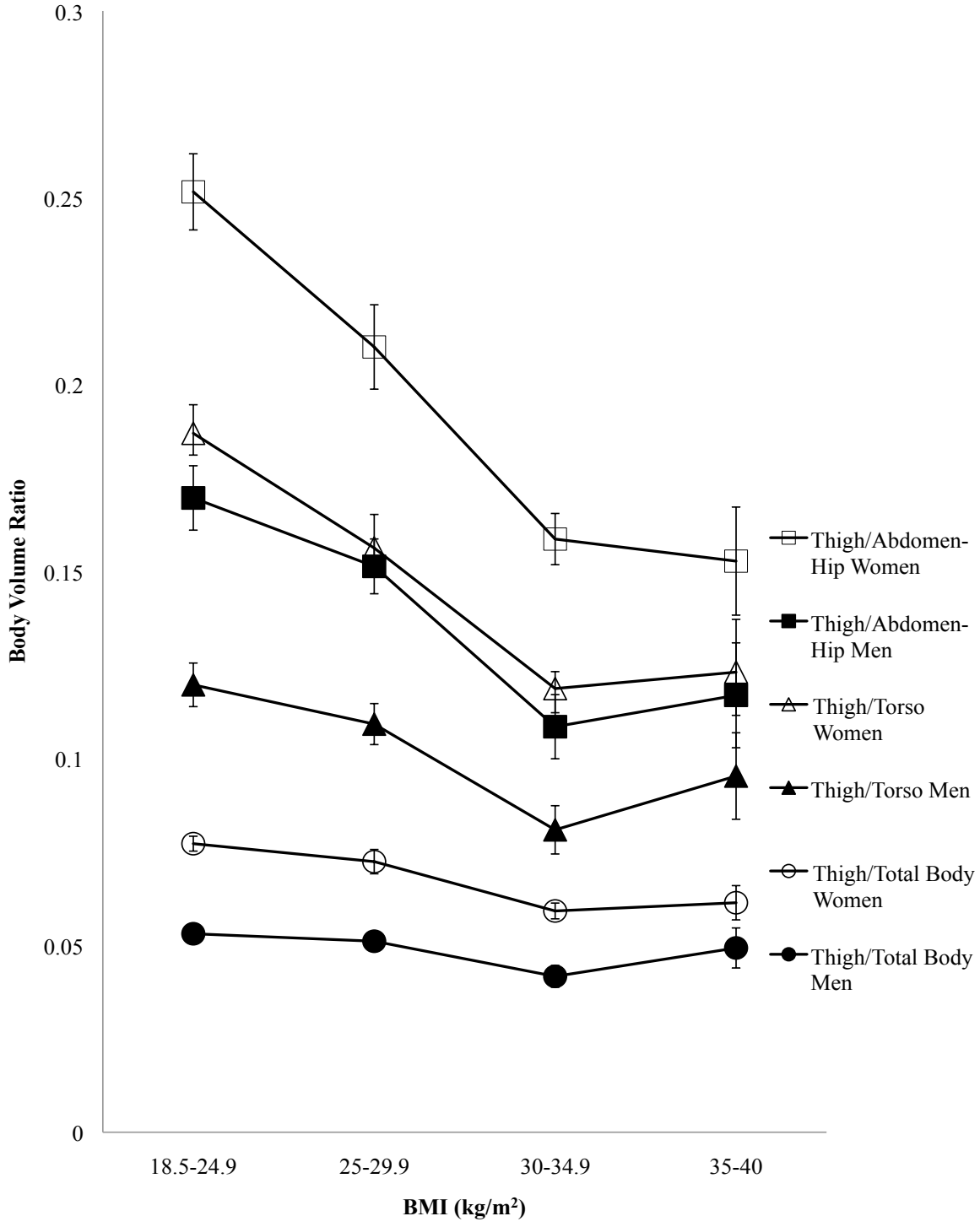

Figure 3.3. Scatter plots of total/regional body volumes assessed by stereovision body imaging and percent body fat, as measured by air displacement plethysmography in men and women, according to BMI classifications

(a) Total body volume according to % body fat in men

(b) Total body volume according to % body fat in women

(c) Torso volume according to % body fat in men

(d) Torso volume according to % body fat in women

(e) Abdomen-hip volume according to % body fat in men

(f) Abdomen-hip volume according to % body fat in women

(g) Thigh volume according to % body fat in men

(h) Thigh volume according to % body fat in women

(a)

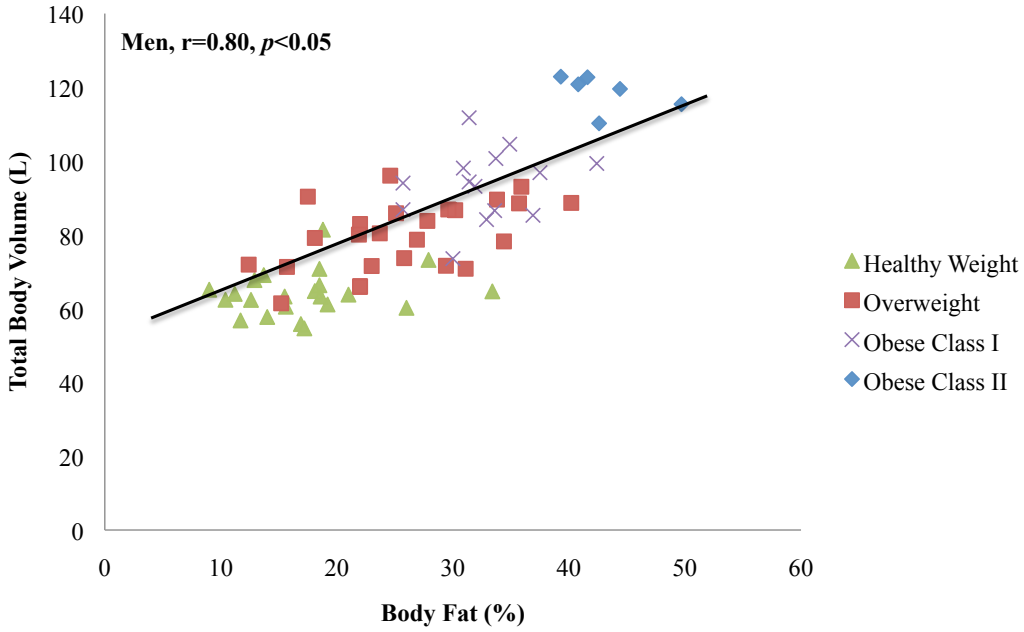
Men, r=0.80, p<0.05
Total Body Volume (L)
Body Fat (%)
0
20
40
60
80
100
120
140
0
10
20
30
40
50
60
Healthy Weight
Overweight
Obese Class I
Obese Class II

(b)

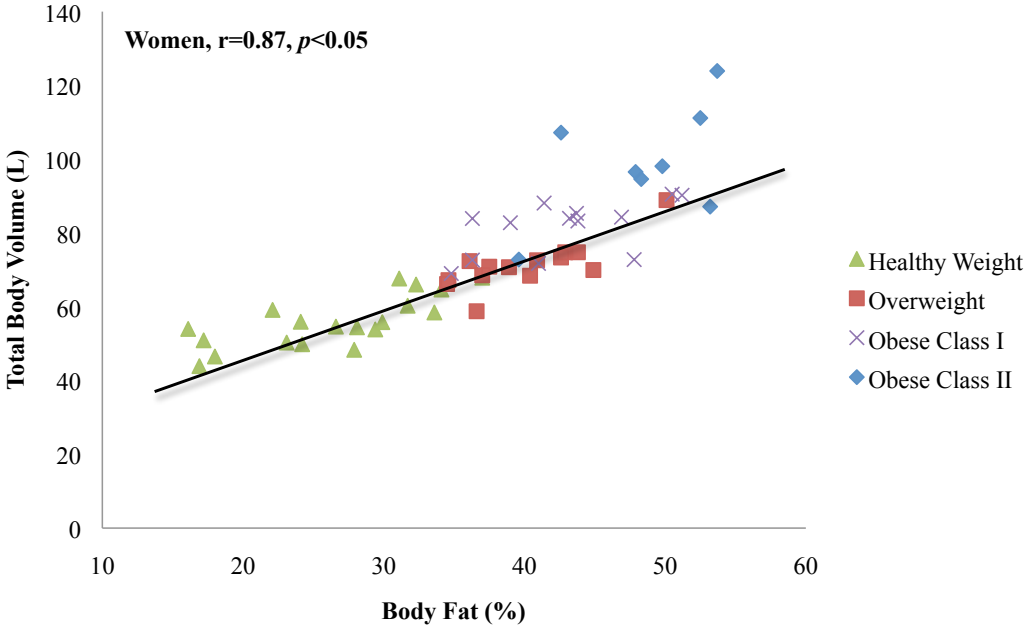
Women, r=0.87, p<0.05
Total Body Volume (L)
Body Fat (%)
0
20
40
60
80
100
120
140
10
20
30
40
50
60
Healthy Weight
Overweight
Obese Class I
Obese Class II

(c)

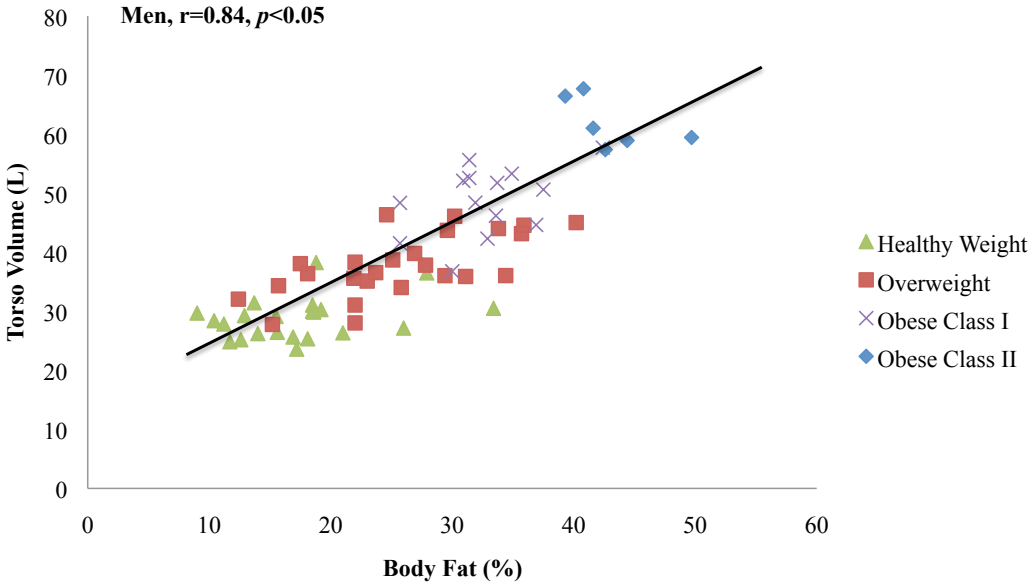
Men, r=0.84, p<0.05
Torso Volume (L)
Body Fat (%)
0
10
20
30
40
50
60
70
80
Healthy Weight
Overweight
Obese Class I
Obese Class II

(d)

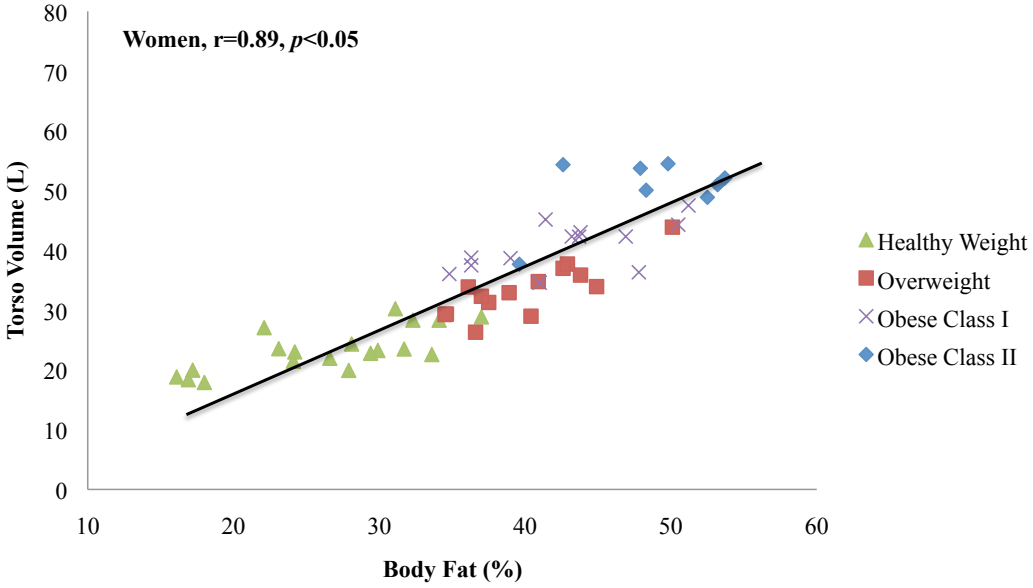
Women, r=0.89, p<0.05
Torso Volume (L)
Body Fat (%)
0
10
20
30
40
50
60
70
80
Healthy Weight
Overweight
Obese Class I
Obese Class II

(e)

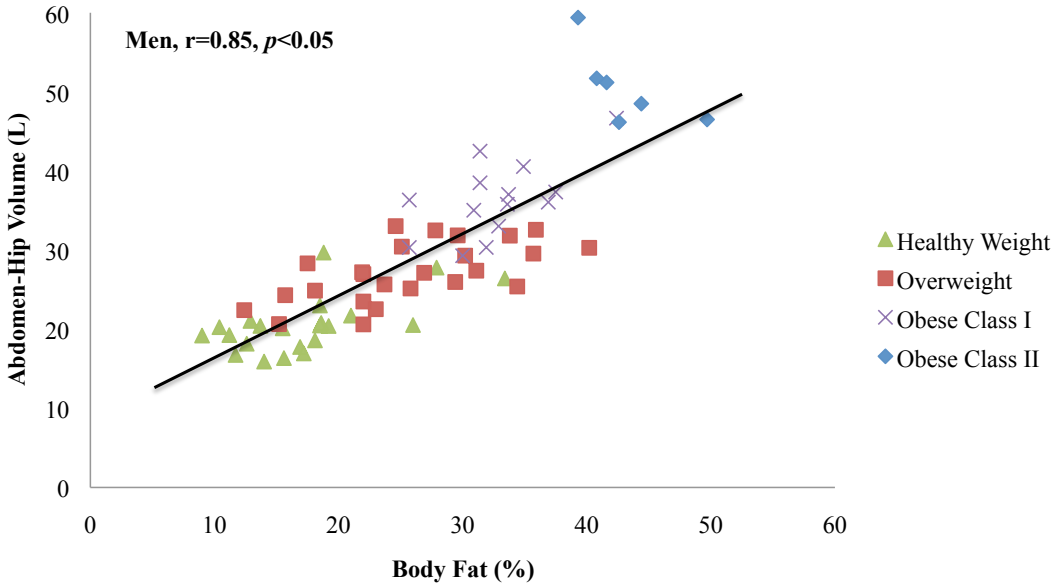
Men, r=0.85, p<0.05
Abdomen-Hip Volume (L)
Body Fat (%)
0
10
20
30
40
50
60
Healthy Weight
Overweight
Obese Class I
Obese Class II

(f)

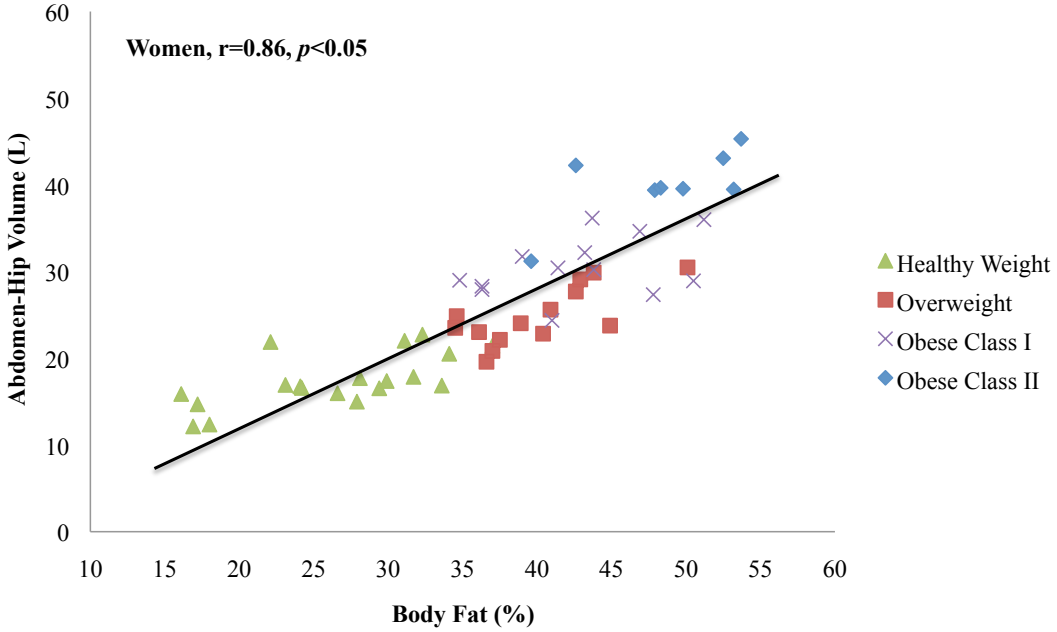
Women, r=0.86, p<0.05
Abdomen-Hip Volume (L)
Body Fat (%)
0
10
20
30
40
50
60
10
15
20
25
30
35
40
45
50
55
60
Healthy Weight
Overweight
Obese Class I
Obese Class II

(g)

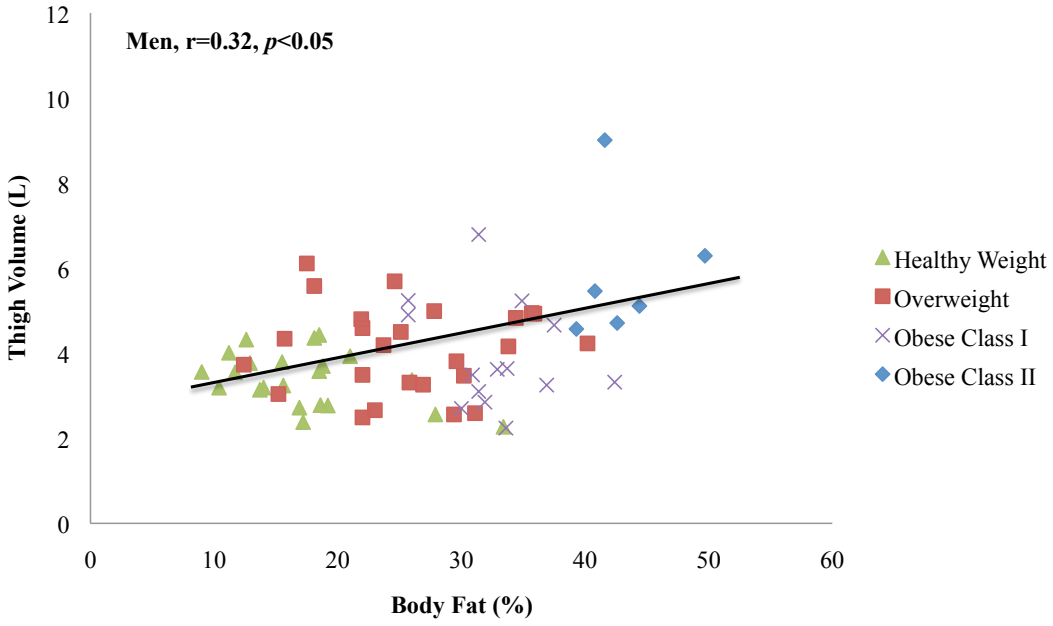
Men, r=0.32, p<0.05
Thigh Volume (L)
Body Fat (%)
0
2
4
6
8
10
12
0
10
20
30
40
50
60
Healthy Weight
Overweight
Obese Class I
Obese Class II

(h)

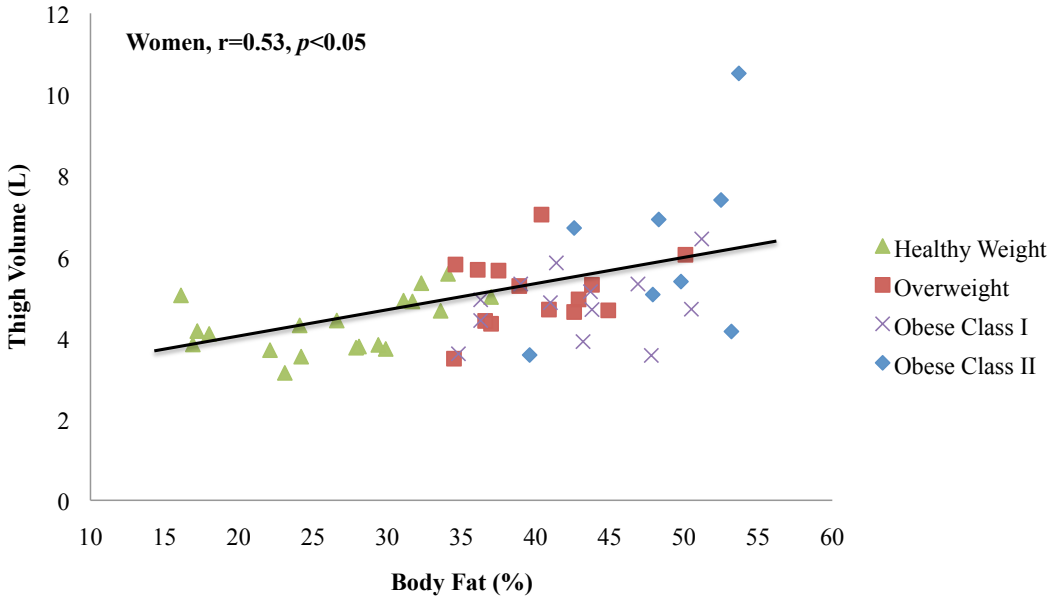
Women, r=0.53, p<0.05
Thigh Volume (L)
Body Fat (%)
0
2
4
6
8
10
12
10
15
20
25
30
35
40
45
50
55
60
Healthy Weight
Overweight
Obese Class I
Obese Class II

Correlations between Body Volumes and Obesity Measures

Age-adjusted partial Pearson correlation coefficients for overall/central obesity measures with whole/regional body volumes and body volume ratios are presented in **Table 3.2**. Total and regional body volumes (torso, abdomen-hip) derived from SBI were closely related with overall obesity measures (BMI and percent body fat) and subcutaneous adiposity volumes. A significant, but weaker relationship has, observed with visceral fat ($p<0.01$). In contrast, thigh volume was not related to visceral adipose tissue.

In men and women, the largest negative correlations for visceral adiposity were observed with thigh to abdomen-hip volume ratio, clearly followed by thigh to torso volume ratio. Only women showed a significant negative relationship with thigh to total body volume ratio and visceral adiposity (**Table 3.2**). In addition, upper body volume ratios, such as torso to total body volume ratio, abdomen-hip to total body volume ratio, and abdomen-hip to torso volume ratio, were positively correlated with these obesity measures (**Table 3.2**).

Odds Ratios for Visceral Fat Tertile, Total/Regional Body Volumes and Volume Ratios

Multinomial logistic regression analysis was conducted to predict tertiles of visceral abdominal fat depots assessed via MRI, according to total/regional body volumes and volume ratios measured by SBI. The odds ratios and 95% confidence intervals by one standard deviation increase of each parameter value for increase in visceral abdominal

Figure 3.4. Scatter plots of visceral adiposity assessed by magnetic resonance imaging according to lower-body volume ratios, as measured by stereovision body imaging in men and women, according to BMI classifications.

(a) Visceral adiposity according to thigh to torso volume ratio in men

(b) Visceral adiposity according to thigh to torso volume ratio in women

(c) Visceral adiposity according to thigh to abdomen-hip volume ratio in men

(d) Visceral adiposity according to thigh to abdomen-hip volume ratio in women

(a)

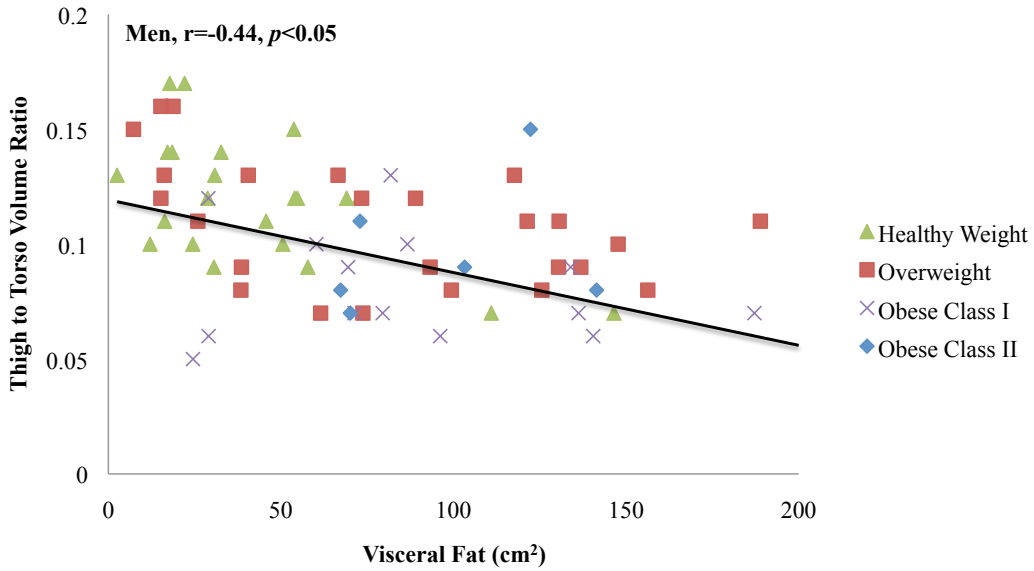
Men, r=-0.44, p<0.05
Thigh to Torso Volume Ratio
0.2
0.15
0.1
0.05
0
0
50
100
150
200
Visceral Fat (cm²)
Healthy Weight
Overweight
Obese Class I
Obese Class II

(b)

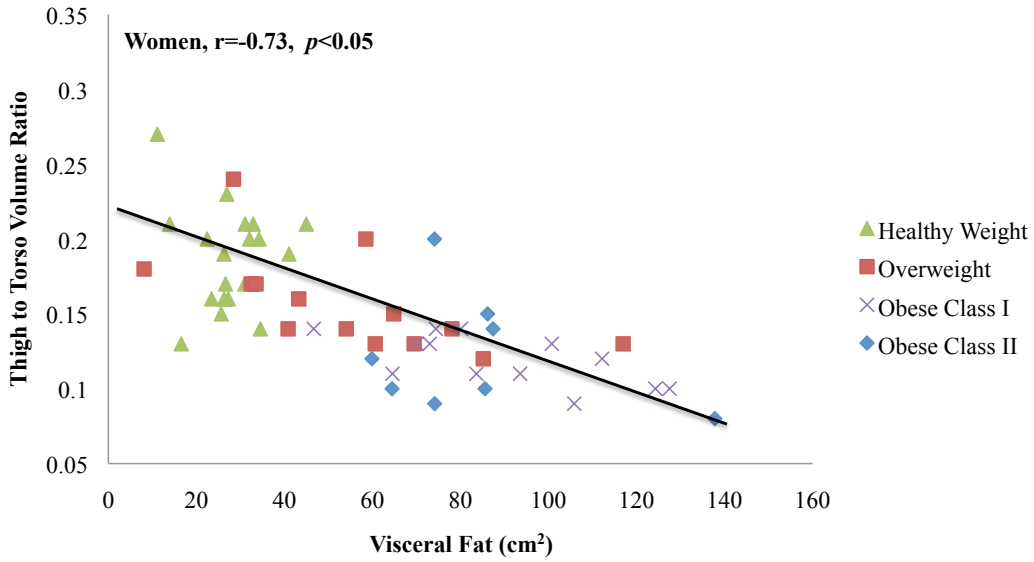
Women, r=-0.73, p<0.05
Thigh to Torso Volume Ratio
0.35
0.3
0.25
0.2
0.15
0.1
0.05
0
20
40
60
80
100
120
140
160
Visceral Fat (cm²)
Healthy Weight
Overweight
Obese Class I
Obese Class II

(c)

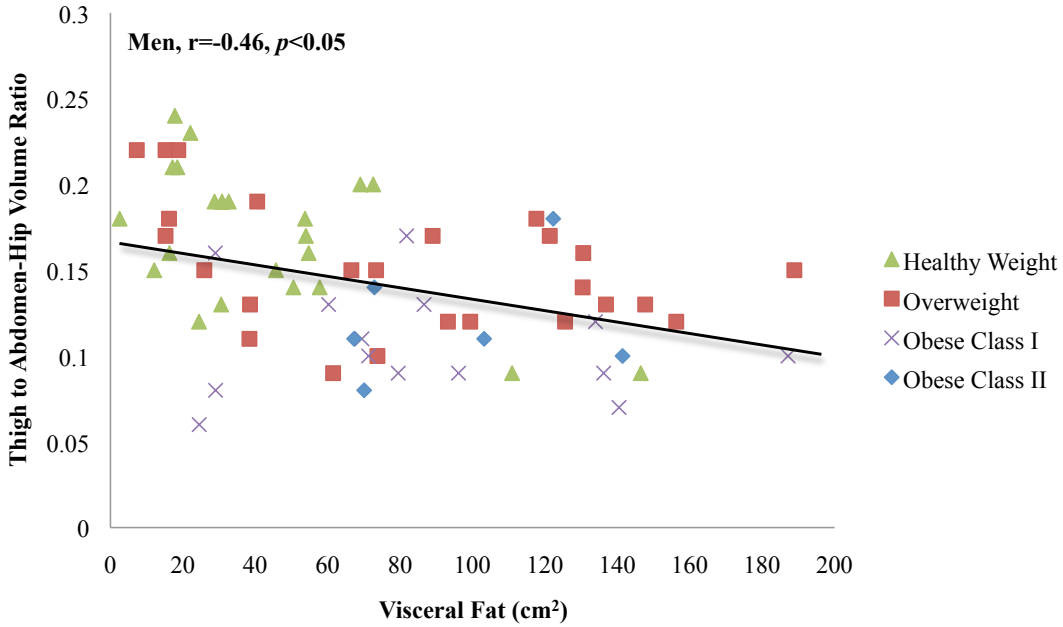
Men, r=-0.46, p<0.05
Thigh to Abdomen-Hip Volume Ratio
0.3
0.25
0.2
0.15
0.1
0.05
0
0
20
40
60
80
100
120
140
160
180
200
Visceral Fat (cm²)
Healthy Weight
Overweight
Obese Class I
Obese Class II

(d)

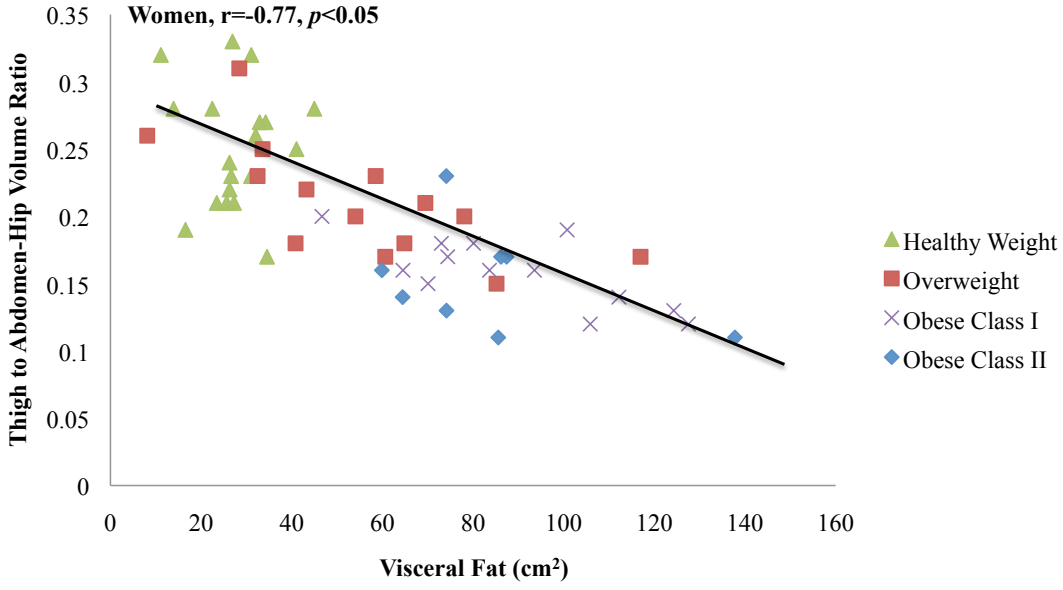
Women, r=-0.77, p<0.05
Thigh to Abdomen-Hip Volume Ratio
0.35
0.3
0.25
0.2
0.15
0.1
0.05
0
0
20
40
60
80
100
120
140
160
Visceral Fat (cm²)
Healthy Weight
Overweight
Obese Class I
Obese Class II

Table 3.2. Age-adjusted partial Pearson correlation coefficients between overall/central obesity measures and total/regional body volumes and body volume ratios, as assessed by air displacement plethysmography, magnetic resonance imaging and stereovision body imaging

Parameters[a]	Overall Obesity Measure		Abdominal Adiposity Volume[d]	
	BMI[b]	% Body Fat[c]	Subcutaneous	Visceral
Men				
Volume:				
Total body	0.90**	0.82**	0.85**	0.39**
Torso	0.92**	0.85**	0.87**	0.40**
Abdomen-hip	0.89**	0.85**	0.88**	0.36**
Thigh	0.47**	0.46**	0.51**	0.20
Volume Ratio:				
Torso to total body	0.74**	0.70**	0.69**	0.36**

Table 3.2 (continued)

Abdomen-hip to total body	0.73**	0.77**	0.75**	0.28*
Abdomen-hip to torso	0.38*	0.49**	0.45**	0.09
Thigh to total body	– 0.30*	– 0.24	– 0.19	– 0.18
Thigh to torso	– 0.45**	– 0.39*	– 0.35**	– 0.26*
Thigh to abdomen-hip	–0.55**	– 0.52**	– 0.46**	– 0.29*
Women				
Volume:				
Total body	0.90**	0.87**	0.85**	0.55**
Torso	0.92**	0.90**	0.88**	0.64**
Abdomen-hip	0.92**	0.88**	0.89**	0.63**
Thigh	0.52**	0.54**	0.48**	0.09

Table 3.2 (continued)

Volume Ratio:				
Torso to total body	0.67**	0.70**	0.68**	0.65**
Abdomen-hip to total body	0.74**	0.69**	0.73**	0.67**
Abdomen-hip to torso	0.25	0.14	0.23	0.14
Thigh to total body	– 5.12**	– 0.46**	– 0.49**	– 0.64**
Thigh to torso	– 0.61**	– 0.60**	– 0.61**	– 0.67**
Thigh to abdomen-hip	– 0.70**	– 0.65**	– 0.68**	– 0.71**

[a] Determined by SBI

[b] Determined by weight in kg divided by height in m^2

[c] Determined by ADP

[d] Determined by MRI

[*] Correlation is significant at 0.05 level (2-tailed)

** Correlation is significant at 0.01 level (2-tailed)

adiposity tertile are demonstrated in **Table 3.3**. Model 1 was unadjusted, model 2 was adjusted for age and sex, and model 3 was adjusted for age, sex, and BMI. Regardless of the adjustment for age and sex (model 1 and 2), higher total and regional body volumes (total body, torso, abdomen-hip), as well as upper body volume ratios (torso to total body, abdomen-hip to total body), were associated with being in a higher visceral adiposity tertile compared to lowest tertile ($p<0.01$).

After adjustment for age and sex (model 2), torso volume and abdomen-hip volume were the strongest variables associated with increased risk for visceral adiposity. Among the body volume ratio parameters, the greatest decrease in the risks of having visceral adiposity was found with thigh to abdomen-hip volume and thigh to torso volume ($p<0.01$) (**Table 3.3**).

However, when the model was adjusted for age, sex, and **BMI group** (model 3), these associations with visceral adiposity were not significant ($p>0.05$). The exceptions were for thigh to torso and thigh to abdomen-hip volume ratios, with the odds ratios for the highest tertile compared with lowest visceral adiposity tertiles being 0.44 and 0.41, respectively ($p<0.05$) (**Table 3.3**).

Discussion

The inverse relationships of abdominal visceral adiposity with lower body volume ratios reported in this study suggest that greater volumes in the lower body are more metabolically favorable than those in the upper regions. In addition, decreased visceral

Table 3.3. Logistic regression analysis to predict tertiles of visceral abdominal fat depots measured by magnetic resonance imaging, according to whole/regional body volume and volume ratios assessed by stereovision body imagining

Parameters[a]	Tertile of Visceral Fat[b]					
	Model 1[c]		Model 2[c]		Model 3[c]	
	Low vs. Middle	Low vs. High	Low vs. Middle	Low vs. High	Low vs. Middle	Low vs. High
Volume						
Total body	3.58** (1.80 – 7.12)	6.98** (3.30 – 14.74)	3.39** (1.65 – 6.94)	3.08** (3.08 – 15.57)	1.89 (0.63 – 5.63)	2.72 (0.82 – 9.03)
Torso	4.36** (2.10 – 9.08)	8.76** (3.95 – 19.47)	3.87** (1.83 – 8.21)	7.75** (3.34 – 17.96)	2.70 (0.79 – 9.24)	3.62 (0.95 – 13.89)
Abdomen-hip	4.93** (2.25 – 10.80)	9.21** (3.98 – 21.31)	4.07** (1.85 – 8.94)	7.50** (3.17 – 17.74)	2.55 (0.74 – 8.75)	2.88 (0.76 – 10.85)
Thigh	1.25 (0.77 – 2.03)	1.44 (0.89 – 2.32)	1.63 (0.92 – 2.90)	2.17* (1.17 – 4.03)	0.95 (0.48 – 1.88)	1.02 (0.49 – 2.13)

Table 3.3 (continued)

Volume Ratio						
Torso to total body	3.49** (1.84 – 6.60)	6.76** (3.30 – 13.88)	2.99** (1.56 – 5.73)	5.33** (2.51 – 11.29)	1.85 (0.81 – 4.22)	1.99 (0.76 – 5.25)
Abdomen-hip to total body	3.64** (1.87 – 7.09)	6.09** (2.98 – 12.44)	3.06** (1.56 – 6.01)	4.65** (2.23 – 9.70)	1.72 (0.71 – 4.17)	1.54 (0.58 – 4.09)
Thigh to total body	0.46** (0.27 – 0.77)	0.23** (0.13 – 0.42)	0.52* (0.29 – 0.91)	0.31** (0.16 – 0.60)	0.64 (0.34 – 1.18)	0.51 (0.24 – 1.06)
Thigh to torso	0.37** (0.21 – 0.64)	0.17** (0.08 – 0.33)	0.42** (0.23 – 0.75)	0.22** (0.11 – 0.46)	0.56 (0.29 – 1.07)	0.44* (0.19 – 0.99)
Thigh to abdomen-hip	0.33** (0.18 – 0.59)	0.14** (0.07 – 0.29)	0.37** (0.20 – 0.68)	0.19** (0.09 – 0.40)	0.54 (0.27 – 1.08)	0.41* (0.17 – 0.99)

Data on exponential β and 95 % confidence intervals are shown.

[a] Determined by SBI

[b] Determined by MRI

[c] Model 1, unadjusted; model 2, adjusted for age, sex; model 3, adjusted for age, sex, BMI group

* Correlation is significant at 0.05 level (2-tailed)

** Correlation is significant at 0.01 level (2-tailed)

adiposity was observed with a high thigh volume in relation to abdomen-hip and torso volumes, independent of age, sex, and BMI groups. Thus, this type of fat distribution in the lower body appears to be metabolically advantageous for both men and women.

Positive effects of the lower body regions on obesity-related health risk factors have been reported previously (119, 177-179). It is plausible that the accumulation of fat in peripheral regions of the body such as thighs, or legs, may restrict the ectopic fat accumulation in the upper body torso, which are more closely linked with metabolic risks (180). Differences in the response rate and introduction of catecholamine-induced lipolysis between gluteal and abdominal fat deposits may explain these adverse effects from a physiological view (181). The reported favorable impact of lower body factors on metabolic health may be related to the adverse effect of inflammatory cytokines on accumulation in abdominal adiposity. In contrast, peripheral adiposity is negatively associated with systemic inflammation stimulated by cytokines (180, 182). Presumably, changes in peripheral body composition could be explained by the proportion of lean (muscle) mass induced by physical activity. However, Wilson et al. (2013) reported that an increased trunk volume, in comparison, to leg volume was due to the elevated fat mass in each body segment, as opposed to the lean mass (183).

Wang et al. (2007) utilized a Hamamatsu photonic laser scanner to assess body volumes, including total body, trunk, arms, and legs, in class II and III obesity participants (n=8 men, 23 =women). These values were compared to those with a BMI < 35 kg/m^2 (184). Men exhibited greater total body, torso, and arm volumes, as well as

torso to total body volume ratio than women; women had a higher leg to total body volume ratio, irrespective of BMI classifications (184). However, no differences were found in leg volume in men and women according to BMI grouping (184). The present study identified significantly greater thigh volumes in women, as compared to men. Men showed significantly higher total and upper body volumes; whereas, women had greater values of lower body volumes and ratios and these findings were consistent across BMI groups between men and women. These results correspond to research that has shown women are more prone to exhibit a gynoid body shape, as opposed to men that have an android body type (115, 116, 171).

The research by Wang et al. (2007) also observed that class II and III obese participants showed greater total body, torso, arm, leg (women only) volumes, and torso to total body volume ratio, and lower leg to total body volume ratio, as opposed to subjects with BMI < 35 kg/m^2 (184). Similarly, the current study observed that obesity class II subjects had greater total body, torso, abdomen-hip, and thigh volume, as opposed to other BMI groups including obesity class I, regardless of sex. In addition, thigh volumes in obese class II participants were larger than those in other BMI groups, but not significant compared to class I. This suggests that the changes in the body volume proportions were subtle among moderately and morbidly obese individuals. Greater differences may have been observed if our sample had been expanded in size or included obesity class III.

Wilson et al. (2013) utilized a trunk to leg volume ratio that was determined by

DXA as a reflection of body shape index (183). A higher value for this measure indicated that the proportion of trunk was greater than the legs, as the upper body volume was divided by the lower body volume. The trunk to leg volume ratio increased across underweight, healthy weight, and overweight participants (1.40, 1.46, 1.57, respectively) (183). This investigation demonstrated that proportions of legs were larger, as compared to trunk volume for underweight individuals, and the proportion of leg volume was smaller than the trunk volume for higher BMI groups. However, no differences were found between the overweight and obese (183). In the current study, upper body volume ratios increased according to the BMI classification, while lower body volume ratios decreased, regardless of sex. These results also conform to Wang et al. (2007) who found that lower body volume factor (leg to total body volume ratio) decreased as BMI classification increased (184). Correspondingly, these suggest that a greater lower body volume may have a beneficial effect on being obese. Thus, as an individual progresses to a higher BMI group, body fat may be more prone to accumulate in the upper body, rather than the lower body region.

The current investigation confirmed the favorable associations between lower body factors and accumulation of visceral adiposity, even after adjustment for age, sex, and BMI, as the odds ratios were 0.44 for thigh to torso volume ratio and 0.41 for thigh to abdomen-hip volume ratio. It is well established that greater fat deposition in thighs or legs is believed to be a protective factor for obesity-related diseases such as cardiovascular disease, coronary heart disease, type 2 diabetes (118, 123, 129, 167) or

longevity/mortality (123, 127); whereas, fat depots in the upper portion of the body are more closely linked to those diseases. In the elderly, Snijder et al. (2003) observed that individuals with larger hip and thigh circumferences exhibited a lower risk of type 2 diabetes occurrences. The odds ratios for prediction of type 2 diabetes for hip and thigh circumferences were 0.55 and 0.79 in men; and 0.63 and 0.62 in women, when adjusted for age, BMI, and waist circumference (167). In contrast, a larger waist circumference was linked to increased incidence of developing type 2 diabetes (167).

A study by McLaughlin et al. (2011) confirmed that thigh fat behaves as a potential protective factor, as the odds ratios regarding the thigh fat to predict insulin resistance was 0.59, after adjustment of sex and BMI (185). Similar findings were observed in college students, with leg (but not arm) fat linked to reduction of cardiovascular risk factors ($p<0.05$) (186). In comparison, Hoyer et al. (2011) found that neither mid-thigh circumference or subcutaneous thigh fat depot was related to risk of type 2 diabetes diagnosis among Japanese Americans; the odds ratios for both were only 0.9 (187) ($p>0.05$).

The unique measurements of body volume and body ratios by SBI incorporated in this present study provide a means for prediction of visceral adiposity volume. Visceral adiposity remains difficult to assess but the 3D SBI utilized in this research permit detection of this type of adiposity.

In summary, thigh volume in relation to torso and abdomen-hip volume determined by SBI were parameters that estimated the risks of possessing visceral adiposity, the

metabolically active fat depot. The favorable effects of lower body components on visceral fat were apparent in both men and women, despite sex differences in body size and shape.

CHAPTER 4. PREDICTION OF ANDROID AND GYNOID BODY ADIPOSITY VIA A THREE-DIMENSIONAL STEREOVISION BODY IMAGING SYSTEM AND DUAL-ENERGY X-RAY ABSORPTIOMETRY

Abstract

Current methods for measuring regional body fat are expensive and inconvenient compared to the relative cost-effectiveness and ease-of-use of a stereovision body imaging (SBI) system. The primary goal of this research is to develop prediction models for android and gynoid fat by body measurements assessed via SBI and dual-energy x-ray absorptiometry (DXA). Subsequently, mathematical equations for prediction of total and regional (trunk, leg) body adiposity were established via parameters measured by SBI and DXA. A total of 121 participants were randomly assigned into primary and cross-validation groups. Body measurements were obtained via traditional anthropometrics, SBI, and DXA. Multiple regression analysis was conducted to develop mathematical equations by demographics and SBI assessed body measurements as independent variables and body adiposity (fat mass and percent fat) as dependent variables. The validity of the prediction models was evaluated by a split sample method and Bland-Altman analysis. The R^2 of the prediction equations for fat mass and percent body fat were 93.2% and 76.4% for android, and 91.4% and 66.5% for gynoid, respectively. The limits of agreement for the fat mass and percent fat were – 0.06 ± 0.87 kg and – 0.11 ± 1.97 % for android and – 0.04 ± 1.58 kg and – 0.19 ± 4.27 % for gynoid. Prediction

values for fat mass and percent fat were 94.6% and 88.9% for total body, 93.9% and 71.0% for trunk, and 92.4% and 64.1% for leg, respectively. The three-dimensional (3D) SBI produces reliable parameters that can predict android and gynoid, as well as total and regional (trunk, leg) fat mass.

Introduction

Measurements of regional body adiposity, such as trunk, thigh, leg, and android fat have been linked closely with obesity-related risks. Thus, these regional areas may provide more information for assessment of health risks, as compared to overall obesity (119, 177-179). This is particularly true with the recent controversy of the efficiency of BMI for predicting obesity-related disease risks (90). One of the previous reports involved with regional adiposity related-risks included android and gynoid fat determined via dual-energy x-ray absorptiometry (DXA) (131, 188, 189). The android adiposity showed a positive correlation with visceral adiposity ($r=0.81$, $p<0.01$), as well as strong associations with metabolic risk factors including triglycerides, homeostatic model assessment of the insulin resistance (HOMA-IR), fasting glucose and insulin (188). These relationships were even stronger when compared to visceral adiposity assessed by computed tomography (CT) (188). In addition, gynoid fat assessed by DXA demonstrated decreased risks for stroke (189) and metabolic risk factors (131). Thus, the ability to predict regional fat distribution, such as android and gynoid fat in an inexpensive and easy manner, would be advantageous for estimating risks associated with

obesity-related diseases in the general population.

Instruments that assess regional body adiposity via advanced techniques include CT (59), DXA (58, 190) and magnetic resonance imaging (MRI) (190). In CT, the differences in the attenuation of X-rays through tissues permits imaging of internal body structures (59). For DXA, a three-compartment model estimates body composition using varying attenuations of X-rays through bones, lean tissue, and fat (58, 62). For the MRI, the basis for production of high quality, 3 dimensional (3D) anatomic images is an abundance of hydrogen nuclei (70). Both CT and DXA involve the usage of radiation during assessment, and DXA is not always possible in morbidly obese subjects due to limits on weight and size (50, 53). Moreover, CT, DXA and MRI are restricted for large scale epidemiological studies that measure a large number of subjects in a given time frame across various locations. All of these methods lack portability, are bulky, and expensive to operate. Thus, more precise, non-invasive, and low cost methods are needed to estimate regional body adiposity.

Previously, body measurements assessed by photonic stereovision body imaging (SBI) were effective in the development of prediction equations for abdominal adiposity determined by MRI (149). The established equations were useful in predicting abdominal adiposity volumes, including total abdominal, subcutaneous, and visceral adiposity, which could replace the MRI and improve the efficiency of assessing abdominal adiposity in field settings. The current project utilized a 3D SBI system as an assessment method for body composition (138, 148), and compared it to android and gynoid fat as

determined by DXA. The advantages of SBI as an evaluative method are: 1) it is a quantifiable, visual representation of body size and shape (**Figure 4.1**); 2) the degree of central obesity can be documented by central obesity depth and width (149); 3) it utilizes a rapid and non-invasive (no radiation exposure) method to obtain various body measurements; and 4) it is cost-effective and portable.

The primary objective of this research was to develop prediction equations for android and gynoid body adiposity assessed via 3D photonic SBI and DXA. Additionally, mathematical models for total body, trunk and leg adiposity were established via parameters measured with SBI and DXA.

Method and Procedures

Design of Study

A total of 121 adults, including 67 men and 54 women, were enrolled in this body composition study. Inclusion criteria for participation were healthy Caucasian or non-White Hispanic men and women, ages 19-65 years old, and BMI category of healthy weight (18.5-24.9 kg/m^2), overweight (25-29.9 kg/m^2), or obese (>30 kg/m^2). Subjects with any known diseases and women who are or could be pregnant, or lactating were excluded. Informed consent documents were obtained from participants and the risks and benefits of the study were explained and informed consents were obtained. The University of Texas at Austin Institutional Review Board approved the study.

Subjects were instructed to restrict consumption of caffeine and alcohol, as well as heavy exercise at least 10 hours prior to the visit. Study participants completed demographic and health questionnaires and then were assessed for traditional anthropometrics, SBI, and DXA.

Assessment of Body Composition

Body composition assessment procedures and descriptions of the devices, including traditional anthropometrics and SBI were described previously (149). Traditional anthropometrics evaluated weight and height, and BMI was calculated as weight in kg divided by height in m^2.

Body circumferences, central obesity measures, and total/regional body volumes and ratios (upper- and lower- body volume ratio factors) were assessed via 3D SBI. SBI utilizes a method of photogrammetry in order to acquire the body images of an individual. Four pairs of CMOS cameras (Videre Design, Menlo Park, CA) capture the image of the body, while four LCD projectors (NEC Corporation, Tokyo, Japan) illuminate the body surface (149). Body circumferences assessed via SBI included chest, waist, hip, upper thigh, lower thigh and knee. Regional body volumes encompassed torso (neck to crotch), abdomen-hip (smallest point of waist to crotch), and thigh (crotch to mid-thigh). Upper-body volume factors involved volume ratios of torso to total body, abdomen-hip to total body, and abdomen-hip to torso. Lower-body volume factors included volume ratios of thigh to total body, thigh to torso, and thigh to abdomen-hip.

Measurements for both central obesity depth and width were taken at the umbilicus level. Central obesity width was defined as the widest length on the coronal plane; central obesity depth, as the length between the mid-point of central obesity width and the umbilicus (149). Waist-to-hip ratio was computed as waist circumference (cm) divided by hip circumference (cm) and waist-to-thigh ratio was obtained as waist circumferences (cm) divided by upper thigh circumference (cm).

DXA was utilized to measure body composition, including android, gynoid, total body, trunk, and leg fat mass, fat-free mass and percent body fat via a Lunar Prodigy (GE Medical Systems, Madison, WI). Subjects laid flat on the scanner table where the X-ray sources were located. All were wearing light weight clothing and metals were removed. The scanning process required 7 to 20 minutes, depending on the size of the subject. The DXA device scans the whole body by interacting with the main computer, using two different energy levels of X-ray beams. These two varying levels of energy go through the body in diverse raster patterns so that the bone mineral density of the spine, hip, forearms and the soft tissues of the whole or specific area (trunk, leg) are measured.

This research focused on android and gynoid fat. For the DXA, the android region was defined as the area between the ribs and the pelvis, and was completely covered by the trunk region. The upper demarcation was 20% of the distance from the iliac crest and the neck; whereas, the lower demarcation was at the top of the pelvis. The gynoid region included the area of the hips and the upper thighs, and it overlapped the leg and trunk areas. For this region, the upper demarcation was below the top of the iliac crest at a

distance of 1.5 times the android height. The total height of the gynoid region was two times the height of the android region (191). Android and gynoid fat regions were computed via Prodigy enCORE software (version 11.0, GE Medical Systems) provided by the manufacturer. The regions of android and gynoid fat depots in men and women that were assessed by DXA are depicted in **Figure 4.1**.

Analysis of Statistics

Participants characteristics including demographics (age, sex), traditional anthropometrics (weight, height, BMI), SBI, and DXA measurements of overall, primary, and cross-validation groups were computed as a measure of descriptive statistics and expressed as mean ± standard error of mean (**Table 4.1**). Comparisons between primary and cross-validation groups were conducted by one-way analysis of variance (ANOVA). The normality of the distributions of quantitative variables was evaluated by histograms and the Kolmogorov-Smirnov test.

Stepwise multiple linear regression analysis utilized body fat mass (kg) and fat percentages (%) (android, gynoid, total body, trunk, leg) derived via DXA as dependent variables, and relevant body measurements assessed by demographics (age, sex) and SBI as independent variables. Independent parameters encompassed ratios of waist to hip, waist to thigh circumferences; circumferences of waist, hip, upper thigh, lower thigh and

Figure 4.1. Body images of men and women determined by a three-dimensional stereovision body imaging and matched figures of dual-energy x-ray absorptiometry, illustrating android and gynoid fat areas

a) Men, BMI 30.8 kg/m^2

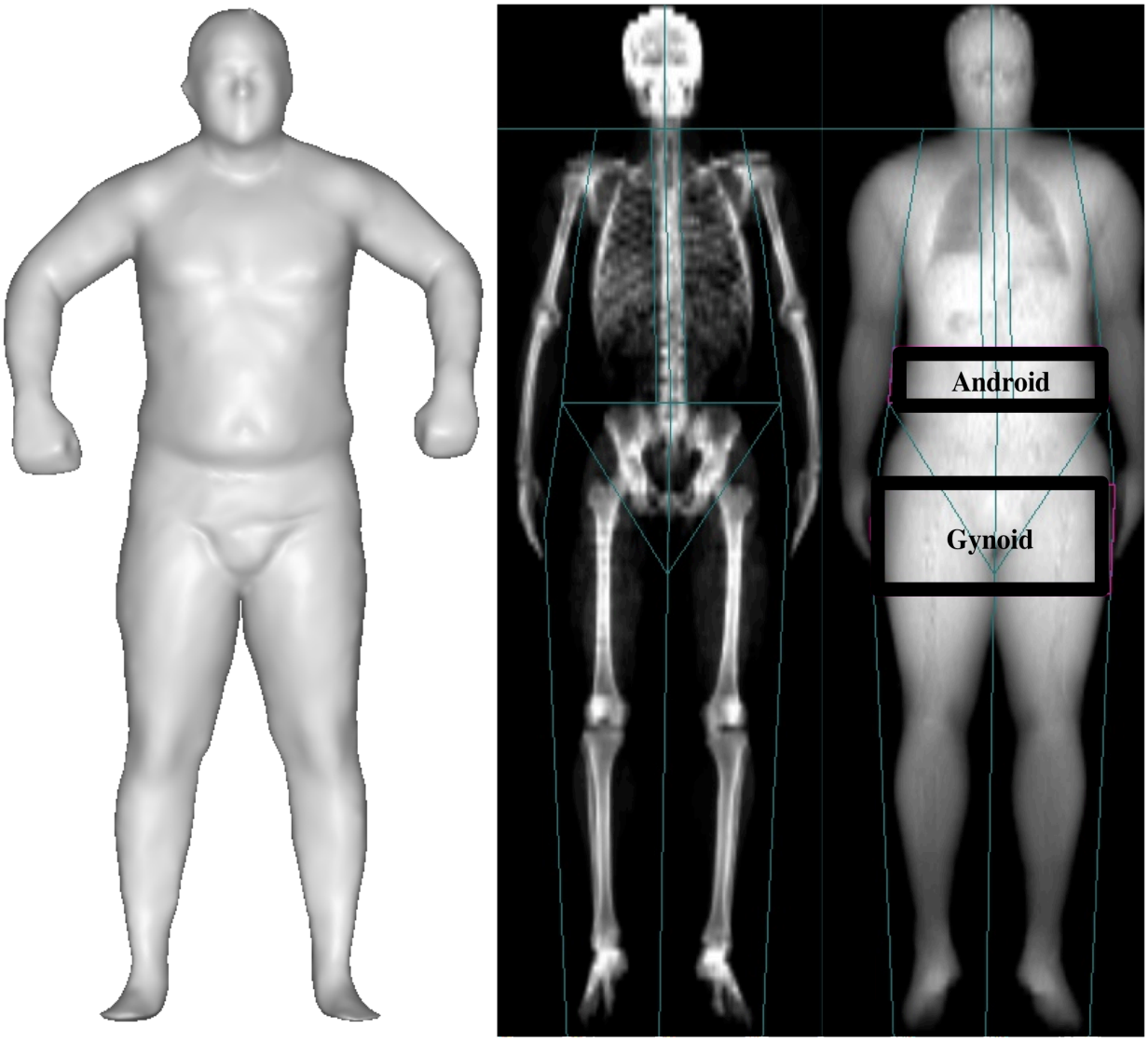

(b) Women, BMI 30.2 kg/m^2

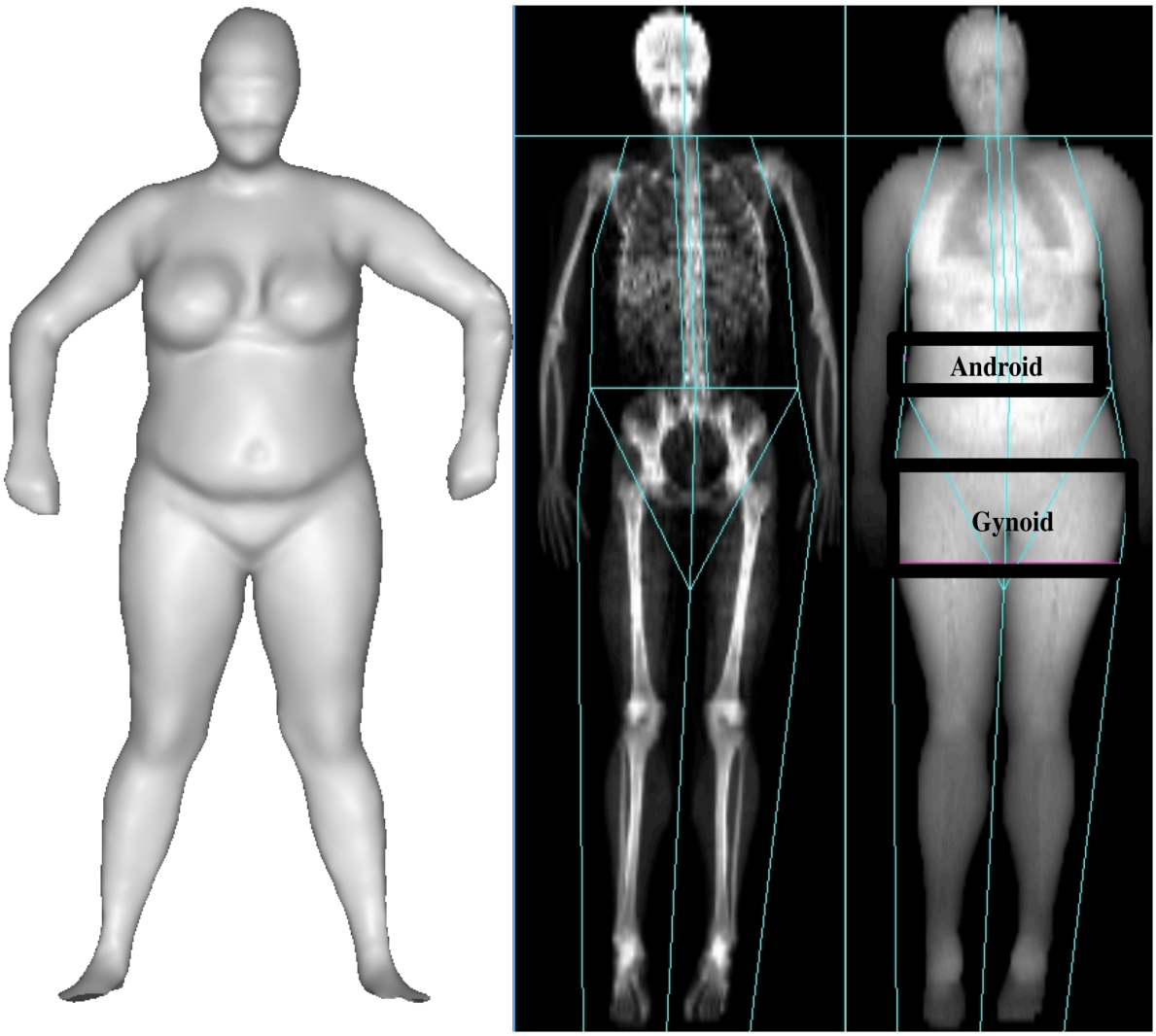

knee; volumes of total body, torso, abdomen-hip and thigh; volume ratios of torso to total body, abdomen-hip to total body, thigh to total body, abdomen-hip to torso, thigh to torso and thigh to abdomen-hip. Central obesity depth and width were calculated to construct prediction models for body adiposity. The impact of demographics, including age and sex, also were included as independent variables in order to examine the associations with android and gynoid body adiposity.

A dummy code was used to label sex as women=0 and men=1 and ethnicity as non-White Hispanic =0 and Caucasian=1. The total participants (n=121) were randomly assigned via the statistics software into primary (n=77, 65%) and cross-validation (n=44, 35%) groups. The prediction equations were developed by using the primary group. In addition, Bland-Altman limits of agreement analysis was implemented to confirm the validity of the developed equations and to visualize the mean differences and 95% limits of agreement for the bias between observed values measured by DXA and predicted values by the equation models (192). Standardized β-coefficients (β) described the output of stepwise multiple regression analysis, which explains the change in terms of the standard deviation unit of the dependent variable that is associated with one standard deviation increase in the independent variable. Variables with a variance inflation factor greater than 10 were eliminated to reduce the impact of collinearity between the parameters.

Table 4.1. Demographics and body composition of primary and cross-validation groups

Parameters	Overall Participants (n=121)	Group		*p*-value[b]
		Primary (n=77)	Cross-Validation (n=44)	
	Mean ± SEM[a]	Mean ± SEM[a]	Mean ± SEM[a]	
Demographics				
Age (years)	34.38 ± 0.98	33.75± 1.27	35.49 ± 1.51	0.39
Sex (%Men/%Women)	55.4/44.6	57.1/42.9	52.3/47.7	0.61
Ethnicity (%Caucasian/Hispanic)	65.3/34.7	61.0/39.0	72.7/27.3	0.20
Traditional Anthropometrics				
Weight (kg)	81.63 ± 1.63	81.71 ± 2.04	81.50 ± 2.75	0.95
Height (cm)	170.34 ± 0.85	169.97 ± 1.00	170.99 ± 1.54	0.56
BMI (kg/m^2)	28.02 ± 0.49	28.24 ± 0.62	27.65 ± 0.77	0.57

Table 4.1 (continued)

Stereovision Body Imaging				
Circumference (cm)				
Waist	91.33 ± 1.27	91.26 ± 1.55	91.46 ± 2.22	0.94
Hip	109.30 ± 1.06	109.45 ± 1.46	109.04 ± 1.43	0.85
Upper thigh	63.81 ± 0.75	63.85 ± 1.03	63.74 ± 1.03	0.94
Lower thigh	42.53 ± 0.47	42.74 ± 0.63	42.16 ± 0.71	0.56
Knee	35.76 ± 0.35	35.75 ± 0.43	35.78 ± 0.59	0.97
Circumference ratio				
Waist-to-hip	0.85 ± 0.01	0.85 ± 0.01	0.85 ± 0.01	0.90
Waist-to-thigh	1.43 ± 0.02	1.43 ± 0.02	1.43 ± 0.04	0.92
Central obesity measure (cm)				

Table 4.1 (continued)

Central obesity depth	15.63 ± 0.34	15.48 ± 0.43	15.89 ± 0.58	0.56
Central obesity width	35.35 ± 0.46	35.30 ± 0.59	35.44 ± 0.74	0.88
Volume (L):				
Total body	77.14 ± 1.64	77.13 ± 2.04	77.16 ± 2.78	0.99
Torso	36.97 ± 1.01	36.95 ± 1.27	37.01 ± 1.69	0.98
Abdomen-hip	27.60 ± 0.84	27.46 ± 1.09	27.83 ± 1.33	0.83
Thigh	4.41 ± 0.12	4.39 ± 0.15	4.44 ± 0.21	0.83
Volume ratio:				
Torso to total body	0.47 ± 0.00	0.47 ± 0.00	0.47 ± 0.01	0.97
Abdomen-hip to total body	0.35 ± 0.00	0.35 ± 0.01	0.36 ± 0.01	0.44
Abdomen-hip to torso	0.74 ± 0.01	0.74 ± 0.01	0.75 ± 0.01	0.17

Table 4.1 (continued)

Thigh to total body	0.06 ± 0.00	0.06 ± 0.00	0.06 ± 0.00	0.54
Thigh to torso	0.13 ± 0.00	0.12 ± 0.00	0.13 ± 0.01	0.45
Thigh to abdomen-hip	0.17 ± 0.01	0.17 ± 0.01	0.17 ± 0.01	0.79
Dual-energy X-ray Absorptiometry				
Fat mass (kg):				
Android	2.77 ± 0.15	2.79 ± 0.19	2.72 ± 0.23	0.80
Gynoid	5.06 ± 0.21	5.07 ± 0.28	5.04 ± 0.29	0.96
Total body	27.46 ± 1.23	27.61 ± 1.61	27.22 ± 1.86	0.88
Trunk	15.30 ± 0.70	15.33 ± 0.92	15.25 ± 1.08	0.96
Legs	9.28 ± 0.46	9.37 ± 0.60	9.12 ± 0.72	0.79
Percent body fat (%):				

Table 4.1 (continued)

Android	9.89 ± 0.19	10.00 ± 0.22	9.69 ± 0.37	0.44
Gynoid	20.11 ± 0.34	19.96 ± 0.40	20.36 ± 0.64	0.58
Total body	32.44 ± 1.09	32.28 ± 1.41	32.74 ± 1.70	0.84
Trunk	56.85 ± 0.64	56.89 ± 0.74	56.78 ± 1.20	0.94
Legs	35.36 ± 0.62	35.25 ± 0.72	35.54 ± 1.17	0.83

[a] Standard error of mean

[b] Significant level determined by one-way analysis of variance (ANOVA)

All statistical analysis and data management was performed using Predictive Analytics Software Statistics 18.0 (IBM SPSS, Chicago, IL). A *p*-value of less than 0.05 was adopted as a statistically significant level.

Results

Description of Statistics

Participants' characteristics and body composition for overall, primary, and cross-validation groups are described in **Table 4.1**. The study sample included men and women, whose age and BMI ranged from 18 to 65 years and 18 to 40 kg/m^2, respectively. None of the parameters were significantly different among participants in the primary and cross-validation groups (p>0.05).

Prediction Equations for Android and Gynoid Body Fat

The final equations for prediction of android and gynoid body adiposity are presented in **Table 4.2**. Changes of prediction value of R^2 and unstandardized/standardized *B* of the demographics and body parameters determined by SBI that were included in the final prediction models for body fat mass and percent body fat are shown in **Table 4.3**. The prediction equations for body fat mass (kg) resulted in higher prediction values (93.2% for android and 91.4% for gynoid), as opposed to the prediction of percent body fat (76.4% for android and 66.5% for gynoid). The android and gynoid fat mass and percent fat equations were composed of a combination of sex,

Table 4.2. Final prediction equations for total and regional body fat mass and percentages via demographics, dual-energy x-ray absorptiometry and stereovision body imaging

Dependent Variable[a]	Predictive Models[b]	Primary Group		Validation Group
		R^2 (%)	SEE[c]	ME (CI)[d]
Fat Mass (kg)				
Android	– 2.54 + 0.10 Torso Volume – 0.65 Sex + 0.13 Central Obesity Depth	93.2*	0.44	– 0.17 (– 1.04, 0.70)
Gynoid	– 5.74 + 0.13 Upper Thigh Circumference + 0.12 Abdomen-Hip Volume – 1.35 Sex	91.4*	0.74	– 0.12 (– 1.93, 1.69)
Total	– 18.85 + 1.25 Central Obesity Depth +2.07 Thigh Volume – 8.37 Sex + 0.62 Torso Volume	94.6*	3.39	– 1.09 (– 13.13, 10.95)
Trunk	– 10.60 + 0.86 Central Obesity Depth + 0.41 Torso Volume – 4.10 Sex	93.9*	2.03	– 0.66 (– 5.18, 3.86)

Table 4.2 (continued)

Leg	– 16.85 + 0.15 Upper Thigh Circumference + 0.53 Knee Circumference –3.42 Sex – 26.13 Thigh to Abdomen-Hip Volume Ratio + 0.92 Thigh Volume	92.4*	1.50	– 0.39 (– 3.52, 2.75)
Percent Fat (%)				
Android	5.72 – 18.13 Thigh to Abdomen-Hip Volume Ratio + 7.23 Waist to Hip Circumference Ratio + 0.08 Central Obesity Depth	76.4*	0.96	– 0.31 (– 2.46, 1.85)
Gynoid	54.90 – 15.48 Waist to Thigh Circumference Ratio – 0.22 Upper Thigh Circumference + 1.68 Sex	66.5*	2.08	0.53 (– 4.15, 5.21)
Total	– 1.89 + 2.01 Central Obesity Depth – 12.98 Sex + 1.53 Thigh Volume	88.9*	4.22	– 1.47 (– 9.12, 6.19)
Trunk	31.62 + 39.14 Waist to Hip Circumference Ratio – 63.48 Thigh to Torso Volume Ratio	71.0*	3.55	0.20 (– 7.73, 8.13)
Leg	47.45 – 13.92 Waist to Thigh Circumference Ratio + 44.92 Thigh to Abdomen-Hip Volume Ratio	64.1*	3.81	0.21 (– 8.12, 8.54)

[a] Dependent variables (body fat mass and fat percentages) measured by dual-energy X-ray absorptiometry.

[b] Independent variables measured by stereovision body imaging. Body measurements include sex, age, upper thigh circumference, knee circumference, stereovision waist to hip circumference ratio, waist to thigh circumference ratio, total body volume, torso volume, abdomen-hip volume, thigh volume, torso volume to total body volume ratio, abdomen-hip volume to total body volume ratio, thigh volume to total body volume ratio, abdomen-hip ratio to torso volume ratio, thigh volume to torso volume ratio, thigh volume to abdomen-hip volume ratio, central obesity depth and central obesity width.

[c] SEE, Standard error of the estimate

[d] Mean error = observed – predicted (confidence interval)

[*] Correlation is significant at 0.05 level (2-tailed)

Table 4.3. Changes of R^2 and *B* values of the demographics and stereovision body imaging parameters included in the prediction equations for total and regional adiposity fat mass and percent fat

Body Fat[a]	Parameters[b]	R^2 Change (%)	Unstandized *B*	Standardized *B*	*p*-value
Fat Mass (kg)					
Android	Torso Volume	85.5	0.10	0.66	<0.001
	Sex	6.0	– 0.65	– 0.20	<0.001
	Central Obesity Depth	1.7	0.13	0.31	<0.001
Gynoid	Upper Thigh Circumference	81.7	0.13	0.46	<0.001
	Abdomen-Hip Volume	5.2	0.12	0.47	<0.001
	Sex	4.5	– 1.35	– 0.27	<0.001
Total Body	Central Obesity Depth	76.8	1.25	0.33	<0.001
	Thigh Volume	12.3	2.07	0.19	<0.001
	Sex	2.4	– 8.37	– 0.29	<0.001
	Torso Volume	3.1	0.62	0.48	<0.001
Trunk	Central Obesity Depth	85.7	0.86	0.40	<0.001
	Torso Volume	2.7	0.41	0.56	<0.001

Table 4.3 (continued)

	Sex	5.6	– 4.10	– 0.25	<0.001
Leg	Upper Thigh Circumference	82.4	0.15	0.26	0.002
	Knee Circumference	3.3	0.53	0.38	<0.001
	Sex	3.6	– 3.42	– 0.33	<0.001
	Thigh to Abdomen Hip Volume Ratio	2.5	– 26.13	– 0.26	<0.001
	Thigh Volume	0.6	0.92	0.22	0.02
Percent Fat (%)					
Android	Thigh to Abdomen Hip Volume Ratio	69.6	– 18.13	– 0.49	<0.001
	Waist to Hip Circumference Ratio	5.2	7.23	0.33	<0.001
	Central Obesity Depth	1.5	0.08	0.16	0.03
Gynoid	Waist to Thigh Circumference Ratio	33.3	– 15.48	– 0.96	<0.001
	Upper Thigh Circumference	29.5	– 0.22	– 0.55	<0.001
	Sex	3.7	1.68	0.24	0.006

Table 4.3 (continued)

Total Body	Central Obesity Depth	53.8	2.01	0.61	<0.001
	Sex	33.4	– 12.98	– 0.52	<0.001
	Thigh Volume	1.6	1.53	0.16	0.002
Trunk	Waist to Hip Circumference Ratio	65.9	39.14	0.54	<0.001
	Thigh to Torso Volume Ratio	5.0	– 63.48	–3.56	0.001
Leg	Waist to Thigh Circumference Ratio	57.9	– 13.92	– 0.48	<0.001
	Thigh to Abdomen Hip Volume Ratio	6.2	44.92	0.37	0.001

[a] Dependent variables (body fat mass and fat percentages) measured by dual-energy X-ray absorptiometry.

[a] Independent variables measured by stereovision body imaging. Body measurements include sex, age, upper thigh circumference, knee circumference, stereovision waist to hip circumference ratio, waist to thigh circumference ratio, total body volume, torso volume, abdomen-hip volume, thigh volume, torso volume to total body volume ratio, abdomen-hip volume to total body volume ratio, thigh volume to total body volume ratio, abdomen-hip ratio to torso volume ratio, thigh volume to torso volume ratio, thigh volume to abdomen-hip volume ratio, central obesity depth and central obesity width.

Figure 4.2. Bland-Altman analysis of agreement for prediction of android and gynoid fat mass and percent fat by stereovision body imaging and measured values by dual-energy x-ray absorptiometry. The solid line in the middle represents the mean values and two dotted lines stand for upper and lower limits of agreement (mean ± 1.96 standard deviation).

(a) Android fat mass (kg)

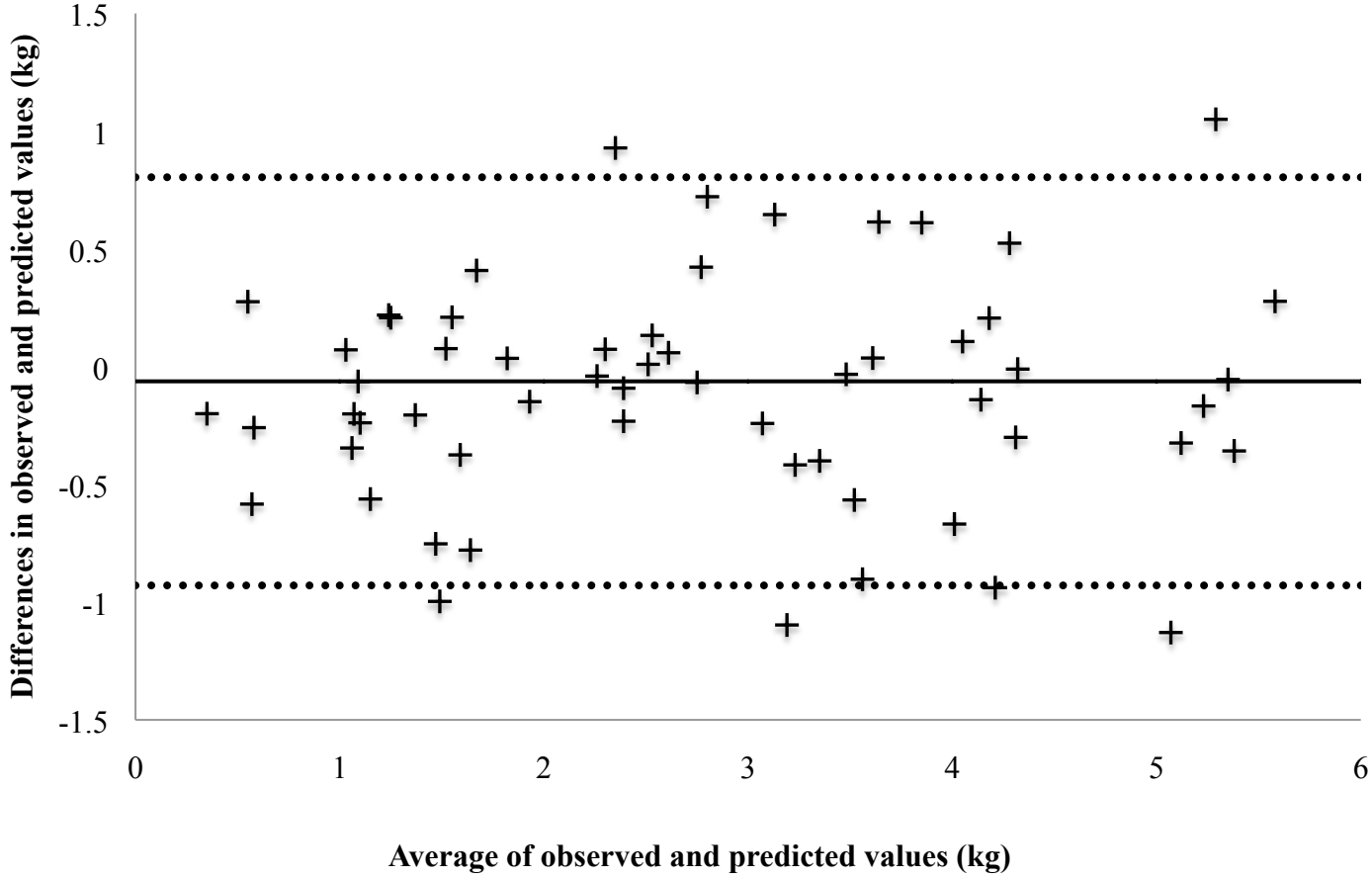

(b) Android fat percentage (%)

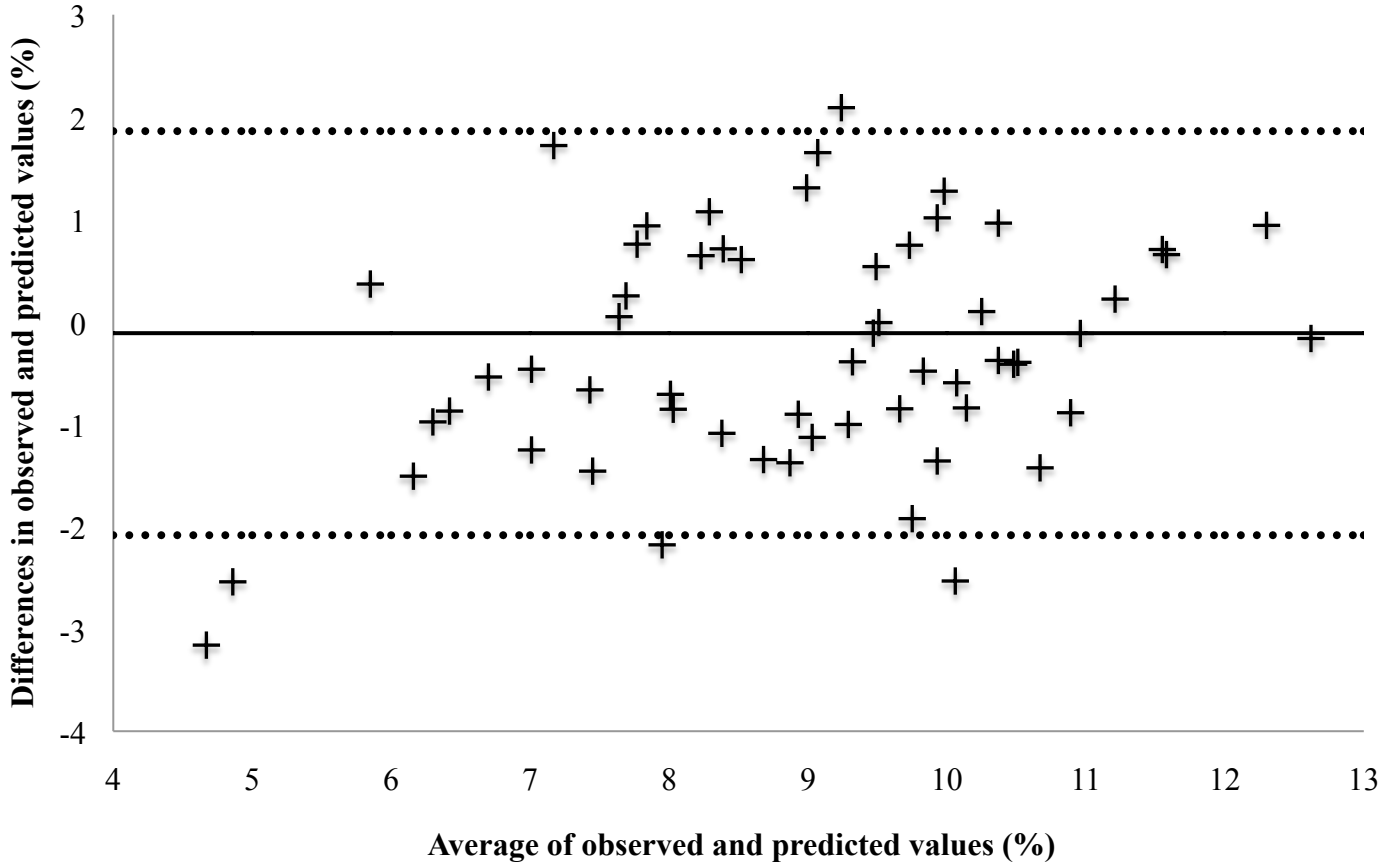

(c) Gynoid fat mass (kg)

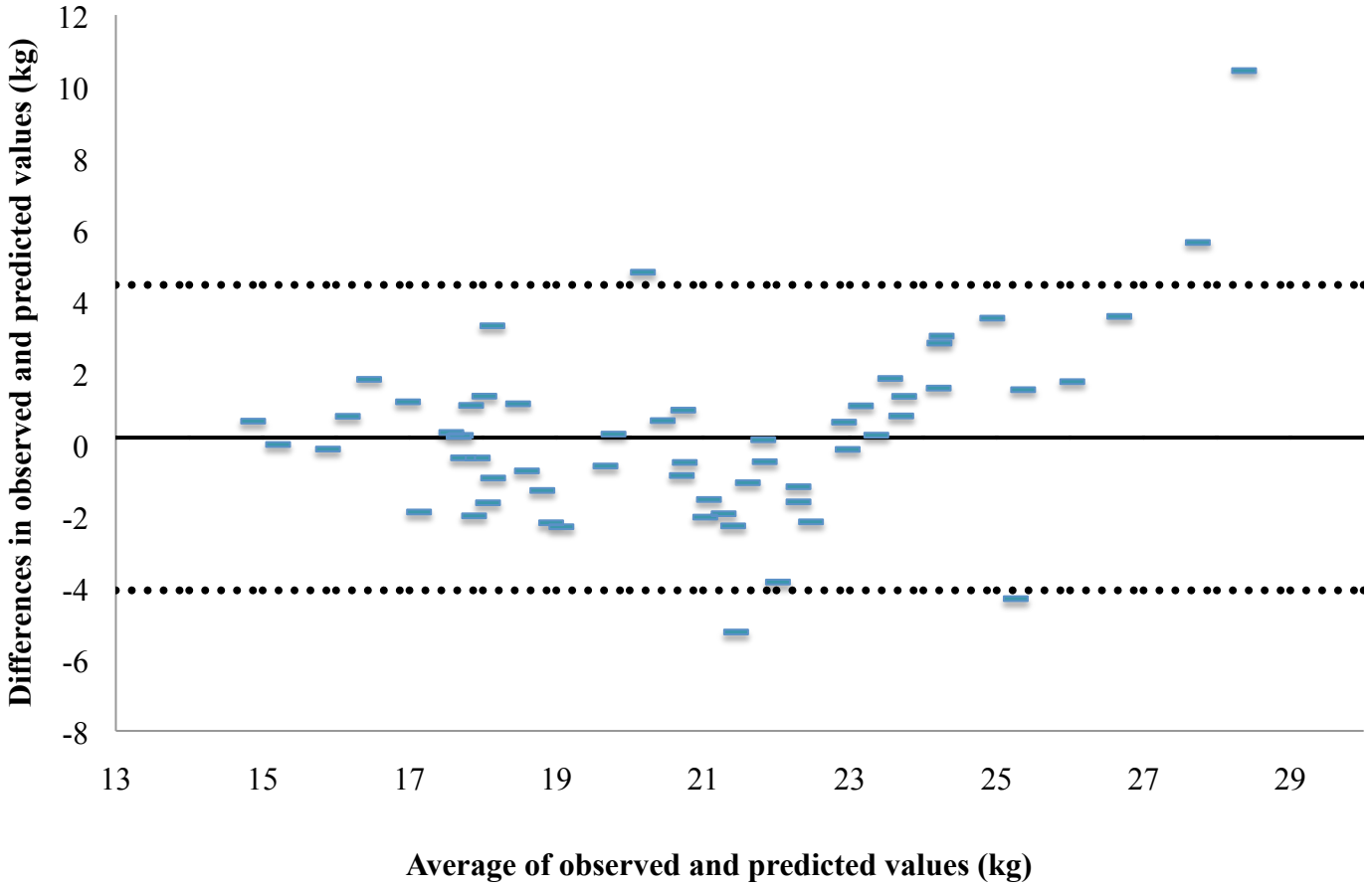

(d) Gynoid fat percentage (%)

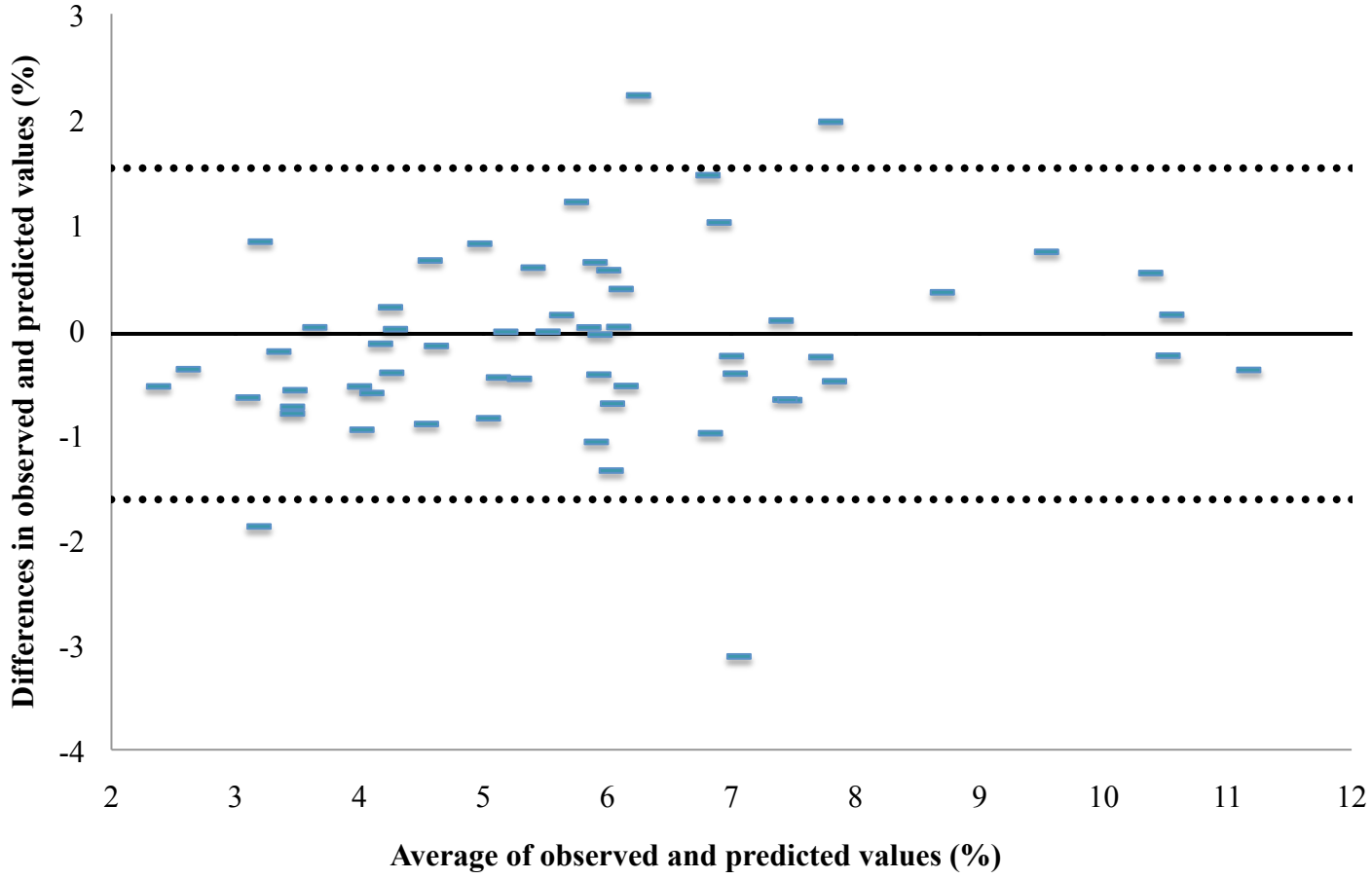

upper thigh circumference, thigh to abdomen-hip volume ratio, waist to hip ratio, waist to thigh circumference ratio, volumes of torso and abdomen-hip, and/or central obesity depth.

Torso volume, sex and central obesity depth were identified for the prediction of android fat mass (R^2=93.2%). For prediction of gynoid fat mass, upper thigh circumference, abdomen-hip volume and sex were selected (R^2=91.4%). Among the independent variables, SBI-measured thigh to abdomen-hip volume ratio, waist to hip ratio and central obesity depth were found to be the most effective parameters that explained android percent body fat, with a R^2 of 76.4%. Similarly, waist to thigh circumference ratio, upper thigh circumference and sex were identified in the stepwise multiple regression analysis for gynoid percent fat (R^2=66.5%).

Prediction Equations for Total and Regional Body Fat

The prediction equations for body fat mass (kg) computed higher prediction values (R^2 from 92.4 to 94.6%), as opposed to the prediction of percent body fat (R^2 from 64.1 to 89.9%) (**Table 4.2**). Each equation contained from three to five parameters, including sex; circumferences of upper thigh and knee; circumference ratios of waist to hip and waist to thigh; volumes of torso and thigh; volume ratios of thigh to torso, thigh to abdomen-hip; and/or central obesity depth. Total body fat exhibited the highest prediction values of 94.6 and 88.9% for fat mass and percent body fat.

Central obesity depth was the most effective parameter for predicting total body fat mass. Also, sex, thigh and torso volumes were included in the model, which resulted in the highest R^2 value of 94.6%. Parameters that explained the highest proportions of total percent body fat were central obesity depth, sex and thigh volume. Central obesity depth and thigh volume showed a positive association with total percent body fat (p<0.05). The explained proportion of the total percent body fat was 88.9%, which was the highest compared to other percent body fat models.

For the trunk fat mass, central obesity depth, torso volume and sex were included in the final model (R^2=93.9%). For the trunk percent fat, waist to hip circumference ratio and thigh to torso ratio determined by SBI were identified as crucial parameters that explained 71.0%. The direction of the standardized β-coefficients showed that having a greater waist to hip circumference ratio (β=0.54, p<0.001*)* and lower thigh to torso ratio (β=-3.56, p=0.001*)* contributed to an increase in trunk percent fat (p<0.05) (**Table 4.3**).

Circumferences of the upper thigh and knee, as well as sex, thigh to abdomen-hip volume ratio, and thigh volume were selected in the prediction model for leg fat mass (R^2 of 92.4%). Significant effects of waist to thigh circumference ratio and SBI measured thigh to abdomen-hip volume ratio were detected by regression analysis for leg percent fat, which explained 64.1% of its proportions (p<0.05).

Cross Validation for the Prediction Equations for Body Fat Mass and Percent Fat

The prediction equations that were developed for estimation of body adiposity by using the primary group were then applied to the cross-validation group in order to confirm the cross-validity of the developed mathematical models. All of the 95% intervals for the mean error (observed value – predicted value) encompassed zero, which assured that the body fat assessed via DXA and predicted body fat by the equation were not statistically different (**Table 4.2**).

Figure 4.2 depicts the mean value (solid line) and 95% limits of agreement (dotted lines) of android (**Figure 4.2a,b)** and gynoid (**Figure 4.2c,d**) fat mass and percent fat via Bland-Altman analysis to examine the absence of systematic bias between observed values assessed by DXA and predicted values computed by prediction equations. Data were randomly dispersed without distinctive patterns within the 95% limits of agreement, which ensured the validity of the prediction equations. The limits of agreement for fat mass and percent fat were – 0.06 ± 0.87 kg and – 0.11 ± 1.97 % for android and – 0.04 ± 1.58 kg and – 0.19 ± 4.27 % for gynoid, respectively (**Figure 4.2)**. A few outliers were observed in the Bland-Altman plots; however, these were not due to data error.

Discussion

The high R^2 values for the equations of android (93.2%) and gynoid (91.4%) adiposity suggested that SBI is a reliable and effective system that can be used to estimate regional body fat mass. This research was the first to develop prediction

equations for android and gynoid adiposity by incorporating body measurements derived via 3D SBI compared to DXA.

Previous studies showed that the upper body fat, such as trunk and android fat, are associated with increased obesity-related risk factors; whereas, lower body fat including thigh, leg and gynoid fat are linked with decreased risk factors (119, 131, 177-179, 189, 193). Particularly, android and gynoid fat determined by DXA showed inverse relationships with metabolic risk factors, in which android fat exhibited a positive association; whereas, gynoid fat deposition had decreased risks (131, 193). In the current research, sex was included in the prediction equations for android and gynoid fat mass, as well as gynoid percent fat, as these reflected the differences in body size and shape between men and women. Moreover, central obesity depth acquired by SBI was entered in the mathematical models for android fat mass and percent fat, implying that this parameter can be used effectively as a surrogate measurement of central obesity. Finally, upper thigh circumference was selected as one of the variables for the prediction of gynoid adiposity fat mass and percent fat. Note that these types of body measurements (upper thigh circumference) cannot be obtained easily without physical contact. The ability to create these measurements electronically reflects the practicality of SBI.

Previous studies have indicated that accumulation of percent fat in the lower body has a protective effect on adiposity-related risk factors, in comparison to fat deposition in the upper body area (130, 193, 194). For instance, large trunk fat measured via DXA was associated with increased insulin resistance in European ($r=0.40$, $p<0.05$) (177) and

elderly women (β=0.65, p<0.05) (119). Trunk fat also was related to greater fasting glucose and post-load glucose in elderly men (β=0.44, p<0.05, β=0.41, p<0.05) and women (β=0.49, p<0.05, β=0.47, p<0.05) (119). In contrast, Zhang et al. (2013) indicated that leg percent fat was negatively linked with adiposity-related risk factors including triacylglycerol, and diastolic blood pressure among adults (p<0.05) (130). Leg percent fat was associated with decreased risks for metabolic syndrome, as the odds ratios for lowest to the highest quintile was 0.22 (130). Correspondingly, Hara et al. (2004) illustrated protective effect of leg percent fat on coronary atherosclerosis while trunk percent fat was associated with increased risks for coronary atherosclerosis (194). Thus, determination of the body fat, especially total and regional body fat mass, in an easy and efficient manner via 3D SBI would improve assessment of clinical health risks.

Previous studies have utilized anthropometric body measurements to develop prediction equations for total and regional adiposity (195-200). Yavari et al. (2011) used body weight to estimate total fat mass (fat mass = 0.59 weight – 16.5; R^2=98%) and trunk fat (trunk fat = 0.32 weight – 11.1; R^2=96%) derived by DXA in women with type 2 diabetes, metabolic syndrome, and healthy participants (195). Ritchie and Davidson (2011) also used simple body measurements [weight, height, BMI, body circumferences (chest, waist, hip, upper and lower legs)] to predict regional body fat mass assessed by DXA. The R^2 for the models were 84.3 and 82.9% for chest; 85.1 and 80.4% for waist; 76.1 and 82.5% for hips; 72.6 and 73.4% for upper legs in men and women, respectively (197). In addition, Scafoglieri et al. (2013) reported the prediction equations for trunk and

leg regional adiposity. The R^2 were 92 and 94% for trunk fat mass and 91 and 86% for trunk percent fat; 94 and 85% for leg fat mass and 76 and 69% for leg percent fat in men and women, respectively (198). Prediction equations by Scafoglieri et al. (2013) utilized numerous anthropometric measurements, by manual methods, such as weight, height, 14 body circumferences via measurement tape, 13 skinfold thicknesses, and 4 bone breadths to develop the prediction equation while regional body fat was assessed by DXA (198). This degree of preciseness yields excellent results, but may not be practical for fast screening of populations.

The present research proposed mathematical equations for the prediction of total and regional (trunk, leg) adiposity (fat mass and percent fat) by integrating body measurements derived via an efficient and rapid method, a 3D photonic SBI. The R^2 of the prediction equations for total body, trunk and legs were 94.6, 93.9, and 92.4% for fat mass; and 88.9, 71.0 and 64.1% for percent body fat, respectively. These predictive values for total and regional (trunk, leg) fat mass, but not fat percentage, were relatively high compared to other equations calculated from previously reported models. This result implied that the relationship between percent body fat and SBI measured parameters were not as close as with body fat mass. These low prediction values indicate that the body parameters incorporated for the equations are not effective surrogate measurements for percent body fat. A greater number of more elaborate measurements as indicated by Scafoglieri et al. (2013) may be helpful (198).

The parameters of regional body volumes and central obesity depth that were used

in this study are unique because simple anthropometric assessment tools cannot easily discern these measurements. In particular, central obesity depth previously has been utilized as a promising indicator of abdominal obesity (149). This variable was selected as an effective predictor for fat mass of total body (R^2 change 76.8%), and trunk (R^2 change 85.7%), as well as percent body fat of total body (R^2 change 53.8%). More specifically, increased values of central obesity depth were linked closely with greater accumulation of the total and regional adiposity (trunk fat mass).

Sex was the one of the most critical components that was incorporated in most of the equations. This finding confirms the disparities of the total and regional adiposity distribution between men and women. However, age was not included in any of the prediction models due to the existence of other stronger variables that were included in the models, such as body volumes and central obesity measurements.

In the current research, measurements, such as upper thigh circumference, that cannot be easily measured were incorporated in the prediction equation models. Additionally, the prediction equations derived from this research by SBI are more practical than other methods because the parameters assessed by the photonic device did not require any physical contact between the subject and researcher. Also, subject burden during assessment is substantially reduced because a large amount of information can be collected within a one second data acquisition period, Finally, the SBI system removes concerns regarding inter and intra-rater reliability, which is problematic in traditional anthropometric measurements (39).

The 3D surface imaging of the human body has received considerable attention due to its broad range of applications, such as body composition assessment in the clothing industry (133), animation in movies and computer games (117), 3D face recognition in biometrics (201), skin scanning in dermatology and cosmetics (135), and planning and evaluation of facial and breast plastic surgery (137). In recent years, this technique has been integrated for obesity assessment as the technique is easy-to-use, safe, cost-effective, and accurate (138). This laboratory previously used 3D laser body scanner to assess body composition, including waist and hip circumferences (165), and body volume (202). The ability to measure body volume compared to hydrodensitometry was highly accurate with a correlation between these two methods of 0.99 (p<0.01) and an intraclass correlation coefficient of 0.99 (p<0.01) (202). In addition, the efficacy of body measurements derived via the 3D photonic imager has been confirmed by predicting abdominal adiposity volume assessed by MRI, as the R^2 values were 89.9, 90.4, and 71.7% for total abdominal, abdominal subcutaneous and abdominal visceral adiposity, respectively (149).

A limitation of this study was the lower prediction values for total and regional (android, gynoid, trunk, leg) percent fat (R^2 ranging from 66.5 to 88.9%), as compared to total and regional fat mass (R^2 ranging from 91.4 to 94.6%). This implies that better body measurements are required to establish mathematical models for body fat percentage. Yet, the mathematical model for percent total body fat exhibited relatively high prediction value (R^2 =88.9%), as opposed to other percent fat equations. Due to the small

sample size, men and women were combined and analyzed together to create the prediction equations. Prediction equations may have been more precise if the analysis was conducted separately. Moreover, ethnicity was not included as a factor for establishing prediction equation due to the small number of non-White Hispanics, as opposed to Caucasians.

In summary, SBI assessed body measurements were effective in developing prediction equations for android (R^2=93.2) and gynoid (R^2=91.4) body, as well as total (R^2=94.6), trunk (R^2=93.9), leg fat mass (R^2=92.4) and total body fat percentage (R^2=88.9). This study confirmed the efficacy of SBI as a reliable instrument that provides information regarding body composition in an efficient and practical manner. The strong predictive values for assessment of android and gynoid, as well as total and regional (trunk, leg) body fat mass suggest that this state-of-the-art instrument could be utilized in field settings to inform consumers on their body status and disease risks. It is believed that the ability to predict regional fat distribution via SBI in an inexpensive and easy method will be advantageous for estimating risks associated with obesity-related diseases in the general population.

CHAPTER 5. CONCLUSIONS

Outcomes of Specific Aims

The primary purpose of this research was to enhance the assessment of total, central, and regional body composition by comparing a three-dimensional (3D) stereovision body imaging (SBI) system versus the "gold standards" of magnetic resonance imaging (MRI), air displacement plethysmography (ADP), and dual-energy x-ray absorptiometry (DXA).

An innovation of this research is the utilization of SBI for body composition assessment of abdominal obesity. The SBI is low cost in comparison to other methods. It is fabricated by four pairs of monochromatic CMOS cameras (Videre Design, Menlo Park, CA; with a resolution of 1280 × 960 with four ultrashort throw NEC 575VT LCD projectors (NEC Corporation, Tokyo, Japan) (138). The projectors are required to illuminate the skin to create artificial textures on the subject, while the cameras capture the surface area of the body figure. Both cameras and projectors are interfaced with the computer, which synchronize their actions. Multiple units are needed to cover the whole body in a limited space and to produce higher resolution of images. Each stereo pair will generate a 3D surface of the covered region (138). The data acquisition time required for obtaining 3D body figures composed of more than 1 million data points is brief, as the subject remains motionless for only 200 milliseconds per scan. The 3D SBI is believed to be an effective and rapid method for the evaluation of body composition of abdominal

obesity. It easily collects diverse body measurements, including volumes, length, breadth, and central obesity parameters, via a low-cost, non-invasive method.

The first aim of the research was to develop mathematical models for the prediction of total abdominal, subcutaneous, and visceral adiposity using measurements derived via traditional anthropometrics, SBI, and a combination of both. These three different approaches for independent predictors were used to establish prediction equations for abdominal adiposity, which was the dependent variable. Equations that contained the strongest predictor variables were selected as the optimal means for predicting total abdominal, subcutaneous and visceral fat. The independent variables included (a) traditional anthropometric body measurements and demographics; (b) SBI parameters and demographics; and (c) a combination of traditional anthropometrics, SBI measurements, and demographics. The dependent variables were volumes of total abdominal, subcutaneous and visceral adiposity measured via MRI. The best total fat for abdominal adiposity prediction equation was selected by traditional anthropometrics: – 470.28 + 7.10 waist circumference – 91.01 sex + 5.74 sagittal diameter. The associated R^2 was 89.9%. For subcutaneous adiposity, the best fat prediction equation was produced by a combination method of traditional anthropometrics and SBI: – 172.37 + 8.57 waist circumference – 62.65 sex – 450.16 stereovision waist-to-hip ratio. This combination method had a R^2 of 90.4%. For visceral adiposity, the best fat prediction equation was established by a SBI method that included the sex of the person: – 96.76 + 11.48 central obesity depth – 5.09 central obesity width + 204.74 stereovision waist-to-hip ratio –

18.59 sex. The corresponding R^2 was 71.7%.

The use of SBI did not improve the R^2 for the total abdominal and subcutaneous adiposity equation models. Yet the prediction values for visceral adiposity increased significantly when parameters derived via SBI were applied to the equations. It should be noted that the final prediction equation for visceral adiposity has two parameters unique to SBI: central obesity width and central obesity depth. It is of great significance that an assessment of visceral adiposity can be made by SBI, as it is very difficult to measure in a low-cost manner. These findings conclude that mathematical equations derived from body measurements obtained by SBI were sufficient predictors of visceral adiposity, the most difficult fat deposition to quantify without utilizing advanced techniques.

The second aim was to determine body size and shape via total/regional body volume and volume ratios assessed by SBI in men and women. The body volumes and body volume ratios, including upper- and lower-body volume ratios, were measured to determine the body size and shape of men and women according to body mass index (BMI) classification and the risks associated with accumulation of visceral adiposity. Men showed higher total body (80.95 L vs. 72.41 L), torso (39.26 L vs. 34.13 L), and abdomen-hip (29.01 L vs. 25.85 L) volumes, and waist circumference (95.21 cm vs. 88.46 cm), as compared to women. Women exhibited greater thigh volumes (4.93 L vs. 3.99 L), hip circumference (112.56 cm vs. 106.68 cm), and lower body-volume ratios [thigh to total body (0.07 vs. 0.05), thigh to torso (0.15 vs. 0.11), and thigh to abdomen-hip (4.93 vs. 4.00); $p<0.05$]. Thigh to torso [odds ratios (OR) 0.44] and abdomen-hip (OR

0.41) volume ratios were associated with decreased risks of accumulating visceral adiposity, even after age, sex, and BMI were taken into account. The innovation of this aim was to utilize the volumes in segments of specific regions of the body via SBI. The body measurements assessed via SBI provided an effective method for determining body size and shape in men and women, as well as for prediction of visceral adiposity deposition in both sexes.

The third aim was to examine the efficacy of SBI for assessment of android and gynoid fat adiposity. Body circumferences, volumes, and volume ratios, as measured via stereovision body imaging, were utilized to develop mathematical models to predict android and gynoid fat mass and percent fat. The validity of these measures of adiposity was tested by comparisons to values that were determined by DXA. SBI body parameters that were used for independent variables consisted of ratios of waist to hip, waist to thigh circumferences; circumferences of waist, hip, upper thigh, lower thigh and knee; volumes of total body, torso, abdomen-hip, and thigh; volume ratios of torso to total body, abdomen-hip to total body, thigh to total body, abdomen-hip to torso, thigh to torso and thigh to abdomen-hip; as well as central obesity depth and width. Demographic parameters (age, sex) also were included as independent variables for the establishment of the prediction models.

The prediction values of the mathematical equations for fat mass and percent body fat were 93.2% and 76.4% for android, and 91.4% and 66.5% for gynoid, respectively. The body measurements derived via SBI were more effective for creating

prediction models for android and gynoid fat mass, as opposed to fat percentages. The high prediction values for total and regional body fat mass indicated that the SBI is a reliable device that can be used for the estimation of body fat mass, but less so for body fat percentage.

Conclusions and Future Directions

Knowledge of specific shapes and sizes of bodies and segments, with varying distribution of total, central and regional fat distribution, may provide beneficial information regarding obesity-related risk factors. The utilization of SBI in the present research enabled the effective assessment of total, central, and regional adiposity for fat mass.

An advantage of SBI is that it is an efficient and reliable instrument that can replace some traditional manual methods to measure various body composition (body circumferences, volumes and lengths) in a rapid manner without the awkwardness that results from the close proximity between the researcher and subject. SBI is easy to fabricate, as it is built with only four pairs of cameras and four projectors. This permits portability of the instrument and makes it ideal for large scale epidemiological studies that requires assessment of numbers of subjects in different locations. The use of SBI for assessment of body size and shape would be a paradigm-shift that provides more practical and cost-efficient means than that currently available by CT, MRI or DXA. For example, the estimated cost for a SBI system is about $10,000, as opposed to several hundred thousand

dollars for other assessment instruments. The ability to accurately estimate total, central and regional adiposity, in particular, would provide health practitioners an enhanced ability to assess and monitor types of obesity.

Nonetheless, a limitation of this research was the prediction values for total and regional (android, gynoid) body fat percentage (76.4% for android, 66.5% for gynoid), as compared to regional fat mass (93.2% for android, 91.4% for gynoid). The lower prediction values for total and regional percent body fat imply that better body measurements are required to establish mathematical models for body fat percentage.

Only Caucasians and non-White Hispanics were included in the subject sample, which suggests that the prediction equations that were developed in this study may not be applicable for other ethnicities, such as Asians or African-Americans. Although SBI can be used in more broad ranges of BMI classification, only healthy weight, overweight, and obese class I participants were recruited in the study in order to form a homogenous group to reduce the variation within the group. This restriction was due to the funding limitations of the grants. Any inferences regarding body size and shape that were associated with age could not be made due to the small sample size within each age group. Moreover, inflammation or metabolic blood markers were not tested in this research, which made it such that researchers were unable to explore the direct associations between SBI assessed body composition or equations and obesity-related risk factors.

The future direction of 3D SBI would be to continue to refine the technique so that a better prediction of percent body fat could be achieved. Also, the research could be expanded to include a broader range of ethnicities, BMIs, and ages to explore the disparities of body size and shape in diverse populations. Particularly, it is believed that SBI could be used for monitoring infant/adolescence growth and development, tracking body size and shape after a patient is diagnosed with certain diseases, or following the application of a new therapy. Finally, monitoring body composition changes according to different types of physical activity (i.e. resistance training versus aerobic) would be helpful for researchers, as well as for the individuals. Knowledge of the precise change in body size and weight could be used as motivations for the individuals to pursue their goals for weight loss and/or maintaining a healthy weight.

In summary, the long-term future of SBI is promising for the assessment of total, central (total abdominal, subcutaneous, visceral), and regional fat mass (android, gynoid), but less so for percent fat at this time. An improved understanding of human body composition was achieved through state-of-the-art 3D SBI and other advanced techniques (MRI, DXA, ADP) tested in this research. This information in this dissertation will provide guidance for researchers and health care practitioners in the assessment of obesity.

REFERENCES

1 Kurukulasuriya LR, Stas S, Lastra G, Manrique C, Sowers JR. Hypertension in obesity. *Med Clin North Am* 2011;95:903-17.

2 Franssen R, Monajemi H, Stroes ES, Kastelein JJ. Obesity and dyslipidemia. *Med Clin North Am* 2011;95:893-902.

3 Logue J, Murray HM, Welsh P*, et al.* Obesity is associated with fatal coronary heart disease independently of traditional risk factors and deprivation. *Heart* 2011;97:564-8.

4 Nguyen NT, Nguyen XM, Lane J, Wang P. Relationship between obesity and diabetes in a US adult population: findings from the National Health and Nutrition Examination Survey, 1999-2006. *Obes Surg* 2011;21:351-5.

5 Mond J, van den Berg P, Boutelle K, Hannan P, Neumark-Sztainer D. Obesity, body dissatisfaction, and emotional well-being in early and late adolescence: findings from the project EAT study. *J Adolesc Health* 2011;48:373-8.

6 Keating CL, Peeters A, Swinburn BA, Magliano DJ, Moodie ML. Utility-based quality of life associated with overweight and obesity: the Australian diabetes, obesity, and lifestyle study. *Obesity (Silver Spring)* 2013;21:652-5.

7 Griffiths LJ, Parsons TJ, Hill AJ. Self-esteem and quality of life in obese children and adolescents: a systematic review. *Int J Pediatr Obes* 2010;5:282-304.

8 National Center for Health Statistics. Health, United States, 2012: With Special Feature on Emergency Care. Hyattsville, MD. 2013.

9 Ogden CL, Carroll MD, Kit BK, Flegal KM. Prevalence of obesity among adults: United States, 2011-2012. *NCHS Data Brief* 2013;1-8.

10 Sturm R, Hattori A. Morbid obesity rates continue to rise rapidly in the United States. *Int J Obes (Lond)* 2013;37:889-91.

11 WHO. Physical status: the use and interpretation of anthropometry. Report of a WHO Expert Committee. WHO Technical Report Series 854. Geneva: World Health Organization, 1995.

12 WHO. Obesity: preventing and managing the global epidemic. Report of a WHO Consultation. WHO Technical Report Series 894. Geneva: World Health Organization, 2000.

13 Wilson PW, D'Agostino RB, Sullivan L, Parise H, Kannel WB. Overweight and obesity as determinants of cardiovascular risk: the Framingham experience. *Arch Intern Med* 2002;162:1867-72.

14 Field AE, Coakley EH, Must A*, et al.* Impact of overweight on the risk of developing common chronic diseases during a 10-year period. *Arch Intern Med* 2001;161:1581-6.

15 Must A, Spadano J, Coakley EH, Field AE, Colditz G, Dietz WH. The disease burden associated with overweight and obesity. *JAMA* 1999;282:1523-9.

16 Ian Janssen SBH, David B Allison, Donald P Kotler, and Robert Ross. Body mass index and waist circumference independently contribute to the prediction of nonabdominal, abdominal subcutaneous, and visceral fat. *Am J Clin Nutr* 2002.

17 Tirosh A, Shai I, Afek A*, et al.* Adolescent BMI trajectory and risk of diabetes versus coronary disease. *N Engl J Med* 2011;364:1315-25.

18 Nevill AM, Stewart AD, Olds T, Holder R. Relationship between adiposity and body size reveals limitations of BMI. *Am J Phys Anthropol* 2006;129:151-6.

19 Heymsfield SB, Scherzer R, Pietrobelli A, Lewis CE, Grunfeld C. Body mass index as a phenotypic expression of adiposity: quantitative contribution of muscularity in a population-based sample. *Int J Obes (Lond)* 2009;33:1363-73.

20 Goodpaster BH, Krishnaswami S, Harris TB*, et al.* Obesity, regional body fat distribution, and the metabolic syndrome in older men and women. *Arch Intern Med* 2005;165:777-83.

21 Bioelectrical impedance analysis in body composition measurement: National Institutes of Health Technology Assessment Conference Statement. *Am J Clin Nutr* 1996;64:524S-32S.

22 Brodie D, Moscrip V, Hutcheon R. Body composition measurement: a review of hydrodensitometry, anthropometry, and impedance methods. *Nutrition* 1998;14:296-310.

23 Ribeiro-Filho FF, Faria AN, Azjen S, Zanella MT, Ferreira SR. Methods of estimation of visceral fat: advantages of ultrasonography. *Obes Res* 2003;11:1488-94.

24 Ginde SR, Geliebter A, Rubiano F*, et al.* Air displacement plethysmography: validation in overweight and obese subjects. *Obes Res* 2005;13:1232-7.

25 Pietrobelli A, Wang Z, Formica C, Heymsfield SB. Dual-energy X-ray absorptiometry: fat estimation errors due to variation in soft tissue hydration. *Am J Physiol* 1998;274:E808-16.

26 Camhi SM, Bray GA, Bouchard C*, et al.* The relationship of waist circumference and BMI to visceral, subcutaneous, and total body fat: sex and race differences. *Obesity (Silver Spring)* 2011;19:402-8.

27 Lee SY, Gallagher D. Assessment methods in human body composition. *Curr Opin Clin Nutr Metab Care* 2008;11:566-72.

28 Lohman T. Skinfolds and body density and their relation to body fatness: A review. *Hum Bio* 1981;53:181-225.

29 Jackson A, Pollock M, Graves J, Mahar M. Reliability and validity of bioelectrical impedance in determining body composition. *J Appl Physiol* 1988;64:529-34.

30 Seip R, Weltman A. Validity of skinfold and girth based regression equations for the prediction of body composition in obese adults. *Am J Hum Bio* 1991;3:91-5.

31 Weltman A, Seip R, Tran L, Zung V. Practical assessment of body composition in adult obese males. *Hum Bio* 1987;59:523-35.

32 Weltman A, Levine S, Seip R, Tran Z. Accurate assessment of body composition in obese females. *Am J Clin Nutr* 1988;48:1179-83.

33 Tran Z, Weltman A. Generalized equation for predicting body density of women from girth measurements. *Med Sci Sports Exerc* 1989;21:101-4.

34 Zamboni M, Turcato E, Armellini F*, et al.* Sagittal abdominal diameter as a practical predictor or visceral fat. *International Journal of Obesity and Related Metabolic Disorders* 1998;22.

35 Ohrvall M, Berglund L, Vessby B. Sagital abdominal diameter compared with other anthropometric measurements in relation to cardiovascular risk. *International Journal of Obesity and Related Metabolic Disorders* 2004;24:497-501.

36 Thomasett A. Bio-electrical properties of tissue impedance measurements. *Lyon Medical* 1962;207:107-18.

37 Hoffer E, Meador C, Simpson D. Correlation of whole-body impedance with total body water volume. *J Appl Physiol* 1969;27:531-4.

38 Houtkooper L, Lohman T, SB G, WH H. Why bioelectrical impedance analysis should be used for estimating adiposity. *Am J Clin Nutr* 1996;64:436S-48S.

39 Wang J, Thornton JC, Bari S*, et al.* Comparisons of waist circumferences measured at 4 sites. *Am J Clin Nutr* 2003;77:379-84.

40 Houtkooper LB, Lohman TG, Going SB, Howell WH. Why bioelectrical impedance analysis should be used for estimating adiposity. *Am J Clin Nutr* 1996;64:436S-48S.

41 Hoffer EC, Meador CK, Simpson DC. Correlation of whole-body impedance with total body water volume. *J Appl Physiol* 1969;27:531-4.

42 Deurenberg P. Limitations of the bioelectrical impedance method for the assessment of body fat in severe obesity. *Am J Clin Nutr* 1996;64:449S-52S.

43 Brozek J, Grande F, Anderson JT, Keys A. Densitometric Analysis of Body Composition: Revision of Some Quantitative Assumptions. *Ann N Y Acad Sci* 1963;110:113-40.

44 Siri WE. Body composition from fluid spaces and density: analysis of methods. In: Brožek J, Henschel A (eds) Techniques for measuring body composition. Washington DC: Natl AcadSciences/Natl Res Council 1961;223-24.

45 Lohman, TG. Assessment of body composition in children. Pediatr Exerc Sci 1986;1:19-30.

46 Ortiz, O, Russell, M, Daley, TL, Baumgartner, RN, Waki, M, et al. Differences in skeletal muscle and bone mineral mass between black and white females and their relevance to estimates of body composition. Am J Clin Nutr 1992;55:8-13.

47 Schutte, JE, Townsend, EJ, Hugg, J, et al. Density of lean body mass is greater in blacks than whites. J Appl Physiol, 1984;56;1647-1649.

48 Pollock ML, Laughridge EE, Coleman B, Linnerud AC, Jackson A. Prediction of body density in young and middle-aged women. *J Appl Physiol* 1975;38:745-9.

49 Lockner DW, Heyward VH, Baumgartner RN, Jenkins KA. Comparison of air-displacement plethysmography, hydrodensitometry, and dual X-ray absorptiometry for assessing body composition of children 10 to 18 years of age. *Ann N Y Acad Sci* 2000;904:72-8.

50 Fogli JJ. Measuring body composition: keeping up with an increasingly obese population. *Obes Res* 2005;13:1134.

51 Bisset R, Khan AN. *Differential diagnosis in abdominal ultrasound*. Elsevier India 2002.

52 Merino-Ibarra E, Artieda M, Cenarro A*, et al.* Ultrasonography for the evaluation of visceral fat and the metabolic syndrome. *Metabolism* 2005;54:1230-5.

53 Koda M, Tsuzuku S, Ando F, Niino N, Shimokata H. Body composition by air displacement plethysmography in middle-aged and elderly Japanese. Comparison with dual-energy X-ray absorptiometry. *Ann N Y Acad Sci* 2000;904:484-8.

54 Biaggi RR, Vollman MW, Nies MA*, et al.* Comparison of air-displacement plethysmography with hydrostatic weighing and bioelectrical impedance analysis for the assessment of body composition in healthy adults. *Am J Clin Nutr* 1999;69:898-903.

55 Dempster P, Aitkens S. A new air displacement method for the determination of human body composition. Med Sci Sports Exerc 1995;27:1692-7.

56 Brožek J, Grande F, Anderson JT, Keys A. Densitometric analysis of body composition: revision of some quantitative assumptions. Ann N Y Acad Sci 1961;110:113-40.

57 Anthropometry Procedures Manual. http://www.cdc.gov/nchs/data/nhanes/bm.pdf 2007.

58 Pietrobelli A, Formica C, Wang Z, Heymsfield SB. Dual-energy X-ray absorptiometry body composition model: review of physical concepts. *Am J Physiol* 1996;271:E941-51.

59 Sjostrom L. A computer-tomography based multi-compartment body composition technique and anthropometric predictions of lean body mass, total and subcutaneous adipose tissue. *Int J Obes (Lond)* 1991;15:19-30.

60 Ross R, Shaw K, Martel Y, de Guise J, Avruch L. Quantification of adipose tissue by MRI: Relationship with anthropometric variables. *J Appl Physiol* 1992;72:384-9.

61 Wagner DR, Heyward VH. Techniques of body composition assessment: a review of laboratory and field methods. *Res Q Exerc Sport* 1999;70:135-49.

62 Mazess RB, Barden HS, Bisek JP, Hanson J. Dual-energy x-ray absorptiometry for total-body and regional bone-mineral and soft-tissue composition. *Am J Clin Nutr* 1990;51:1106-12.

63 Schoeller D, Tylavsky F, Baer D*, et al.* QDR 4500A dual energy X-ray absorptiometer underestimates fat mass in comparison with criterion methods in adults. *Am J Clin Nutr* 2005;82:1018-25.

64 Weyers AM, Mazzetti SA, Love DM, Gomez AL, Kraemer WJ, Volek JS. Comparison of methods for assessing body composition changes during weight loss. *Med Sci Sports Exerc* 2002;34:497-502.

65 Schoeller DA, Tylavsky FA, Baer DJ*, et al.* QDR 4500A dual-energy X-ray absorptiometer underestimates fat mass in comparison with criterion methods in adults. *Am J Clin Nutr* 2005;81:1018-25.

66 Visser M, Fuerst T, Lang T, Salamone L, Harris TB. Validity of fan-beam dual-energy X-ray absorptiometry for measuring fat-free mass and leg muscle mass. Health, Aging, and Body Composition Study--Dual-Energy X-ray Absorptiometry and Body Composition Working Group. *J Appl Physiol (1985)* 1999;87:1513-20.

67 Tylavsky F, Lohman T, Blunt BA*, et al.* QDR 4500A DXA overestimates fat-free mass compared with criterion methods. *J Appl Physiol (1985)* 2003;94:959-65.

68 Sardinha LB, Lohman TG, Teixeira PJ, Guedes DP, Going SB. Comparison of air displacement plethysmography with dual-energy X-ray absorptiometry and 3 field methods for estimating body composition in middle-aged men. *Am J Clin Nutr* 1998;68:786-93.

69 Guo Y, Franks PW, Brookshire T, Antonio Tataranni P. The intra- and inter-instrument reliability of DXA based on ex vivo soft tissue measurements. *Obes Res* 2004;12:1925-9.

70 Huettel S, Song A, MaCarthy G. *Functional magnetic resonance imaging*. Sinauer Associates: Sunderland, MA; 2004.

71 Fox CS, Massaro JM, Hoffmann U*, et al.* Abdominal visceral and subcutaneous adipose tissue compartments: association with metabolic risk factors in the Framingham Heart Study. *Circulation* 2007;116:39-48.

72 Wajchenberg BL. Subcutaneous and visceral adipose tissue: their relation to the metabolic syndrome. *Endocr Rev* 2000;21:697-738.

73 Phillips LK, Prins JB. The link between abdominal obesity and the metabolic syndrome. *Curr Hypertens Rep* 2008;10:156-64.

74 Despres JP, Lemieux I, Bergeron J*, et al.* Abdominal obesity and the metabolic syndrome: contribution to global cardiometabolic risk. *Arterioscler Thromb Vasc Biol* 2008;28:1039-49.

75 Britton KA, Fox CS. Ectopic fat depots and cardiovascular disease. *Circulation* 2011;124:e837-41.

76 Sardinha LB, Teixeira PJ, Guedes DP, Going SB, Lohman TG. Subcutaneous central fat is associated with cardiovascular risk factors in men independently of total fatness and fitness. *Metabolism* 2000;49:1379-85.

77 Kanaya AM, Harris T, Goodpaster BH*, et al.* Adipocytokines attenuate the association between visceral adiposity and diabetes in older adults. *Diabetes Care* 2004;27:1375-80.

78 Hayashi T, Boyko EJ, Leonetti DL*, et al.* Visceral adiposity is an independent predictor of incident hypertension in Japanese Americans. *Ann Intern Med* 2004;140:992-1000.

79 Montani JP, Carroll JF, Dwyer TM, Antic V, Yang Z, Dulloo AG. Ectopic fat storage in heart, blood vessels and kidneys in the pathogenesis of cardiovascular diseases. *Int J Obes Relat Metab Disord* 2004;28 Suppl 4:S58-65.

80 Jeong JW, Jeong MH, Yun KH*, et al.* Echocardiographic epicardial fat thickness and coronary artery disease. *Circ J* 2007;71:536-9.

81 Lim S, Meigs JB. Ectopic fat and cardiometabolic and vascular risk. *Int J Cardiol* 2013;169:166-76.

82 Despres JP, Lemieux I. Abdominal obesity and metabolic syndrome. *Nature* 2006;444:881-7.

83 Aasen G, Fagertun H, Halse J. Regional fat mass by DXA: high leg fat mass attenuates the relative risk of insulin resistance and dyslipidaemia in obese but not in overweight postmenopausal women. *Scand J Clin Lab Invest* 2008;68:204-11.

84 Preis SR, Massaro JM, Robins SJ*, et al.* Abdominal subcutaneous and visceral adipose tissue and insulin resistance in the Framingham heart study. *Obesity (Silver Spring)* 2010;18:2191-8.

85 Taylor AE, Ebrahim S, Ben-Shlomo Y*, et al.* Comparison of the associations of body mass index and measures of central adiposity and fat mass with coronary heart disease, diabetes, and all-cause mortality: a study using data from 4 UK cohorts. *Am J Clin Nutr* 2010;91:547-56.

86 Bradlee ML, Singer MR, Qureshi MM, Moore LL. Food group intake and central obesity among children and adolescents in the Third National Health and Nutrition Examination Survey (NHANES III). *Public Health Nutr* 2010;13:797-805.

87 Pouliot MC, Despres JP, Lemieux S*, et al.* Waist circumference and abdominal sagittal diameter: best simple anthropometric indexes of abdominal visceral adipose

tissue accumulation and related cardiovascular risk in men and women. *Am J Cardiol* 1994;73:460-8.

88 Theorell-Haglow J, Berne C, Janson C, Sahlin C, Lindberg E. Associations between short sleep duration and central obesity in women. *Sleep* 2010;33:593-8.

89 Rexrode KM, Carey VJ, Hennekens CH*, et al.* Abdominal adiposity and coronary heart disease in women. *JAMA* 1998;280:1843-8.

90 Ashwell M, Gunn P, Gibson S. Waist-to-height ratio is a better screening tool than waist circumference and BMI for adult cardiometabolic risk factors: systematic review and meta-analysis. *Obes Rev* 2012;13:275-86.

91 Waist circumference and waist–hip ratio: report of a WHO expert consultation G, 8–11, 2008.

92 Obesity in Asia C, Huxley R, Barzi F*, et al.* Waist circumference thresholds provide an accurate and widely applicable method for the discrimination of diabetes. *Diabetes Care* 2007;30:3116-8.

93 Huxley R, Mendis S, Zheleznyakov E, Reddy S, Chan J. Body mass index, waist circumference and waist:hip ratio as predictors of cardiovascular risk--a review of the literature. *Eur J Clin Nutr* 2010;64:16-22.

94 Koster A, Leitzmann MF, Schatzkin A*, et al.* Waist circumference and mortality. *Am J Epidemiol* 2008;167:1465-75.

95 Ohrvall M, Berglund L, Vessby B. Sagittal abdominal diameter compared with other anthropometric measurements in relation to cardiovascular risk. *Int J Obes Relat Metab Disord* 2000;24:497-501.

96 Sampaio LR, Simoes EJ, Assis AM, Ramos LR. Validity and reliability of the sagittal abdominal diameter as a predictor of visceral abdominal fat. *Arq Bras Endocrinol Metabol* 2007;51:980-6.

97 Koren D, Marcus CL, Kim C*, et al.* Anthropometric predictors of visceral adiposity in normal-weight and obese adolescents. *Pediatr Diabetes* 2013;14:575-84.

98 Iribarren C, Darbinian JA, Lo JC, Fireman BH, Go AS. Value of the sagittal abdominal diameter in coronary heart disease risk assessment: cohort study in a large, multiethnic population. *Am J Epidemiol* 2006;164:1150-9.

99 de Souza NC, de Oliveira EP. Sagittal abdominal diameter shows better correlation with cardiovascular risk factors than waist circumference and BMI. *J Diabetes Metab Disord* 2013;12:41.

100 Hoenig MR. MRI sagittal abdominal diameter is a stronger predictor of metabolic syndrome than visceral fat area or waist circumference in a high-risk vascular cohort. *Vasc Health Risk Manag* 2010;6:629-33.

101 Valsamakis G, Chetty R, Anwar A, Banerjee AK, Barnett A, Kumar S. Association of simple anthropometric measures of obesity with visceral fat and the metabolic syndrome in male Caucasian and Indo-Asian subjects. *Diabet Med* 2004;21:1339-45.

102 Vazquez G, Duval S, Jacobs DR, Jr., Silventoinen K. Comparison of body mass index, waist circumference, and waist/hip ratio in predicting incident diabetes: a meta-analysis. *Epidemiol Rev* 2007;29:115-28.

103 Price GM, Uauy R, Breeze E, Bulpitt CJ, Fletcher AE. Weight, shape, and mortality risk in older persons: elevated waist-hip ratio, not high body mass index, is associated with a greater risk of death. *Am J Clin Nutr* 2006;84:449-60.

104 Hsieh SD, Yoshinaga H. Abdominal fat distribution and coronary heart disease risk factors in men-waist/height ratio as a simple and useful predictor. *Int J Obes Relat Metab Disord* 1995;19:585-9.

105 Lee CM, Huxley RR, Wildman RP, Woodward M. Indices of abdominal obesity are better discriminators of cardiovascular risk factors than BMI: a meta-analysis. *J Clin Epidemiol* 2008;61:646-53.

106 Browning LM, Hsieh SD, Ashwell M. A systematic review of waist-to-height ratio as a screening tool for the prediction of cardiovascular disease and diabetes: 0.5 could be a suitable global boundary value. *Nutr Res Rev* 2010;23:247-69.

107 Parikh RM, Joshi SR, Menon PS, Shah NS. Index of central obesity - A novel parameter. *Med Hypotheses* 2007;68:1272-5.

108 Sebo P, Beer-Borst S, Haller DM, Bovier PA. Reliability of doctors' anthropometric measurements to detect obesity. *Prev Med* 2008;47:389-93.

109 Freedman DS, Katzmarzyk PT, Dietz WH, Srinivasan SR, Berenson GS. Relation of body mass index and skinfold thicknesses to cardiovascular disease risk factors in children: the Bogalusa Heart Study. *Am J Clin Nutr* 2009;90:210-6.

110 Mason C, Katzmarzyk PT. Effect of the site of measurement of waist circumference on the prevalence of the metabolic syndrome. *Am J Cardiol* 2009;103:1716-20.

111 Mason C, Katzmarzyk PT. Variability in waist circumference measurements according to anatomic measurement site. *Obesity (Silver Spring)* 2009;17:1789-95.

112 Ross R, Berentzen T, Bradshaw AJ*, et al.* Does the relationship between waist circumference, morbidity and mortality depend on measurement protocol for waist circumference? *Obes Rev* 2008;9:312-25.

113 Bosy-Westphal A, Booke CA, Blocker T*, et al.* Measurement site for waist circumference affects its accuracy as an index of visceral and abdominal subcutaneous fat in a Caucasian population. *J Nutr* 2010;140:954-61.

114 Ryo M, Maeda K, Onda T*, et al.* A new simple method for the measurement of visceral fat accumulation by bioelectrical impedance. *Diabetes Care* 2005;28:451-3.

115 Haslam D, Sattar N, Lean M. ABC of obesity. Obesity--time to wake up. *BMJ* 2006;333:640-2.

116 Ludescher B, Machann J, Eschweiler GW*, et al.* Correlation of fat distribution in whole body MRI with generally used anthropometric data. *Invest Radiol* 2009;44:712-9.

117 Magnenat-Thalmann N, Seo H, Cordier F. Automatic modeling of animatable virtual humans: A survey. Fourth International Conference on 3-D Digital Imaging and Modeling:2-10.

118 Goodpaster BH, Thaete FL, Kelley DE. Thigh adipose tissue distribution is associated with insulin resistance in obesity and in type 2 diabetes mellitus. *Am J Clin Nutr* 2000;71:885-92.

119 Snijder MB, Dekker JM, Visser M*, et al.* Trunk fat and leg fat have independent and opposite associations with fasting and postload glucose levels: the Hoorn study. *Diabetes Care* 2004;27:372-7.

120 Aasen G, Fagertun H, Tonstad S, Halse J. Leg fat mass as measured by dual X-ray absorptiometry (DXA) impacts insulin resistance differently in obese women versus men. *Scand J Clin Lab Invest* 2009;69:181-9.

121 Park JS, Cho MH, Ahn CW, Kim KR, Huh KB. The association of insulin resistance and carotid atherosclerosis with thigh and calf circumference in patients with type 2 diabetes. *Cardiovasc Diabetol* 2012;11:62.

122 Van Pelt RE, Jankowski CM, Gozansky WS, Schwartz RS, Kohrt WM. Lower-body adiposity and metabolic protection in postmenopausal women. *J Clin Endocrinol Metab* 2005;90:4573-8.

123 Heitmann BL, Frederiksen P. Thigh circumference and risk of heart disease and premature death: prospective cohort study. *BMJ* 2009;339:b3292.

124 Peppa M, Koliaki C, Hadjidakis DI*, et al.* Regional fat distribution and cardiometabolic risk in healthy postmenopausal women. *Eur J Intern Med* 2013;24:824-31.

125 Van Pelt RE, Evans EM, Schechtman KB, Ehsani AA, Kohrt WM. Contributions of total and regional fat mass to risk for cardiovascular disease in older women. *Am J Physiol Endocrinol Metab* 2002;282:E1023-8.

126 Smith DA, Ness EM, Herbert R*, et al.* Abdominal diameter index: a more powerful anthropometric measure for prevalent coronary heart disease risk in adult males. *Diabetes Obes Metab* 2005;7:370-80.

127 Lissner L, Bjorkelund C, Heitmann BL, Seidell JC, Bengtsson C. Larger hip circumference independently predicts health and longevity in a Swedish female cohort. *Obes Res* 2001;9:644-6.

128 Seidell JC, Han TS, Feskens EJ, Lean ME. Narrow hips and broad waist circumferences independently contribute to increased risk of non-insulin-dependent diabetes mellitus. *J Intern Med* 1997;242:401-6.

129 Seidell JC, Perusse L, Despres JP, Bouchard C. Waist and hip circumferences have independent and opposite effects on cardiovascular disease risk factors: the Quebec Family Study. *Am J Clin Nutr* 2001;74:315-21.

130 Zhang X, Hu EA, Wu H, Malik V, Sun Q. Associations of leg fat accumulation with adiposity-related biological factors and risk of metabolic syndrome. *Obesity (Silver Spring)* 2013;21:824-30.

131 Fu X, Song A, Zhou Y*, et al.* Association of regional body fat with metabolic risks in Chinese women. *Public Health Nutr* 2013;1-9.

132 Keckeisen M, Stoev S, Feurer M, Strasser W. Interactive cloth simulation in virtual environments. IEEE Virtual Reality Conference, 2003;71-8.

133 Paquette S. 3D scanning in apparel design and human engineering. IEEE Computer Graphics and Applications 1996;16:11-5.

134 Medioni G, Waupotitsch R. Face recognition and modeling in 3D. IEEE International Workshop on Analysis and Modeling of Faces and Gestures, 2003:232-3.

135 Lagarde J, Rouvraise C, Black D, Diridollou S, Gall Y. Skin topography measurement by interference fringe projection: A technical validation. Skin Res Technol 2001;7:112-21.

136 Lee S. Three-dimensional photography and its application to facial plastic surgery. Arch Facial Plastic Surg 2004;6:410-4.

137 Galdino M, Nahabedian M, Chiaramonte M, Geng J, Klatsky S, Manson P. Clinical applications of three-dimensional photography in breast surgery. Plastic Reconstr Surg 2002;110:58-70.

138 Xu B, Yu W, Yao M, Pepper MR, Freeland-Graves JH. Three-dimensional surface imaging system for assessing human obesity. *Opt Eng* 2009;48:nihpa156427.

139 Wells JC, Douros I, Fuller NJ, Elia M, Dekker L. Assessment of body volume using three-dimensional photonic scanning. *Ann N Y Acad Sci* 2000;904:247-54.

140 Wells JC, Cole TJ, Bruner D, Treleaven P. Body shape in American and British adults: between-country and inter-ethnic comparisons. *Int J Obes (Lond)* 2008;32:152-9.

141 Wells JC, Charoensiriwath S, Treleaven P. Reproduction, aging, and body shape by three-dimensional photonic scanning in Thai men and women. *Am J Hum Biol* 2011;23:291-8.

142 Wells JC, Treleaven P, Cole TJ. BMI compared with 3-dimensional body shape: the UK National Sizing Survey. *Am J Clin Nutr* 2007;85:419-25.

143 Wells JC, Cole TJ, Treleaven P. Age-variability in body shape associated with excess weight: the UK National Sizing Survey. *Obesity (Silver Spring)* 2008;16:435-41.

144 Liu TH, Chiou WK, Lin JD, Yu CY. Implementation of whole body scanner for determining somatotype index at Chang Gung Memorial Hospital. *Chang Gung Med J* 2001;24:697-707.

145 Lin JD, Chiou WK, Weng HF, Tsai YH, Liu TH. Comparison of three-dimensional anthropometric body surface scanning to waist-hip ratio and body mass index in correlation with metabolic risk factors. *J Clin Epidemiol* 2002;55:757-66.

146 Lin JD, Chiou WK, Weng HF, Fang JT, Liu TH. Application of three-dimensional body scanner: observation of prevalence of metabolic syndrome. *Clin Nutr* 2004;23:1313-23.

147 Chuang YC, Wang MH, Huang DH, Yang CH, Lin JD. To construct a forecasting model of the anthropometric chronic disease risk factor score. *Chang Gung Med J* 2006;29:135-42.

148 Yu W, Xu B. A Portable Stereo Vision System for Whole Body Surface Imaging. *Image Vis Comput* 2010;28:605-13.

149 Lee JJ, Freeland-Graves JH, Pepper MR, Yao M, Xu B. Predictive equations for central obesity via anthropometrics, stereovision imaging and MRI in adults. *Obesity (Silver Spring)* 2014;22:852-62.

150 Kahn SE, Hull RL, Utzschneider KM. Mechanisms linking obesity to insulin resistance and type 2 diabetes. *Nature* 2006;444:840-6.

151 Fabbrini E, Sullivan S, Klein S. Obesity and nonalcoholic fatty liver disease: biochemical, metabolic, and clinical implications. *Hepatology* 2010;51:679-89.

152 Flegal KM, Carroll MD, Ogden CL, Curtin LR. Prevalence and trends in obesity among US adults, 1999-2008. *JAMA* 2010;303:235-41.

153 Smith SR, Lovejoy JC, Greenway F*, et al.* Contributions of total body fat, abdominal subcutaneous adipose tissue compartments, and visceral adipose tissue to the metabolic complications of obesity. *Metabolism* 2001;50:425-35.

154 SK Vasan NT, S Christopher, FS Geethanjali, TV Paul, CB Sanjeevi. Anthropometric measurements for the prediction of the metabolic syndrome: a cross-sectional study on adolescents and young adults from southern india *Heart Asia* 2011;3:2-7.

155 Stanforth PR, Jackson AS, Green JS*, et al.* Generalized abdominal visceral fat prediction models for black and white adults aged 17-65 y: the HERITAGE Family Study. *Int J Obes Relat Metab Disord* 2004;28:925-32.

156 Goel K, Gupta N, Misra A*, et al.* Predictive Equations for Body Fat and Abdominal Fat With DXA and MRI as Reference in Asian Indians. *Obesity* 2008;16:451-6.

157 Zwane PE, Sithole M, Hunter L. A preliminary comparative analysis of 3D body scanner, manually taken girth body measurements and size chart measurements. Int J Consum Stud 2010;34:265-271.

158 Sironi AM, Petz R, De Marchi D*, et al.* Impact of increased visceral and cardiac fat on cardiometabolic risk and disease. *Diabet Med* 2012;29:622-7.

159 Misra A, Vikram NK. Clinical and pathophysiological consequences of abdominal adiposity and abdominal adipose tissue depots. *Nutrition* 2003;19:457-66.

160 Brundavani V, Murthy SR, Kurpad AV. Estimation of deep-abdominal-adipose-tissue (DAAT) accumulation from simple anthropometric measurements in Indian men and women. *Eur J Clin Nutr* 2006;60:658-66.

161 Demerath EW, Sun SS, Rogers N*, et al.* Anatomical patterning of visceral adipose tissue: race, sex, and age variation. *Obesity (Silver Spring)* 2007;15:2984-93.

162 Demura S, Sato S. Prediction of visceral fat area in Japanese adults: proposal of prediction method applicable in a field setting. *Eur J Clin Nutr* 2007;61:727-35.

163 Ross R, Leger L, Guardo R, De Guise J, Pike BG. Adipose tissue volume measured by magnetic resonance imaging and computerized tomography in rats. *J Appl Physiol* 1991;70:2164-72.

164 Seidell JC, Bakker CJ, van der Kooy K. Imaging techniques for measuring adipose-tissue distribution--a comparison between computed tomography and 1.5-T magnetic resonance. *Am J Clin Nutr* 1990;51:953-7.

165 Pepper MR, Freeland-Graves JH, Yu W*, et al.* Validation of a 3-dimensional laser body scanner for assessment of waist and hip circumference. *J Am Coll Nutr* 2010;29:179-88.

166 Toth MJ, Tchernof A, Sites CK, Poehlman ET. Effect of menopausal status on body composition and abdominal fat distribution. *Int J Obes Relat Metab Disord* 2000;24:226-31.

167 Snijder MB, Dekker JM, Visser M*, et al.* Associations of hip and thigh circumferences independent of waist circumference with the incidence of type 2 diabetes: the Hoorn Study. *Am J Clin Nutr* 2003;77:1192-7.

168 Parikh M, Issa R, Vieira D*, et al.* Role of Bariatric Surgery as Treatment for Type 2 Diabetes in Patients Who Do Not Meet Current NIH Criteria: A Systematic Review and Meta-Analysis. *J Am Coll Surg* 2013;217:527-32.

169 Bergman RN, Stefanovski D, Buchanan TA*, et al.* A better index of body adiposity. *Obesity (Silver Spring)* 2011;19:1083-9.

170 Hayashi T, Boyko EJ, McNeely MJ, Leonetti DL, Kahn SE, Fujimoto WY. Visceral adiposity, not abdominal subcutaneous fat area, is associated with an increase in future insulin resistance in Japanese Americans. *Diabetes* 2008;57:1269-75.

171 Cornier MA, Despres JP, Davis N*, et al.* Assessing adiposity: a scientific statement from the American Heart Association. *Circulation* 2011;124:1996-2019.

172 Haarbo J, Marslew U, Gotfredsen A, Christiansen C. Postmenopausal hormone replacement therapy prevents central distribution of body fat after menopause. *Metabolism* 1991;40:1323-6.

173 Reubinoff BE, Wurtman J, Rojansky N*, et al.* Effects of hormone replacement therapy on weight, body composition, fat distribution, and food intake in early postmenopausal women: a prospective study. *Fertil Steril* 1995;64:963-8.

174 Kanaley JA, Sames C, Swisher L*, et al.* Abdominal fat distribution in pre- and postmenopausal women: The impact of physical activity, age, and menopausal status. *Metabolism* 2001;50:976-82.

175 National Health and Nutrition Examination Survey, Anthropometry Procedures Manual, The Centers for Disease Control and Prevention, 2007.

176 Massey Jr FJ. The Kolmogorov-Smirnov test for goodness of fit. *Journal of the American statistical Association* 1951;46:68-78.

177 Boutcher SH, Dunn SL, Gail Trapp E, Freund J. Regional adiposity distribution and insulin resistance in young Chinese and European Australian women. *Scand J Clin Lab Invest* 2011;71:653-7.

178 Grunfeld C, Rimland D, Gibert CL*, et al.* Association of upper trunk and visceral adipose tissue volume with insulin resistance in control and HIV-infected subjects in the FRAM study. *J Acquir Immune Defic Syndr* 2007;46:283-90.

179 Azuma K, Heilbronn LK, Albu JB*, et al.* Adipose tissue distribution in relation to insulin resistance in type 2 diabetes mellitus. *Am J Physiol Endocrinol Metab* 2007;293:E435-42.

180 Manolopoulos KN, Karpe F, Frayn KN. Gluteofemoral body fat as a determinant of metabolic health. *Int J Obes (Lond)* 2010;34:949-59.

181 Wahrenberg H, Lonnqvist F, Arner P. Mechanisms underlying regional differences in lipolysis in human adipose tissue. *J Clin Invest* 1989;84:458-67.

182 Tchernof A, Despres JP. Pathophysiology of human visceral obesity: an update. *Physiol Rev* 2013;93:359-404.

183 Wilson JP, Kanaya AM, Fan B, Shepherd JA. Ratio of trunk to leg volume as a new body shape metric for diabetes and mortality. *PLoS One* 2013;8:e68716.

184 Wang J, Gallagher D, Thornton JC*, et al.* Regional body volumes, BMI, waist circumference, and percentage fat in severely obese adults. *Obesity (Silver Spring)* 2007;15:2688-98.

185 McLaughlin T, Lamendola C, Liu A, Abbasi F. Preferential fat deposition in subcutaneous versus visceral depots is associated with insulin sensitivity. *J Clin Endocrinol Metab* 2011;96:E1756-60.

186 Sanchez-Lopez M, Ortega FB, Moya-Martinez P*, et al.* Leg fat might be more protective than arm fat in relation to lipid profile. *Eur J Nutr* 2013;52:489-95.

187 Hoyer D, Boyko EJ, McNeely MJ, Leonetti DL, Kahn SE, Fujimoto WY. Subcutaneous thigh fat area is unrelated to risk of type 2 diabetes in a prospective study of Japanese Americans. *Diabetologia* 2011;54:2795-800.

188 Kang SM, Yoon JW, Ahn HY*, et al.* Android fat depot is more closely associated with metabolic syndrome than abdominal visceral fat in elderly people. *PLoS One* 2011;6:e27694.

189 Toss F, Wiklund P, Franks PW*, et al.* Abdominal and gynoid adiposity and the risk of stroke. *Int J Obes (Lond)* 2011;35:1427-32.

190 Ross R, Leger L, Morris D, de Guise J, Guardo R. Quantification of adipose tissue by MRI: relationship with anthropometric variables. *J Appl Physiol* 1992;72:787-95.

191 GE Healthcare. Lunar enCore Safety and Specification Manual. 2009.

192 Bland JM, Altman DG. Statistical methods for assessing agreement between two methods of clinical measurement. *Lancet* 1986;1:307-10.

193 Wiklund P, Toss F, Weinehall L*, et al.* Abdominal and gynoid fat mass are associated with cardiovascular risk factors in men and women. *J Clin Endocrinol Metab* 2008;93:4360-6.

194 Hara M, Saikawa T, Kurokawa M, Sakata T, Yoshimatsu H. Leg fat percentage correlates negatively with coronary atherosclerosis. *Circ J* 2004;68:1173-8.

195 Yavari R, McEntee E, McEntee M, Brines M. Anthropometric variables accurately predict dual energy x-ray absorptiometric-derived body composition and can be used to screen for diabetes. *PLoS One* 2011;6:e24017.

196 Holmes JD, Andrews DM, Durkin JL, Dowling JJ. Predicting in vivo soft tissue masses of the lower extremity using segment anthropometric measures and DXA. *J Appl Biomech* 2005;21:371-82.

197 Ritchie CB, Davidson RT. Regional body composition in college-aged Caucasians from anthropometric measures. *Nutr Metab (Lond)* 2007;4:29.

198 Scafoglieri A, Tresignie J, Provyn S*, et al.* Accuracy and concordance of anthropometry for measuring regional fat distribution in adults aged 20-55 years. *Am J Hum Biol* 2013;25:63-70.

199 Arthurs KL, Andrews DM. Upper extremity soft and rigid tissue mass prediction using segment anthropometric measures and DXA. *J Biomech* 2009;42:389-94.

200 Demura S, Sato S, Noguchi T. Prediction of segmental percent fat using anthropometric variables. *J Sports Med Phys Fitness* 2005;45:518-23.

201 Liu CH, Ward J. The use of 3D information in face recognition. *Vision Res* 2006;46:768-73.

202 Pepper MR, Freeland-Graves JH, Yu W, Stanforth PR, Xu B. Evaluation of a rotary laser body scanner for body volume and fat assessment. *J Test Eval* 2010;39:1-6.